

Rock Mass Behavior Under
Hydropower Embankment Dams
with Focus on Fracture Erosion
and Rock Mass Stability

Alexander Bondarchuk

DOCTORAL THESIS

Division of Mining and Geotechnical Engineering

Rock Mass Behavior Under
Hydropower Embankment Dams
with Focus on Fracture Erosion
and Rock Mass Stability

Alexander Bondarchuk

Luleå University of Technology
Department of Civil, Mining and Environmental Engineering
Division of Mining and Geotechnical Engineering

Printed by Universitetstryckeriet, Luleå 2012

ISSN: 1402-1544
ISBN 978-91-7439-409-2

Luleå 2012

www.ltu.se

PREFACE

The research presented in this thesis was carried out as a part of "Swedish Hydropower Centre - SVC". SVC has been established by the Swedish Energy Agency, Elforsk and Svenska Kraftnät together with Luleå University of Technology, The Royal Institute of Technology, Chalmers University of Technology and Uppsala University.

Participating hydro power companies are: Andritz Hydro Inepar Sweden, Andritz Waplans, E.ON Vattenkraft Sverige, Fortum Generation, Holmen Energi, Jämtkraft, Karlstads Energi, Linde Energi, Mälarenergi, Skellefteå Kraft, Sollefteåforsens, Statkraft Sverige, Statoil Lubricants, Sweco Infrastructure, Sweco Energuide, SveMin, Umeå Energi, Vattenfall Research and Development, Vattenfall Vattenkraft, VG Power and WSP.

I really want to thank my supervisors Associate Professor Maria Ask (LTU), Adjunct Professor Lars-Olof Dahlström (LTU / NCC AB, Gothenburg), and the LTU resources Professor Erling Nordlund and Professor Sven Knutsson, who help me to develop this project and have patience with me.

I would like to express my gratitude to my project reference group, for their support and good suggestions how to improve my work. This group consists of: M.Sc. Anders Isander (E.ON Gothenburg), Dr. Peter Viklander (Vattenfall, Luleå / WSP Samhällsbyggnad, Stockholm), Dr. Fredrik Johansson (KTH, Stockholm / SWECO, Stockholm), and Dr. Staffan Swedenborg (NCC AB, Gothenburg).

I would like to thank Vattenregleringsföretagen in general, and Gunnar Sjödin and his colleagues Birgitta Rådman och Svante Andersson in particular for allowing me to use the Håckren dam in my case study, and for providing data and help during my two visits to the dam.

I want to thank M.Sc. Mark Christianson (Itasca, Minnesota, USA), Dr. Eva Hakami (Itasca, Stockholm, Sweden), Assistant Professor Ping Zhang (LTU), Adjunct Professor Jonny Sjöberg (Itasca, Luleå, Sweden / LTU), and Dr. José Lemos (LNEC, Lisbon, Portugal) who helped me to implement my ideas into the numerical models.

I would like to thank my colleagues Lecturer Tomas Villegas, PhD David Saiang, who gave me hints how to solve the different problems.

I would like also to thank all my colleges at LTU, who have shown interest in my work and who have cared for me.

I am very grateful to the coffee-machine which kept me awake and provided energy for the work.

SUMMARY

There are over 190 large hydropower- and regulation dams in Sweden. The peak of dam construction occurred between 1950 and 1980, and those dams have now been in operation for about 30 to 60 years. Time has a negative influence on dam performance. The variations in load in the reservoir during operation induce displacements along existing discontinuities in the rock mass. Such displacements contribute to the degradation processes in a dam complex by influencing the water seepage and pore pressure, and may induce fracture erosion.

It is important to increase the understanding of rock mass stability, hydro-geological properties and the response of a dam to applied loads in the short- and long-term perspectives. An urgent challenge for the hydropower industry in Sweden is to maintain good stability and functionality of their aging hydropower dams. Several hydropower dams must be examined and, if necessary, upgraded to ensure that the safety of these dams complies with the best international practice and standards. These measures must be taken to improve safety, address new calculation- and assessment models, as well as account for new environmental conditions (i.e. climate change and more precipitation), and these actions are costly and time consuming that require large investments of time and money by the hydropower industry.

The objective of this doctoral thesis is to study the consequences on rock mass stability and fracture erosion induced by variations in loading conditions of a dam complex. The method in use is the coupled hydro-mechanical distinct-element method UDEC [Itasca, 2005]. The long-term developments of displacement along fractures, and distributions of pore pressure, leakage and flow velocity are studied in numerical models that are based on a real embankment dam in Sweden, the Håckren dam.

Conceptual models were first developed [Bondarchuk, 2008], and further analyzed to evaluate important factors in terms of normal- and shear displacements under a dam and its reservoir. Two 2D orthogonal conceptual models with seven parameters were developed. One parameter at the time was varied to investigate the influence of that parameter. The results suggest that sub-horizontal discontinuities and sub-vertical discontinuities leads to an increased water leakage under the dam. The amount of displacement depends on the direction of the dip angle of the sub-horizontal discontinuities. The magnitude and direction of in-situ stresses and the fracture frequency are also major factors that are affecting rock mass stability.

Subsequently, the conceptual model was modified to a real case, using as much site-specific data as possible to populate the model. Two 2D orthogonal models were developed. New data were collected using commonly used engineering geology methods. The satisfying validation of the model with real monitoring data suggest that this approach is robust and cost-effective, although some minor improvements can be applied within budget. A long-term evaluation of rock mass stability in terms of displacements, water flow- and velocity, and pore pressure distribution has been conducted over ten idealized years of operation (Paper IV). The results show that the rock mass is stable in most parts. Displacements are occurring in the dam that will alter the distribution of the void space, and lead to highly irregular preferential flow paths with widely varying velocities and may result in the erosion process of the surfaces of the discontinuities and gouge material in it, and gradual deterioration of the grout curtain.

SAMMANFATTNING

Det finns över 190 kraftverks- och regleringsdammar i Sverige. De flesta dammarna färdigställdes från år 1950 – 1980 och de har nu varit i drift mellan 30 och 60 år. Tid har en dokumenterat negativ effekt på en damms prestanda. Varierande belastningar från vattenreservoaren under drift kan orsaka små förskjutningar av berggrundens sprickzoner. Dessa rörelser bidrar till nedbrytning av dammen och dess reservoar. Ett ökat vattenläckage och en förändrad portrycksfördelning kan leda till initiering av sprickerosion i berggrunden.

Det är viktigt att öka förståelsen om berggrundens stabilitet, dess hydrogeologiska egenskaper och respons på belastningar från dammen ur olika tidsperspektiv. Ett angeläget arbete för svensk vattenkraftindustri är att säkerställa de åldrande dammarnas funktion och säkerhet. För att uppdatera och säkerställa det stora antalet dammar enligt nya beräknings- och bedömningsmodeller samt ändrade förutsättningar kommer många dammar att behöva uppdateras, och åtgärdas för att öka dess säkerhet, varför kraftindustrin framöver kommer att göra mycket stora investeringar.

Syftet med denna doktorsavhandling är att studera vilka konsekvenser varierande belastningar från damm och reservoar har på berggrundens stabilitet och dess sprickerosion. Jag använder den kopplade hydromekaniska distinkt-element metoden UDEC [*Itasca*, 2005]. Små förskjutningar längs berggrundens sprickor har studerats över lång tid tillsammans med portrycksfördelning, vattenläckage och vattenflödes hastighet. De numeriska modellerna har en verklig damm som förebild med platsspecifika indata, nämligen Håckren fyllningsdamm i centrala Sverige.

Två vinkelräta konceptuella modeller i 2D har utvecklats [*Bondarchuk*, 2008]. Berggrundens normal- och skjuvförskjutningar analyserades. Resultaten visar att sub-horisontella och sub-vertikala strukturer kan samverka och ge upphov till vattenläckage under dammen. Beteendet beror på bankningsplanens stupningsriktning. Sprickfrekvensen och de primära spänningarnas storlek och riktning är andra viktiga faktorer för berggrundens beteende.

De två konceptuella modellerna har anpassats till en verklig dam genom att använda så mycket platsspecifik data som möjligt. Ny data samlades in med hjälp av vanlig förekommande ingenjörsgelogiska metoder. En god överensstämmelse mellan modellresultat och övervakningsdata indikerar att angreppssättet är robust och kostnadseffektivt även om vissa förbättringar kan genomföras inom givna budgetramar. Små förskjutningar längs berggrundens sprickor har studerats över en period som motsvarar 10 driftår tillsammans med portrycksfördelning, vattenläckage och vattenflödes hastighet. Resultaten visar att berggrunden till största delen är stabil men att små förskjutningar sker och att dessa påverkar distributionen av öppna porer som i sin tur leder till mycket oregelbundna flödesmönster som kan orsaka sprickerosion längs sprickytor och sprickfyllnadsmaterial. I förlängningen kan detta påverka injekteringsskärmens beständighet och därmed berggrundens täthet under dammen.

TABLE OF CONTENTS	PAGE
PREFACE	i
SUMMARY	ii
SAMMANFATTNING	iii
TABLE OF CONTENTS	iv
LIST OF PAPERS	vi
1. INTRODUCTION	1
<i>1.1 Project motivation</i>	<i>1</i>
<i>1.2 Aim and approach</i>	<i>3</i>
<i>1.4 Outline of thesis</i>	<i>4</i>
2. EMBANKMENT DAM AND FOUNDATION ROCK MASS	5
<i>2.1 Embankment dams</i>	<i>5</i>
<i>2.1.1. Definitions</i>	<i>5</i>
<i>2.1.2 Safety guidelines</i>	<i>6</i>
<i>2.2 Foundation rock mass</i>	<i>7</i>
<i>2.2.1 Requirements for foundation rock of embankments dams</i>	<i>7</i>
<i>2.2.2 Grout curtains and drainage systems</i>	<i>7</i>
3. LOADS AND HYDRO-MECHANICAL BEHAVIOR OF ROCK JOINTS	9
<i>3.1 Mechanical effect of loads from the dam and water in the reservoir</i>	<i>9</i>
<i>3.2 Strength of discontinuities</i>	<i>11</i>
<i>3.3 Hydro-mechanical behavior of rock joints</i>	<i>12</i>
<i>3.3.1 Theory in fluid flow</i>	<i>13</i>
<i>3.3.2 Hydro-mechanical behavior during joint normal closure</i>	<i>15</i>
<i>3.3.3 Hydro-mechanical behavior during shear displacement</i>	<i>16</i>
<i>3.4 Erosion</i>	<i>17</i>
4. A COUPLED HYDRO-MECHANICAL MODEL OF EMBANKMENT DAM	18
<i>4.1 Continuum equivalent and discontinuum models</i>	<i>18</i>
<i>4.2 Description of the UDEC distinct element code</i>	<i>18</i>

4.3 <i>Concept and numerical approach</i>	19
5. RESPONSE OF TYPICAL SWEDISH ROCK MASS TO THE CONSTRUCTION AND FIRST STAGES OF OPERATION OF A HYDROPOWER EMBANKMENT DAM (Paper I, Paper II)	21
6. VALIDATION OF CONCEPTUAL MODEL ON CASE STUDY – HÅCKREN DAM (Paper III)	23
7. EVALUATION OF ROCK MASS RESPONSE IN LONG-TERM PERSPECTIVE WITH RESPECT TO DEFORMATION AND POSSIBLE EROSION (Paper IV)	25
8. CONCLUSIONS	27
9. RECOMMENDATIONS	29
REFERENCES	30

Paper I

Paper II

Paper III

Paper IV

LIST OF PAPERS

This doctoral thesis comprises the following papers:

Paper I

Bondarchuk A, Ask M V S, Dahlström L-O and Nordlund E (2011). Rock Mass Behavior Under Hydropower Embankment Dams: A Two-Dimensional Numerical Study. *Rock Mech. and Rock Eng.*, Springer DOI 10.1007/s00603-011-0173-2

Paper II

Bondarchuk A, Ask M, Dahlström L, Nordlund E and Knutsson S (2009). Hydro-mechanical numerical analysis of rock mass behavior under a Swedish embankment hydropower dam *Long Term Behavior of Dams*. Bauer, E., Semprich, S. & Zenz, G. (eds.). p. 113-118.

Paper III

Bondarchuk A, Ask M V S, Dahlström L-O and Nordlund E (2012). Rock mass stability of the Häckren hydropower embankment dam in central Sweden: Part I — Developing and validating 2D UDEC numerical models. Submitted for publication in the *Rock Mechanics and Mining Science*

Paper IV

Bondarchuk A, Ask M V S, Dahlström L-O and Nordlund E (2012). Rock mass stability of the Häckren hydropower embankment dam in central Sweden: Part II – Investigating fracture erosion. Submitted for publication in the *Rock Mechanics and Mining Sciences*

1. INTRODUCTION

1.1. Project motivation

Globally, dams are built to store water for irrigation, municipal use, hydropower electricity generation, and/or flood prevention [e.g. *Wahlström*, 1974]. Size and complexity of dams range from small and structurally simple constructions in small streams to large and structurally more complex dams in large rivers [e.g. *Wahlström*, 1974]. The type and design of individual dams depends on factors such as amount of available water, topography, geology, and type and amount of local material available for constructing the dam [e.g. *Fell et al.*, 2005].

Embankment, concrete and masonry dams are used for hydropower electricity generation. Embankment dams are mainly composed of naturally occurring materials [e.g. *Fell et al.*, 2005]). The main construction component of concrete dams is concrete, and masonry dams comprise building of structures from individual units laid in and bound together.

Over 190 large hydropower- and regulation dams were constructed for electricity production in Sweden (Figure 1.1) [e.g. *Bérburé*, 2004; *Axheim*, 2011]. About 100 of these are combined concrete- and embankment dams, whereas 50 of them are pure embankment dams. The first of these dams were constructed in early 20th century, but the peak of dam construction was from 1950 to 1980. The number of dams completed each year varied from over 10 to 34 dams/year within this period. The large dams are producing about 12% of the electricity in Sweden [e.g. *Swedish Energy Agency*, 2006]. Production of hydropower energy has the advantages of being flexible and instantaneous; therefore, it is often used to produce electricity at times of day or season when energy demand is higher than normal [e.g. *Ljunggren*, pers. comm., 2005], with low degree of energy waste [e.g. *Korsfeldt et al.*, 2007]. Energy production from hydropower is important for Sweden, and it is important that the dams are functioning with as few interruptions as possible.

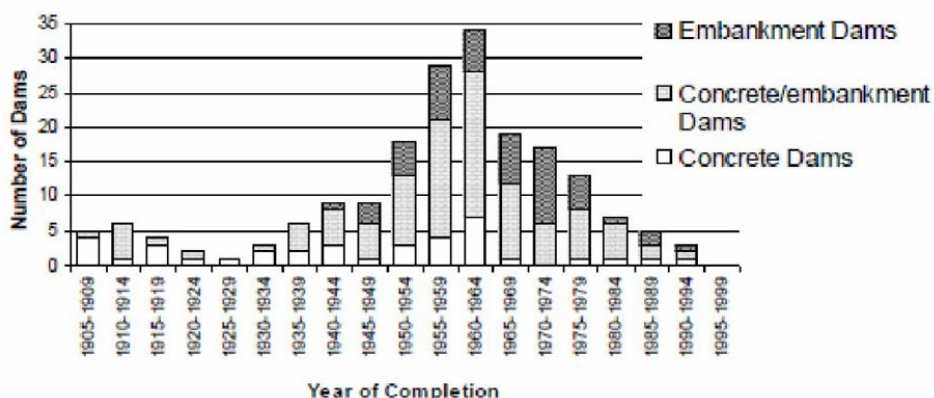


Figure 1.1 The number and types of dams in Sweden plotted against the year of their completion [from *Axheim*, 2011].

In addition to a negative impact on the overall energy production, a dam accident, or a major failure, potentially would cause large damage to society (e.g. human life and infrastructure)

downstream of a hydropower dam. To predict and mitigate effects from dam accidents and failures, the International Commission on Large Dams, ICOLD has developed and established guidelines for dam safety [e.g. *ICOLD*, 1974; 1995; 2002]. ICOLD is a non-governmental international organization, and a forum for the exchange of knowledge and experience in dam engineering. In Sweden, dam owners have established guidelines for the safety of dams, the hydropower industry dam safety guidelines, RIDAS [e.g. *RIDAS*, 2002]. The behavior of the foundation rock under a hydropower embankment dam is investigated in this thesis project. Anticipated results of the thesis include improved knowledge on parameters of the foundation rock that lead to potential instability of the foundation, together with how these parameters influence the integrity of the grouting curtain. These results are important for predict and mitigate effects of dam accidents and failures.

Many studies have been addressing dam stability issues. However, most studies are focusing on the dam construction itself [e.g. *Johansson*, 1997; *Windelhed*, 2001], and/or causes of failure and accidents [e.g. *ICOLD*, 1974; 1983; 1995; *Foster*, 2000]. Geophysical studies may be useful for studying the internal structure of dams and their foundation [e.g. *Bérubé*, 2004]. Dam incidents are often caused by overtopping, embankment leakage or piping, foundation leakage or piping, flow erosion, slope protection damage, and deformation. Other researches have attempted to predict the likelihood for dam failure based on statistical analysis of dam incidents [e.g. *Samad et al.*, 1987; *Cheng*, 1993]. The mechanical behavior of foundation rock under a hydropower dam, and the interaction between the construction and the foundation rock have been studied using experimental [e.g. *Reinius*, 1988] and numerical analyses [e.g. *Barla et al.*, 2004; *Dolezalova*, 2004; *Vasconcelos Braga Farinha*, 2010].

This thesis is one of the few attempts to investigate the hydro-mechanical behavior of the foundation rock under hydropower embankment dams (conceptual and real case) using the coupled hydro-mechanical discrete-element numerical code UDEC [*Itasca*, 2005]; It is the first study to consider the behavior of Swedish foundation rocks and conditions. The foundation rock consists of a rock mass, which is intact rock intersected by discontinuities.

Numerical analyses may advance the knowledge on the response of the foundation rock, interaction, and stability of the foundation rock and the hydropower dam, which is important information for determining the status of a hydropower dam. It allows the detailed investigation of complex interaction of a wide range of parameters over a selected cross-section of investigation. As the result, numerical analyses may help identifying the type of maintenance needed to ensure the functionality and safety of a hydropower dam. Different aspects of the life time of a dam may be investigated using numerical analyses. Numerical analyses may be a part of the design procedure to help identifying possible scenarios of rock mass behavior in response to construction and future exploitation of dam. It may be implemented as an instrument, which would allow to identify the reasons of malfunctioning of the dam in term of foundation rock. It may be used as a tool to predict the effectiveness of remedial measures or reconstruction of the dam.

Variation in static and cyclic loading at different stages in the life of a hydropower embankment dam may induce deformation in the foundation rock. This deformation may lead to displacement of the soil material within the embankment dam, and of the grout curtain. Increased water flow through the grout curtain is one plausible effect that may change the pressure distribution in the foundation rock and result in higher water loss. Both an increase in water flow and a change in pressure redistribution may have negative effects on dam stability, and, hence, increase the risk for dam failure.

1.2 Aim and approach

This doctoral thesis project concerns an urgent problem for the hydropower industry: How to maintain good stability and functionality of aging hydropower dams. Several hydropower dams must be examined and, if necessary, upgraded to ensure that the safety of these dams complies with the best international practice and standards. These measures must be taken to improve safety, address new calculation- and assessment models, as well as account for new environmental conditions (i.e. climate change and more precipitation). These actions all require large investments of time and money by the hydropower industry.

The objective of this doctoral thesis is to study the consequences on rock mass stability and fracture erosion induced by variations in loading conditions of a dam complex. The method in use is the coupled hydro-mechanical distinct-element method UDEC [Itasca, 2005]. The long-term developments of displacement along fractures, and distributions of pore pressure, leakage and flow velocity are studied in numerical models that are based on a real embankment dam in Sweden, the Håckren dam.

This work is a direct continuation of the licentiate thesis project by *Alexander Bondarchuk* [2008], in which a conceptual numerical model was developed to study the rock mass response to the construction of a hydropower dam and the filling of the reservoir. The conceptual model consisted of seven parameters, and the potential impact of individual parameters was investigated by varying one parameter a time.

The overarching aim for both the licentiate and doctoral theses is to *forward the knowledge about the foundation rock mass response to (a) static loading from the weight of a hydropower dam; and (b) cyclic loading from the annual variation in water load of its reservoir*. The studies are focused on Swedish conditions. The following approach was developed to address the overarching aim and the objective of this thesis:

1. Conduct in-depth analyses of the results from the conceptual model of the licentiate project. The results are included in Papers I and II;
2. Modify the conceptual model to a case study on a real dam by populating the UDEC model with site specific data, and validate the new model using real monitoring data. The results from this approach is included in Papers II and III; and
3. Perform long-term analyses of rock mass deformation and develop a method for interpreting the results in terms of fracture erosion and rock mass stability. This approach is addressed in Paper IV.

Anticipated results from this thesis include an improved understanding of degradation processes in the foundation rock mass, with focus on fracture erosion and rock mass stability. This understanding is important for the development of appropriate maintenance actions for high risk dams in Sweden, for example regarding reinforcement and grouting. The approach could also be adopted in the planning process, if new hydropower dams would be constructed in Sweden.

The Håckren dam in central Sweden has been selected as the case study. A series of engineering geology field methods (i.e. mapping, rock mass classification, Schmidt hammer test, coring of samples) and laboratory tests (Point Load Strength index, Tilt test, and index properties) have been performed. Additional information regarding the geology, monitoring of the inflow into the inspection tunnel and pore pressure redistribution in the foundation rock has been provided by the owners of the dam. All the information has been evaluated and the selected values are applied into the numerical model. The rock mass is studied along two orthogonal profiles, and the analyzes have been made during ten idealized years, where each year represents one cycle of filling and emptying of the reservoir by ± 25 m.

1.3 Outline of thesis

This doctoral thesis consists of eight main parts:

The motivation and objectives are presented in Chapter 1, “*Introduction*”.

Chapter 2, “*Embankment dam and foundation rock mass*” first briefly reviews different types of embankment dams and overview the incidents and their causes. The second part describes the foundation rock mass requirements for different type of embankment dams. The grout curtain and drainage systems aspects are also presented in Chapter 2.

Chapter 3, “*Loads and hydro-mechanical behavior of rock joints*” reviews the research regarding the loads caused by the construction and exploitation of the dams. The second part summaries the theory behind the mechanical strength of the discontinuities. A short review of the theory in fluid flow is presented, followed by the description of the hydro-mechanical properties of the discontinuities. Aspects of erosion of the discontinuities are also covered in Chapter 3.

Chapter 4, “*A coupled hydro-mechanical model of embankment dam*” describes the difference between the continuum equivalent and discontinuum models. Then it presents the UDEC distinct element code. Afterwards there is a description of the process of transformation of the concept into the numerical code.

Chapters 5-7 are based on Papers I, II,III and IV and include a short summary of these papers.

Chapter 8 contains conclusions obtained from this research.

Chapter 9 presents the recommendations for the future work.

2. EMBANKMENT DAM AND FOUNDATION ROCK MASS

2.1 Embankment dams

2.1.1. Definitions

Several definitions of embankment dams exist. A common feature for all definitions is that an embankment dam is a dam constructed of natural materials [e.g. *National Research Council*, 1983; *Goldin and Rasskazov*, 1992; *Varshney*, 1995]. Embankment dam may be characterized as a dam, in which the bulk of the construction consists of naturally occurring materials, e.g. soil, clay, sand, gravel, and natural boulder or quarried fragmented rock. Embankment dams may be subdivided into two major groups:

(1) Earth-fill embankment dams; and (2) Rock-fill embankment dams.

Earth-fill embankment dams are primarily constructed of compacted earth, either homogeneous or zoned, and contain more than 50% of earth. Rock-fill dams contain more than 50% of compacted and dumped permeable rock fill. The latter dams must have an impermeable (water tight) upstream blanket, or an impermeable core [e.g. *National Research Council*, 1983].

National Research Council [1983] proposed three criteria to base the classification of embankment dams:

- (1) The predominant material of the dam (it could consist of either rock or earth);
- (2) The method used to place material in the embankment; and
- (3) The geometric configuration or layout of the zones of the dam.

Goldin and Rasskazov [1992] suggested a larger number of criteria to classify embankment dams than, for example, the *National Research Council* [1983]. His criteria include type of material, design, construction technology, height, and seepage preventions measures. However this work is concentrated on the behavior of the foundation rock under the embankment dams than the embankment dams itself, so only simplified classification based on structure is introduced.

Homogeneous embankment dams

Homogeneous embankment consists almost entirely of one type of the material (Figure 2.1). This type of dam has evolved to reduce the construction costs in areas where only one main type of material is available near the dam site. Usually homogeneous embankment dams consist of low permeability material and require flatter slopes than zoned embankment dams.



Figure 2.1 Homogeneous embankment dam [*Goldin and Rasskazov*, 1992]

Zoned embankment dams

Zoned embankment dams are made up of two or more different types of material (Figure 2.2). This type of dam includes different sections, including a 'core', which is an impermeable zone inside the dam, and a 'shell', which is the outer zone on both sides of dam. The 'shells' are

usually made from permeable material, and if several different types of material are available, those with higher permeability are placed on the outer faces. Separation of different zones in the dam is performed with the help of filters.



Figure 2.2 Zoned embankment dam with thin central core [Goldin and Rasskazov, 1992]

A standard Swedish embankment dam with a central impermeable core is presented in Figure. 2.3 [RIDAS, 2002].

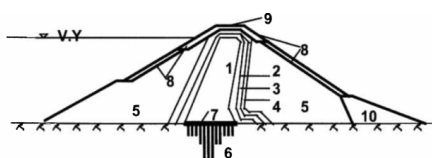


Figure 2.3 Standard Swedish embankment dam with a central impervious core according to RIDAS [2002]

2.1.2 Safety guidelines

Dam failures are rated as one of the major low-probability, high-loss events [e.g. *National Research Council*, 1983]. Studies of past dam failures show three major causes: seepage and internal erosion in the embankment, seepage and erosion of the foundation, and overtopping [e.g. *ICOLD*, 1995].

Realizing importance of historic performance of dams in assessing dam safety, ICOLD carried out extensive review of incidents of large dams, i.e. more than 15 m high. The most common causes of accidents and failures were investigated [e.g. *ICOLD*, 1974; 1983; 1995; *Foster et al.*, 2000]. Other researchers have attempted to predict the likelihood of dam failure based on the statistical analysis of dam incidents, for example *Samad et al.* [1987] and *Cheng* [1993]. Although piping through the foundation of the embankment dam is not the biggest threat to the integrity of the dam, nearly 15% of all known failures are caused by piping. This shows that hydrological properties of the rock are important for the stability of embankment dams, and that closer attention should be paid to these properties during numerical analyses.

According to Swedish law, the dam owners have the responsibility for dam safety [Mcgrath, 2000]. Although the Swedish government gives permission for the construction of a dam, the dam owners normally operate and maintain their dams. Therefore, owners are working in non-regulatory environment. Individual towns are responsible for emergency planning for accidents while Country Councils have responsibility for major events such as dam failures.

In 1997, the first guidelines for Swedish dam owners were finalized, the Hydropower Industry Dam Safety Guidelines, RIDAS. These guidelines were review in 2002. There are three main objectives for the RIDAS guidelines, namely to: (1) Define requirements and establish guidelines for adequate and uniform dam safety; (2) Constitute a basis for a uniform evaluation of dam safety and identify measures needed to improve dam safety; and (3) Support authorities in their supervision of dam safety.

2.2 Foundation rock mass

2.2.1 Requirements for foundation rock of embankment dams

The foundation rock or rock mass under an embankment dam has two main purposes [e.g. *National Research Council*, 1983]: to provide stable support with little deformation and settlement under all conditions of saturation and loading; and, for economic purposes, to provide resistance to leakage of water. Homogeneous and zoned embankment dams require different types of the foundation rock [e.g. *Singh*, 1995]. Homogeneous embankment dams may have uniform quality of the rock across the entire foundation, while zoned embankment dams generally have different quality of the foundation rock for the outer shells and the impermeable core.

The foundation rock of the outer shells should be resistant against sliding and major settlements, whereas minor foundation settlements may be tolerated without any damage to the construction of the dam. The physical properties of this foundation rock are equal or better than the properties of the dam shell [e.g. *Singh*, 1995].

For the zoned embankment dam, the contact area between the impermeable core and the foundation rock is the most critical in terms of integrity of the core [e.g. *Singh*, 1995]. To guarantee the integrity of that contact area, the foundation rock should consist of hard rock with few joints and fault plains [e.g. *Goldin and Rasskazov*, 1992; *Singh*, 1995]. These conditions are usually obtained by removing weak, weathered rock until rock with required quality is reached, and by using consolidated grouting to reduce the permeability of the foundation rock [e.g. *Singh*, 1995; *Goldin and Rasskazov*, 1992].

The interface between embankment dam and foundation rock is a critical contact for all types of embankment dams. Poor bonding between the two may lead to piping along the contact area, which later may develop into seepage paths and internal erosion [e.g. *National Research Council*, 1983]. Improper treatment of foundation discontinuities, and/or together with inadequate filters between the embankment dam and joints in the foundation rock, may also lead to piping in the embankment dam, and subsequently to collapse due to internal erosion [e.g. *National Research Council* 1983]. To reduce a risk of incidents there have been proposed methodology of preparation of foundation rocks before construction reservoir [e.g. *RIDAS*, 2002; *USACOE*, 2004].

2.2.2 Grout curtains and drainage systems

Control of the seepage is necessary procedure to prevent excessive uplift pressure and erosion of material in open joints. It is usually carried out with the grouting and the drainage systems. Blanket- and curtain grouting are the two main grouting programs that normally are used for embankment dam construction (Figure 2.4). Near-surface rocks are often weathered and highly fractured because of natural causes as well as activities related to the preparation and construction of the dam. Blanket grouting is used to reduce seepage losses, seepage velocities through a relatively permeable near-surface zone, and the possibility of transporting embankment material into foundation. Blanket grouting is introduced by drilled shallow holes with different patterns, depending on the type of the dam and the geological conditions and it is usually restricted to the upper 5m to 20 m [e.g. *Duncan*, 1999; *Fell et al.*, 2005; *RIDAS*, 2007; *Weaver and Bruce*, 2007]. Grout curtain is designed to create a narrow barrier through an area of high permeability. It usually consists of a single row of grout holes that are drilled and grouted to the base of the permeable rock, or to such depths that acceptable hydraulic gradients are achieved. For large dams on foundation rocks, and dams on very permeable rock, three, five or

even more lines of grout holes may be grouted [e.g. *Fell et al.*, 2005]. Sometimes the vertical depth of the grout curtain is accepted as two thirds of the height of the dam [e.g. *Vattenfall*, 1988; *RIDAS* 2007; *Weaver and Bruce*, 2007].

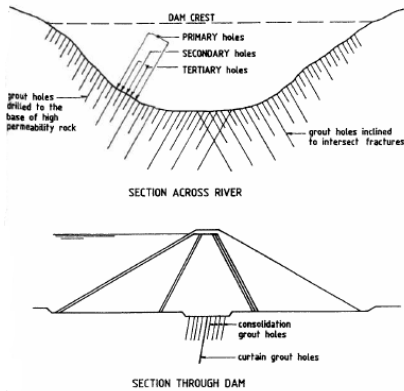


Figure 2.4 Consolidation (blanket) and grout curtain under an embankment dam with central core [*Fell et al.*, 2005]

The introduction of cement grout into discontinuity void space affects its mechanical as well as hydrological properties. *Swedenborg* [2001] carried out laboratory tests on a cement grouted crystalline rock samples and implemented numerical analyze to estimate mechanical effects of grouting. It shows a slight reinforcing effect for surface grouting operations such as under the dams. Filling the discontinuities of the rock mass with cement substance reduces their hydraulic conductivity hence reducing seepage rate and seepage exit gradient [e.g. *Fell et al.*, 2005; *Hwang and Houghtalen*, 1996; *Swedenborg*, 2001]. (Figure 2.5)

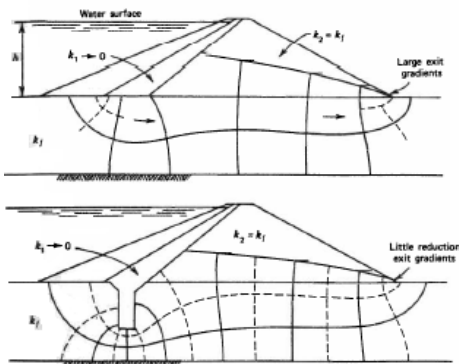


Figure 2.5 Effect of partial cutoff on position of line of seepage [*Fell et al.*, 2005]

The drainage curtain is usually represented by the line of boreholes drilled downstream from the grout curtain to collect and control seepage under the dam and that way reduce the uplift pressure. Reduction of uplift pressure leads to increasing effective normal stress acting on the discontinuities in the rock mass and consequently leads to increased safety [*Vasconcelos Braga Farinha*, 2010]. The drainage curtain is usually made from the drainage gallery.

3. LOADS AND HYDRO-MECHANICAL BEHAVIOR OF ROCK JOINTS

3.1 Mechanical effect of loads from the dam and water in the reservoir

Reinius [1988] investigated stresses and deformation of the foundation rock before and after filling up water in the reservoir based on the simple analogue experimental model of an embankment dam to obtain an approximate idea what forces and stresses act on the foundation rock of the embankment dam due to load (Figure 3.1). Reinius [1988] found that horizontal tension stresses occur in the foundation rock when the dam load is placed on the rock surface (Figure 3.2), and that they further increase when the water level of the reservoir is raised to the full storage level (Figure 3.3). Tensional stresses may lead to an increase in the width of the discontinuities. He suggests two causes for the tension stresses and opening cracks: The first one is related to differential settlement, due to sloping foundation in the direction of the longitudinal dam axis (Figure 3.4) and rapid changes of the rock quality. The second cause is that the soil and water pressures are acting in a direction perpendicular to the long axis of the dam. Cracks with widths of several millimeters may cause considerable water leakage, and they may be a way for transportation of the material from the core.

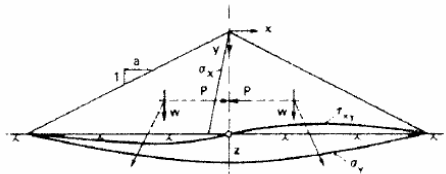


Figure 3.1 Forces and stresses in a triangular, prismatic earth fill dam [Reinius, 1988]

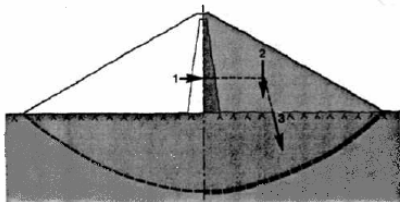


Figure 3.2 Embankment dam with central core. Stresses redistribution in foundation rock after construction of embankment dam. [Reinius, 1988]

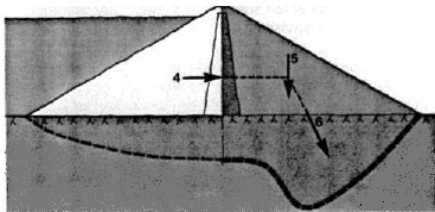


Figure 3.3 Embankment dam with central core. Stresses redistribution in foundation rock after impounding the reservoir. [Reinius, 1988]

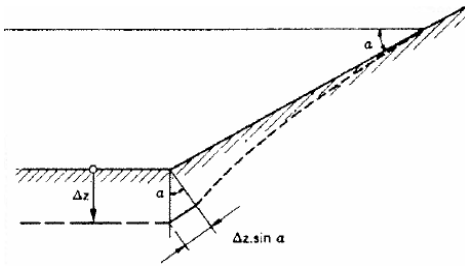


Figure 3.4 Elongation along a rock slope caused by settlement of the rock surface Δz by the weight of the dam [Reinius, 1988]

The cycling variation of the water in the reservoir causes cycling loading on the foundation rock which leads to irrecoverable strain within rock mass which may be as important as design [Goodman, 1980]. As the reservoir behind the dam rises the rock under the dam deforms. When the reservoir is lowered for any reason, rock mass tries to restore its original condition however there is still some permanent deformations left. Repeated cycles of loading and unloading in response of cyclic variation of the water in the reservoir would produce a series of loops, hysteresis. The example of such response of rock mass is presented on Figure 3.5. In long-term perspective such process results in accumulation of deformation in the foundation rock of the dam. Considering that the intact rock matrix is generally stiff compare to the joints [Rutqvist, 1990] and dam engineering usually does not operate with high magnitude stresses as in mine industry, it logical that all deformations are occurring along the discontinuities in the rock mass.

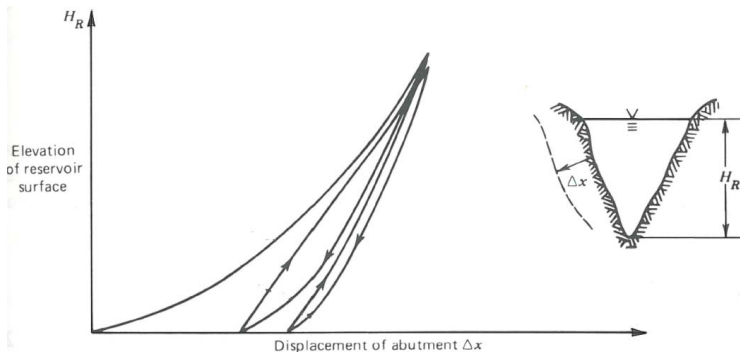


Figure 3.5 Permanent foundation deformation caused by cycles of reservoir filling and emptying [Goodman, 1980]

A discontinuity is any mechanical discontinuity in a rock mass having different strength properties. There are several other types of discontinuities, for example fault, bedding, cleavage, and foliation [e.g. *Wyllie and Mah* 2004]. At shallow depth gravity driving sliding on the discontinuities and rotation of the individual rock block plays a dominant role [e.g. *Hoek et al.*, 1997]. Since discontinuity governs the stability of the rock system, therefore it is very essential to assess the shear strength of the discontinuities. However, determination of shear strength is associated with some uncertainty. Several factors must be considered, such as aperture, the wall strength, the roughness, the scale effect, the presence of filling material and presence of water. To model stress-strain response, shear and normal stiffness are required parameters, together with dilation angle [e.g. *Johansson*, 2005].

3.2 Strength of discontinuities

Estimation of shear strength may be done under laboratory conditions, although the results should be taken with precaution due to scale effect reasons. In-situ measurements will also consider the scale effect, however, these test are associated with high cost and requires much time [e.g. *Johansson, 2005*]. There are also two empirical methods: Barton's empirical failure criteria and back analysis of failures, which is based on calculation shear strength parameters using experience or from other sites with similar characteristics.

A fundamental quantity for shear strength of discontinuities is the basic friction angle, ϕ_b . This is approximately equal to the residual friction angle, ϕ_r [e.g. *Hoek et al., 1997*]. The basic friction angle is related to the size and shape of the grains, exposed on the discontinuity surface. It may be measured by testing sawn or ground rock surfaces [e.g. *Wyllie and Mah, 2004*]. The basic friction angle normally varies within 25 to 40° for common rock types.

A natural discontinuity surface in hard rock is never as smooth as sawn specimens which are used in laboratory tests for estimation of basic friction angle. The undulation and asperities on a natural joint have a significant influence on its shear resistance. Generally the surface roughness of the joint increases its shear strength [e.g. *Hoek et al., 1997*]. Patton [1966] demonstrated the importance of roughness in terms of shear resistance in shear test using "saw-tooth" specimens (Figure 3.6).

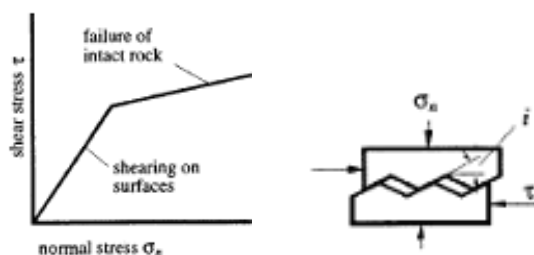


Figure 3.6 Influence of roughness of joints on shear resistance [*Hoek et al., 1997*].

Based on detailed studies of natural joints, Barton [1973] proposed that the peak shear strength could be expressed as:

$$\tau = \sigma_n \cdot \tan \left[\phi_b + JRC \cdot \log_{10} \left(\frac{JCS}{\sigma_n} \right) \right] \quad (\text{Eq. 3.1})$$

where σ_n is the normal stress acting on the discontinuity, ϕ_b is the basic friction angle, JRC is the joint roughness coefficient, and JCS is the wall compressive strength. ISRM has published suggested methods for the estimation of JRC [e.g. *ISRM, 1978*]. They recommend tilt- and shear tests to estimate JRC, which is obtained from:

$$JRC = \frac{\alpha - \phi_b}{\log_{10} \left[\frac{JCS}{\sigma_n} \right]} \quad (\text{Eq. 3.2})$$

where α is the tilt angle, and σ_n is the normal stress acting on the discontinuity when sliding occurs. If no laboratory tests are available, they propose to estimate JRC by comparing the roughness of the surface of the discontinuity with standard profiles [e.g. *Barton and Choubey, 1977*].

The scale effect is an important factor for estimating the shear strength. Smaller sized samples have higher peak shear strength than larger ones [e.g. *Hoek et al.*, 1997]. They suggest that JRC decreases with increasing scale, which lead to a reduction of shear strength of the discontinuity. An increase in scale also lead to a reduction of the average JCS, because the possibility for weaknesses in the sample increase with an increasing sample size [e.g. *Hoek et al.*, 1997].

The influence of the infilling on the shear strength properties of a discontinuity depends on the thickness and strength properties of the infilling material [e.g. *Hoek and Bray*, 1981, *Swedenborg*, 2001]. If the thickness of the asperity is more than 25-50% of the amplitude of the asperities, there will be little or no rock-to-rock contact and shear strength properties of discontinuity will be dictated by properties of the infilling material [e.g. *Goodman*, 1980]. When water is present in discontinuities, the shear strength is reduced even more, as the result of a decrease in effective normal stress [e.g. *Hoek and Bray*, 1981]

Barton [1974] performed a series of direct shear test to determine peak friction angle and cohesion for filled discontinuities, and proposed that the infilling can be subdivided in two groups: The first group comprises of clays, with friction angles from about 8-20°, and cohesion values up to about 200 kPa. The second group comprises of faults, shear zones, and breccias, with friction angles from about 25-45° and cohesion values up to about 100 kPa. Barton [1974] also found that the residual friction angle only is about 2-4° lower than the peak friction angle, while the residual cohesion is zero.

A second criterion by *Barton* [1974] regards whether there has been previous displacement along the discontinuity. He proposed two general categories: Recently displaced discontinuities, and undisplaced discontinuities, respectively. Recently displaced discontinuities include faults, shear zones, clay mylonites, and bedding-surface shears. Their shear strength is assumed to be close to the residual strength, and there will be a small reduction in strength when further displacement takes place. Undisplaced discontinuities include igneous and metamorphic rocks that have weathered along discontinuity surfaces to form clay layers. Further subdivisions of these two categories have been made to include normal- and over-consolidated materials [e.g. *Wyllie and Mah*, 2004], and these discontinuities have significantly different peak strength values.

Today there is no theoretical model or empirical correlation which would allow accurately determine the shear strength of filled discontinuities. The best test method available today is in situ shear tests [e.g. *ISRM*, 1975; *Matsuoka et al.*, 2001].

Parameters for describing the relation between stress and strain for discontinuities include normal- and shear stiffness, K_n and K_s , respectively, maximum closure, δ_0 , and the dilation angle, ψ_{dis} [e.g. *Johansson*, 2005; *Bandis et al.*, 1983]. Normal stiffness is measured while the sample is subjected to normal deformation, and the normal deformation is measured with sensitive gauges. The shear stiffness and dilation angle are determined in shear tests, where the constant normal load is applied to the sample, and rate of shear loading is kept on same level.

3.3 Hydro-mechanical behavior of rock joints

Dams are constructed to store large volumes of water on foundation rocks that are never homogenous, but rather consist of many discontinuities. Some discontinuities may form a connection between the storage area and the downstream side of the dam, where the water loss due to seepage is high. When water is filled into the dam reservoir, the different elevation of the water on both sides of the dam result in a hydraulic gradient. In addition, the cross sectional area through which water flow can take place decreases, because the low permeability of the dam body increase the velocity of seeping water [e.g. *Bandara and Imbulana*, 1996]. Increase in velocity may lead to erosion of material in the foundation rock, which may lead to piping. *Fell et*

al. [2005] formulated required conditions that contribute to the development of piping: (1) There must be a seepage flow path and a source of water; (2) There must be erodible material within the flow path and this material must be carried by the seepage flow; (3) There must be unprotected exit, from which the eroded material may escape; and (4) For a pipe to form, the material being piped, or the material directly above, must be able to form and support “roof” for the pipe.

3.3.1 Theory in fluid flow

The movement of water in foundation rock occurs predominantly along discontinuities, because the hydraulic conductivity of intact rock is much lower than the discontinuities. Consequently, the conductivity of foundation rock is strongly affected by the characteristics of the discontinuities [e.g. *Wyllie and Mah, 2004*]. The flow of water in a jointed rock mass may be carried out either assuming that rock mass is a continuum or that the rock is a non-continuum [e.g. *Thiel, 1989; Wyllie and Mah, 2004*]. The continuum approach is used for the rock mass where discontinuities spacing is sufficiently close that the fractured rock acts hydraulically as a granular porous media and is considered as a permeable homogeneous material with a coefficient of permeability, k (Figure 3.7).

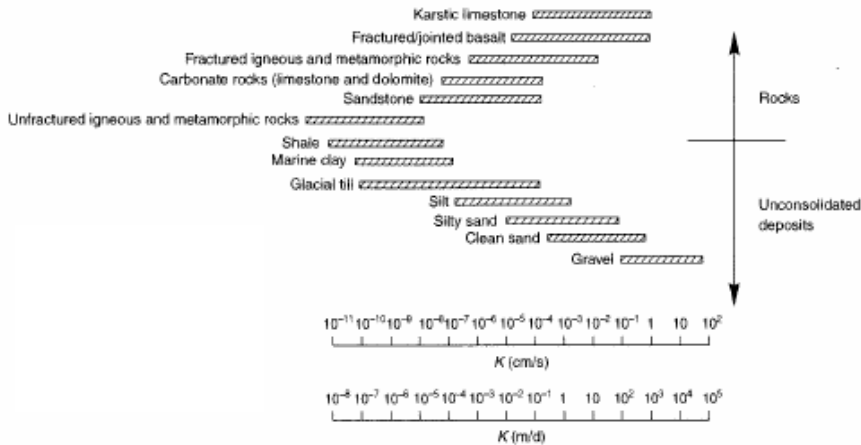


Figure 3.7 Hydraulic conductivity of various geologic materials [*Wyllie and Mah, 2004*]

According to Darcy law, water flow through a material proportionally to the hydraulic gradient [e.g. *Darcy, 1856*]:

$$Q = k \cdot I \cdot A \tag{Eq. 3.3}$$

where Q is rate of flow, I is the gradient or head loss between two points and A is the cross-section area. Darcy’s law is only applicable to the laminar flow, and cannot be used for turbulent flow [e.g. *Wyllie and Mah, 2004*]. If boundary conditions and permeability of the material is known, the pore pressure, u may be calculated at different points in the material using Darcy’s law:

$$u = \gamma_w \cdot h \tag{Eq. 3.4}$$

where γ_w is the unit weight of the water, and h is the pressure height. *Terzaghi* [1943] used Eq. 3.4 to develop the principle of effective stresses:

$$\sigma' = \sigma - u \tag{Eq. 3.5}$$

where σ' is effective stress, u is pore pressure, and σ is total stress.

The equivalent hydraulic conductivity (Figure 3.8) of an array of parallel, smooth, clean discontinuities may be expressed as [e.g. *Wyllie and Mah, 2004*]:

$$K \approx \frac{g \cdot e^3}{12 \cdot \nu \cdot b} \quad (\text{Eq. 3.6})$$

where g is the gravitational acceleration, e and b are the discontinuity aperture and spacing, respectively, and ν is the coefficient of kinematic viscosity.

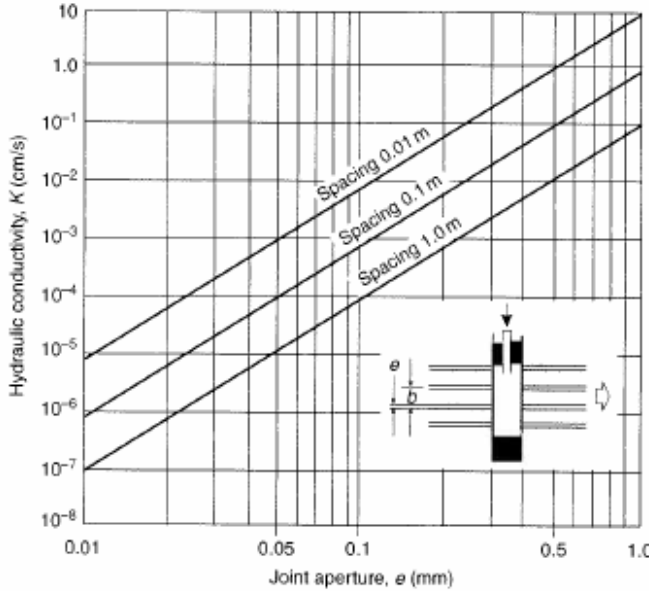


Figure 3.8 Influence of joint aperture and spacing on hydraulic conductivity in the direction of a set of smooth parallel joints in a rock mass [*Wyllie and Mah, 2004*]

The hydraulic conductivity is very sensitive to the aperture, hence small changes in the aperture significantly reduce the conductivity. Eq. 3.6 can be applied only to laminar flow in planar, smooth, parallel discontinuities and represents the highest equivalent hydraulic conductivity for a fracture system. However, the presence of filling material in the discontinuities reduces their hydraulic conductivity, so Eq. 3.6 modifies into:

$$K = \frac{e \cdot K_f}{b} + K_r \quad (\text{Eq. 3.7})$$

where K_f is the hydraulic conductivity of the filling, and K_r is that of intact rock.

Based on Darcy's law, an expression for hydraulic conductivity and the area expressed in width, w and aperture, e , the flow between two parallel planar plates may be expressed with the cubic law:

$$Q = -\frac{\rho_w \cdot g \cdot w \cdot a^3}{12 \cdot \nu_w} \quad (\text{Eq. 3.8})$$

where ρ_w is the density of water, ν_w is the kinematic viscosity of water, g is gravitational acceleration, w is discontinuity spacing, and a is aperture.

It is difficult to model the movement of water in the rock mass using a discontinuous approach, because the flow is influenced by a number of parameters (Figure 3.9). As stated above, a

reduction in aperture result in a substantial reduction of the hydraulic conductivity, and it also result in ejection of infilling material (e.g. water). *Thiel* [1989] discuss the issue of modeling based on the spacing between the discontinuities and the size of rock mass or structure in question.

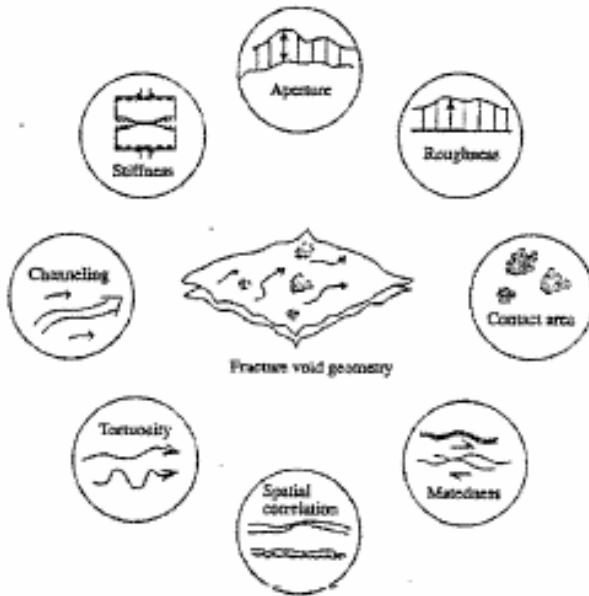


Figure 3.9 Properties of discontinuities that affect the flow [*Hakami*, 1995]

3.3.2 Hydro-mechanical behavior during joint normal closure

The dependence of aperture and flow behavior in the rock discontinuities from normal stress have been studied by many authors [*Barton et al.*, 1985; *Rutqvist*, 1990; *Cammarata et al.*, 2007; *Cook*, 1992]. Figure 3.10 shows the typical mechanical and hydro-mechanical behavior of the rock discontinuities under normal stress. This behavior is non-linear and the rate of close is higher at the lower normal stresses, which means the increase of the discontinuity's normal stiffness with increasing normal stress. This figure shows also the scale dependence where the normal closure of the discontinuity increases with sample size [*Vasconcelos Braga Farinha*, 2010].

Experimental results shows that fracture transmissivity is decreasing with increasing normal stress, however there is apparent residual transmissivity (T_r) at high stress when the discontinuity appears to be mechanically compressed, Figure 3.10 [*Vasconcelos Braga Farinha*, 2010] The residual transmissivity indicates that the fluid flow at high stress is governed by tube-like flow channels [*Rutqvist and Stephansson*, 2003]

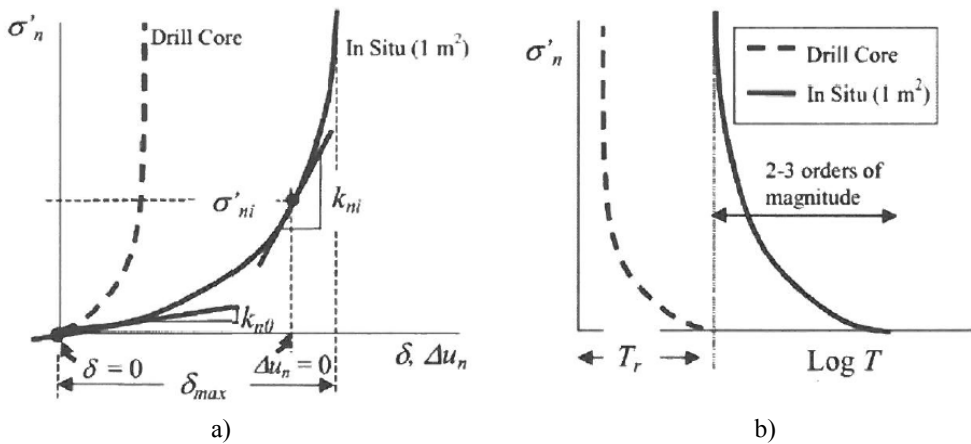


Figure 3.10 Typical mechanical (a) and hydro-mechanical (b) fracture responses under normal closure [Vasconcelos Braga Farinha, 2010]. σ'_n - effective discontinuity normal stress, σ'_{ni} - effective discontinuity normal stress at initial conditions, k_{n0} - discontinuity normal stiffness at zero normal stress, k_{ni} - discontinuity normal stiffness at an initial effective stress, Δu_n - discontinuity normal displacement, Δu_s - discontinuity shear displacement, δ - discontinuity normal closure, δ_{max} - maximum discontinuity normal closure, T - fluid transmissivity, T_r - residual transmissivity at high compressive strength.

3.3.3 Hydro-mechanical behavior during shear displacement

Deformation of discontinuity can take the following forms: normal closure, opening, shear and dilation. All these deformations change the hydraulic properties of rock and so its conductivity. To make a model combining all these deformations it necessary to know a precise characterization of joint roughness morphology and its development with shear displacement in the case of the share loading conditions [Archambault et al. 1997] In shear loading condition case a hydro-mechanical coupling is sophisticated and experimental work is difficult to perform, so less research is dedicated to this problem [Chen et al., 2000; Boulon et al., 1993; Makurat et al., 1990; Vasconcelos Braga Farinha, 2010]. The difficulty comes from the evolution of roughness morphology on the discontinuity surfaces with applied normal stress and shear displacement [Archambault et al., 1997].

Effect of normal loading is very significant for conductivity at process of sharing [Bandis et al., 1985; Chen et al., 2000; Archambault et al., 1997]. Increase of the normal stress results larger damaged zones, reduction of cumulative dilatancy with fewer void spaces and decrease of aperture for the same shear displacement on the discontinuity plane. For lower normal stress and longer shear displacement the aperture in the void spaces will be larger because of the greater cumulative dilatancy. The perturbations of closure-opening (contractancy - dilatancy) for a matched joint under shearing loading occurs within 2 mm of shear displacement or even less. The fluid flow will follow the tortuous paths, around the contact areas with widely varying velocities and preferential channels. [Archambault et al., 1997]. This non-linear flow is a result of inertial losses arising from entrance and exhaust boundaries, constrictions and obstructions, and initiation of turbulence due to localized eddy formation [Chen et al., 2000]

3.4 Erosion

Movement of water along flow channels in the discontinuities results in water-rock interaction. This interaction includes physical and chemical reactions. Colback and Wild [1965] showed that the influence of water-rock interaction on rock mass strength is significant. Construction of dam and following filling of the reservoir transmits large loads to the foundation and causes changes in aperture of the discontinuities, which in turn modifies the natural flow path. Additionally the rock mass is subjected to large difference in hydraulic head between upstream and downstream side of the dam. The cyclic loading caused by variation of water in the reservoir contributes to continuous change in flow path [Goodman, 1980; Vasconcelos Braga Farinha, 2010]. Farinha [2010] reported that majority of recorded failures were due to problems in the foundation rock mass because of the weathering processes. Subsurface erosion and dissolution were the most significant. These processes resulted in loose of strength and lack of shear resistance along weak planes of unfavorable direction.

Process of erosion is very complicated. However our understanding of long-term behavior of rock mass during geological wear and erosion may be drawn from the results of accelerating testing methods [Momber, 2004]. The main evaluation parameter in mechanical erosion is the erosion rate, usually given through the following equation

$$E_R = \frac{m_1 - m_2}{t_e} = \frac{\Delta W}{t_e} \quad (\text{Eq. 3.9})$$

where E_R – is the erosion rate, ΔW – weight loss, t_e – time of exposure.

High-speed fluid flow tests show that two most important parameters influencing the erosion performance, which are flow velocity and exposure time [Momber, 2004]. The functions for both parameters in turn may be subdivided into two sections: an incubation period and an erosion period. Incubation period is characterized by “invisible damage”, because no material is removed and the target material seems to be undamaged. The critical flow velocity, which is also called “erosive velocity” separates incubation and erosion period. It is the velocity of water in a channel above which erosion occur. In term of dam stability, water pressure are the most crucial aspect, however the discharge is also relevant factor. It is connected very close with seepage velocity, which should be limited in order to avoid erosion of material in open discontinuities [Vasconcelos Braga Farinha, 2010].

4. A COUPLED HYDRO-MECHANICAL MODEL OF EMBANKMENT DAM

4.1 Continuum equivalent and discontinuum models

There are two approaches to simulate hydro-mechanical coupling behavior of fractured rock mass. The first one uses the equivalent continuum models, the second one applies the discrete fracture network [Vasconcelos Braga Farinha, 2010]. The choice between the approaches depends on several factors such as the size and spacing of the discontinuities when compared to the size of the problem, and on the discontinuity pattern.

In equivalent continuum models, the properties of the material should be modified in such a way that they represent major characteristics of the rock mass's physical behavior. The water flow within the model creates deformations in continuous media, which alters the permeability. This approach requires correlation between stress or strain and permeability to be previously established.

In distinct element method the rock mass is presented as an assemblage of discrete blocks. The discontinuities are treated as boundary conditions between the blocks. The flow of the water occurs through the discontinuities and voids in the model. A fully coupled hydro-mechanical analysis implies that fracture conductivity is dependent on mechanical deformation of the joint aperture; conversely, joint water pressures affect the mechanical behavior [Itasca, 2005]. Discontinuum modeling of the hydro-mechanical behavior of the jointed rock mass requires mechanical and hydraulic properties of the discontinuities such as orientation and spacing of the discontinuities, joint normal and shear stiffness, joint apertures and residual aperture.

4.2 Description of the UDEC distinct element code

The Universal Distinct Elements Code (UDEC) of Itasca [2005] is a two-dimensional program based on the distinct element method for discontinuum analyses. It simulates the response of discontinuous media (such as a jointed rock mass) subjected to static or dynamic loading. UDEC is most suitable code for fulfilling the objectives of this thesis, based on the assumption that the behavior of the rock mass is primarily controlled by the major discontinuities in the foundation rock.

In the UDEC the discontinuities are treated as boundary conditions between blocks; large displacements along discontinuities and rotations of blocks are allowed. The relative motion of the discontinuities is also governed by linear or nonlinear force-displacement relations for movement in both the normal and shear directions. The model is the Coulomb slip criterion, which assigns elastic stiffness, frictional, cohesive and tensile strengths, and dilation characteristics to a joint. A modified version of this model includes displacement weakening as a result of loss in cohesive and tensile strength at the onset of shear failure.

In the normal direction, the stress-displacement relation is assumed to be linear and governed by the stiffness k_n such that

$$\Delta\sigma_n = -k_n \Delta u_n \quad (\text{Eq. 4.1})$$

where $\Delta\sigma_n$ – effective normal stress increment, Δu_n - the normal displacement increment. There is also a limiting tensile strength, T , for the joint. If the tensile strength is exceeded (i.e., if $\sigma_n < -T$), then $\sigma_n = 0$.

In shear, the response is controlled by a constant shear stiffness, k_s . The shear stress, τ_s , is limited by a combination of cohesive (C) and frictional (θ) strength. Thus, if

$$|\tau_s| \leq C + \sigma_n \tan \theta = \tau_{\max} \quad (\text{Eq. 4.2})$$

then

$$\Delta\tau_s = -k_s \Delta u_s^e \quad (\text{Eq. 4.3})$$

or else, if

$$|\tau_s| \geq \tau_{\max} \quad (\text{Eq. 4.4})$$

then

$$\tau_s = \text{sign}(\Delta u_s) \tau_{\max} \quad (\text{Eq. 4.5})$$

where Δu_s^e - the elastic component of the incremental shear displacement, Δu_s - the total incremental shear displacement.

UDEC has the capability to perform the analysis of fluid flow through the fractures of a system of impermeable blocks. A fully coupled mechanical-hydraulic analysis is performed in which fracture conductivity is dependent on mechanical deformation of the joint aperture; conversely, joint water pressures affect the mechanical behavior [Itasca, 2005]. Flow is modelled by means of the parallel plate model, and the flow rate per unit width therefore is expressed by the cubic law.

4.3 Concept and numerical approach

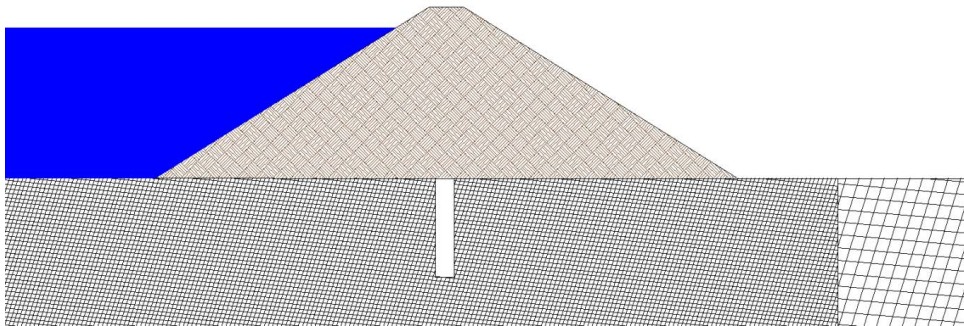
Construction of the embankment dam results in application of the external load on the foundation rock followed by the redistribution of the stresses within it. Following filling of the reservoir and cyclic loading caused by the variation of the water table results in increasing load on dam in downstream direction and foundation rock. An embankment dam is soft that generates a specific loading pattern, with higher stresses under the dam centre than at the upstream and downstream sides. Therefore in numerical simulation the embankment dam is represented by the solid impermeable block with linearly elastic and isotropic conditions (Paper I). The hydrostatic pressure is applied directly on the interface between the dam and foundation rock. In Paper III the dam body has been modified and adopted to the case study of the Håckren dam so it consists of two sections (outer shell and core) (Figure 4.1a). The intact block material within the dam body is simulated as linearly elastic, isotropic. Discontinuities are introduced into the both sections of the dam, however in the core they are set to be impermeable. Such approach allows more accurate transfer of the hydrostatic pressure of water on the interface between the dam and foundation on the upstream side.

Other critical area of the dam system is the interface between the dam and foundation. However the objectives of the thesis do not cover the monitoring and evaluation of the behavior of this interface. In Paper I this interface is simulated as an artificial discontinuity with high strength properties (friction angle, cohesion and tensile strength), which prevents dam to slide along it. In Paper III the hydraulic properties of the interface under the two sections of the dam are different (under the core is impermeable, under the outer shell is permeable) while the mechanical properties are the same.

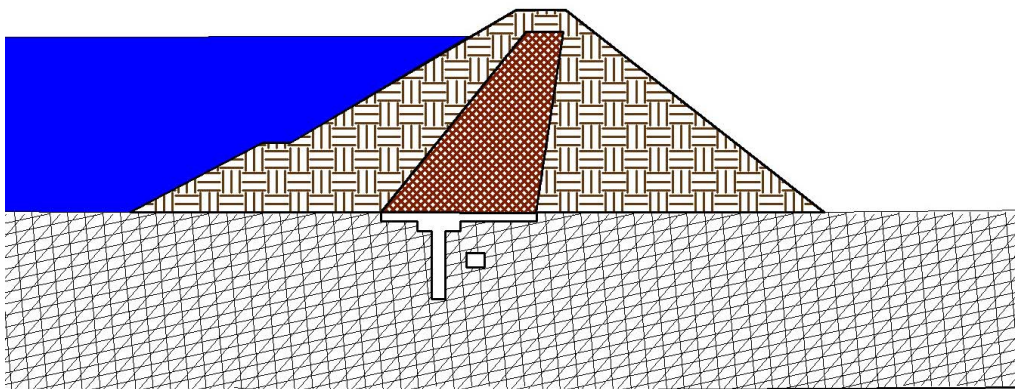
In numerical simulations it is usual that grout curtain is simulated as impermeable barrier with zero hydraulic conductivity (impermeable) [e.g. Barla *et al.*, 2004]. However the complete

sealing of the discontinuities by cement suspension is not possible [Idel, 1980] especially which have an aperture lower than 0.1 mm. In this thesis grout curtain is simulated as a permeable barrier, however the aperture of grouted discontinuities is set to residual values which is 0,05 mm.

The construction and exploitation of the dam disturbs not only the rock mass under the dam but also the adjacent rock mass such as floor and bank of the reservoir. The process of opening discontinuities on the upstream side under the reservoir may be a start point of development of seepage under the dam. To study the effect of cyclic loading of the water table on the discontinuities which are striking parallel to the river valley an additional cross-section B (cross-section A is perpendicular to the river valley) has been simulated. (Figure 4.1b)



a)



b)

Figure 4.1 Two different representations of embankment dam a) Conceptual model, Paper I
b) Håckren dam, Paper III

5. RESPONSE OF TYPICAL SWEDISH ROCK MASS TO THE CONSTRUCTION AND FIRST STAGES OF OPERATION OF A HYDROPOWER EMBANKMENT DAM (Paper I, Paper II)

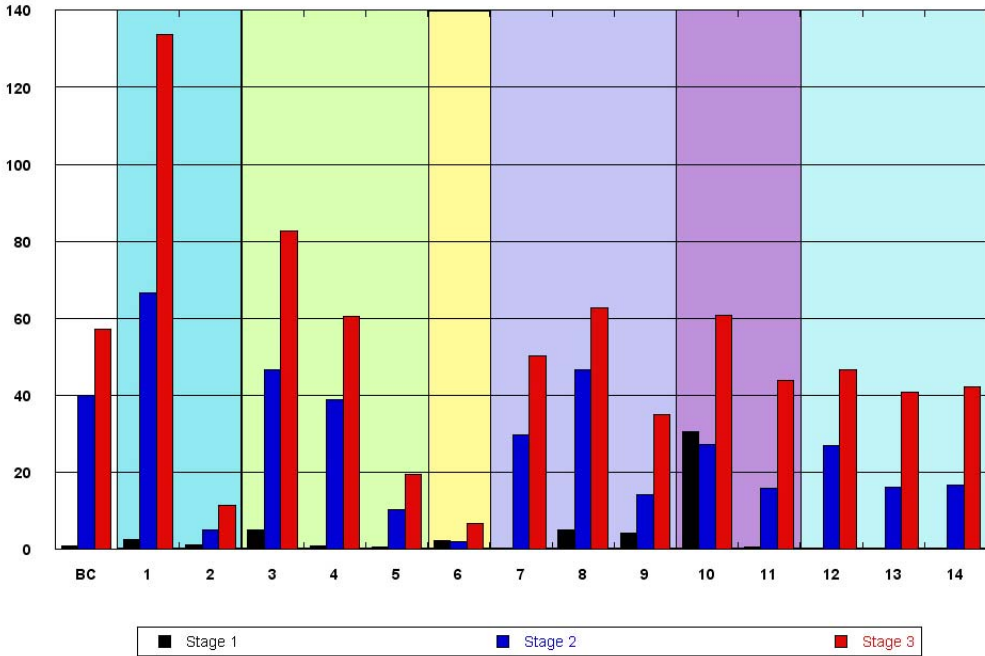
A properly functioning dam complex requires a stable foundation rock and a competent grout curtain. This implies that the rock mass should withstand loads from the dam and its reservoir over short- and long-time perspectives. Several factors influence stability of the foundation rock, including state of stress, rock mass strength, rock mass deformability, geological structures, and hydraulic properties of the rock mass. To evaluate different factors, sensitivity analyses have been performed for two cross-sections of the river valley; one cross-section is oriented along the river valley, and second one is perpendicular. The sensitivity analyses included variation of one parameter at the time in the base case (BC) model, which represents the typical rock mass in Sweden. During the sensitivity analyses the monitoring of location and magnitude of normal- and shear displacement in the foundation rock and the grout curtain during three important stages of the life time of the conceptual dam is performed: (1) Construction of the dam; (2) The first filling of its reservoir; and (3) One cyclic water load to mimic a seasonal variation of precipitation.

Results of sensitivity analyses show (Figure 5.1) that the construction of the dam (Stage 1) generally induces limited shear and normal displacements in the rock mass, with the exception for the model with highly fractured rock. The first filling of reservoir (Stage 2) results in further development of displacements for the model with highly fractured rock. At the same time, parameters such as high differential stress field and low joint friction angle also show significant displacements. All shear displacements occur at the downstream side of the dam, while normal displacements located close to the grout curtain at the interface between dam and foundation. Cyclic loading caused by variations of the water table in the reservoir (Stage 3) results in development of displacements in the rock mass. The models with high differential stress, low friction angle and small joint spacing show the most significant displacements. Resulted shear displacements occur downstream of the dam, in the same area as in Stage2. Significant normal displacement is observed only for case with high differential stress, and the location of it is in the vicinity of the grout curtain at the interface between the dam and the foundation rock. Sensitivity analyses shows that high differential stresses, friction angles and small joint spacing result in the most adverse effect on the stability of the rock mass in term shear and normal deformations.

Significant displacements are observed in the grout curtain and they are induced by the same models as for the rest of the rock mass in the foundation. However the scale of their displacements is significantly lower. This implies that the range of study parameters used in the sensitivity analyses does not have significant affect on the integrity of the grout curtain at the early stages of the life time of the dam.

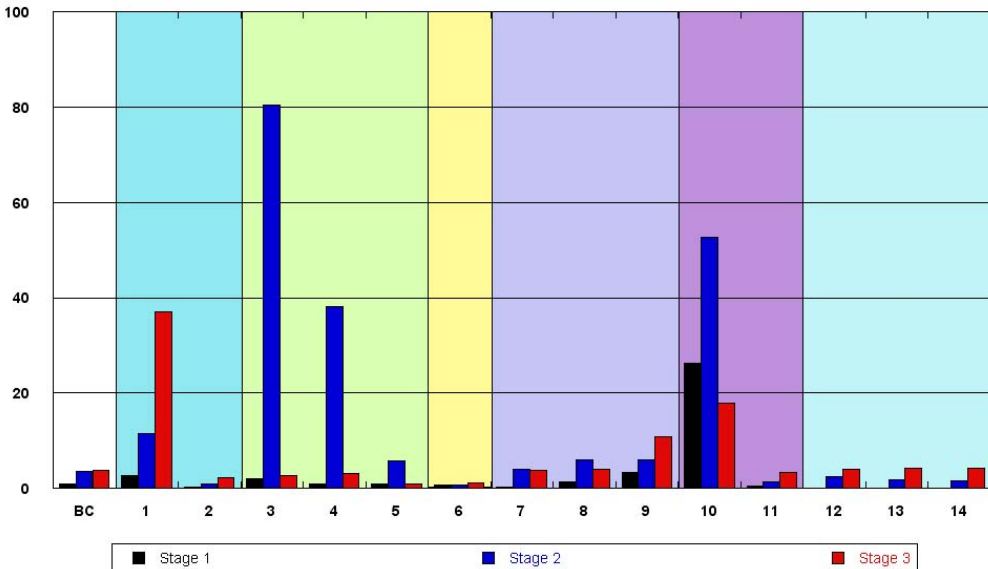
Sensitivity analyses of cross-section B identifies that most displacement occur at the banks during first filling (Stage 2) and variation of the water table (Stage 3). The same parameters which are significant for cross-section A are also important for cross-section B, in term of displacements.

Normalised Max Shear deformation CS A



a)

Normalised Max Normal displacement CS A



b)

Figure 5.1 Normalized values of maximum shear (a) and normal (b) displacements of Cross-section A against Stage 1 of BC model. Black color shows Stage 1 (construction of the dam), blue – Stage 2 (first filling of the reservoir), red – Stage 3 (cyclic variation of the water table in the reservoir)

6. VALIDATION OF CONCEPTUAL MODEL ON CASE STUDY – HÅCKREN DAM (Paper III)

In the conceptual numerical study it is identified that seasonal variations (also referred as cyclic variations) in load from the water in the storage basin may induce substantial shear- and normal deformation of the rock mass under certain conditions [Bondarchuk *et al.* 2011]. The three most important conditions were stress state, fracture frequency, and fracture friction angle. It appears that displacements along pre-existing discontinuities due to cyclic variations in load from the storage basin may be substantial enough to increase the fracture erosion. However, the results must be validated by running a model based on a real dam using the developed approach. The numerical model is populated with existing and new geological and rock mechanical data obtained by using robust and commonly used engineering geology field investigation methods for collecting data. It should be noted that we have aimed at keeping the new site investigation costs at a minimum with the intension to investigate if this approach for collecting new data is satisfactory, or if more cost-intense investigation methods are needed.

The Håckren embankment dam was selected as a case study because of the following characteristics: (1) It is a zoned embankment dam; (2) To the greatest extent, it is founded on rock; (3) It has a high regulation amplitude (26.9 m); and (4) For Swedish conditions, the amount of available data is unusual large (5) It has an inspection/drainage tunnel. The analysis of the condition of the rock mass at the Håckren dam site was carried out by UDEC. The analysis studied the deformations, flow and pore pressure distribution under the Håckren dam and in the reservoir in close vicinity.

The results show good agreement with available monitored data in terms of the pore pressure and water leakage (Figure 6.1) into the inspection tunnel. The available results suggests that we have developed a realistic proper numerical model by using a combination of simple and low-cost (~10 kEUR) field- and laboratory tests and pre-existing data. However, we recommend improving the core collection so that uniaxial strength tests can be performed, and the model incorporates site data on uniaxial compressive strength, Poisson's ratio, Young's Modulus, and friction angle. In addition, we also recommend including two contrasting stress fields into the sensitivity analyses in order to improve the understanding of the role of in situ stresses. With these limitations in mind, it remains apparent that we have developed reliable methodology for collecting data and evaluate of the condition of the rock mass under the dam and in the storage basin.

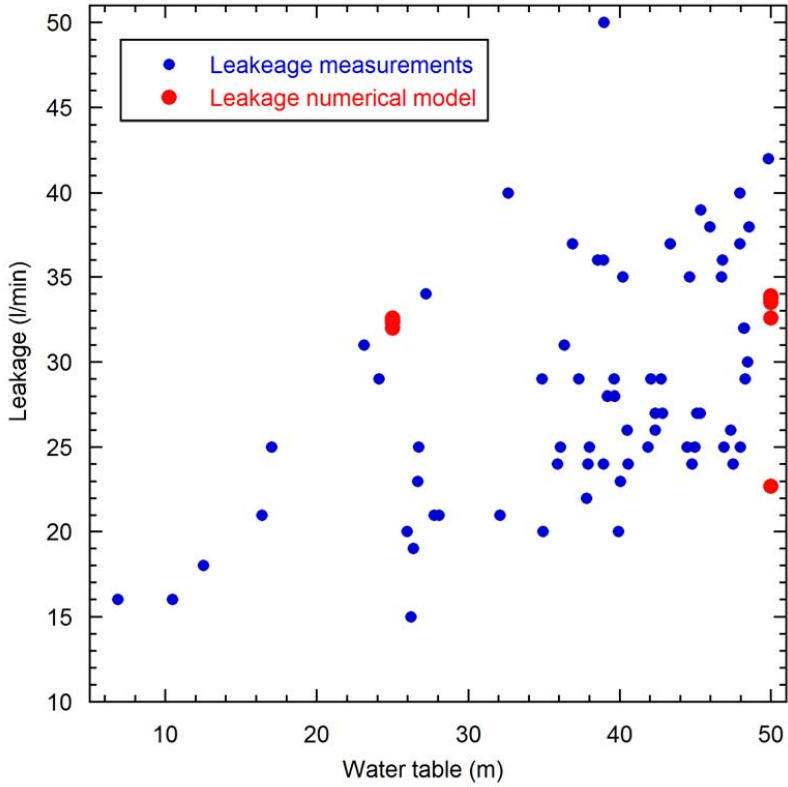


Figure 6.1 Leakage plotted against the depth of the water table in the inspection tunnel for real leakage measurements (blue filled circles) from 1966 to 1976, and numerical modeling data (red filled circles).

7. EVALUATION OF ROCK MASS RESPONSE IN LONG-TERM PERSPECTIVE WITH RESPECT TO DEFORMATION AND POSSIBLE EROSION (Paper IV)

On the field scale, where the rock mass contains fissures, fractures, bedding planes, contacts and zones of altered rock, most rock does not exhibit perfect elasticity. The extent of irrecoverability of strain due to load cycles may be as important as design [Goodman, 1980]. This process is very important for dam engineering because seasonal variation of the water in the reservoir apply cyclic loading on the foundation rock during exploitation. In long-term perspective this results in accumulation of deformation in the foundation rock of the dam.

The other critical factor in term of stability and functionality of dam is the flow of water in the fractured rock mass. Loads imposed by dam construction and exploitation causes relative displacements both in tangential and normal direction to the plane of discontinuity, therefore altering the hydraulic properties of pre-existing fractures [Pine and Batchelor, 1984]. These movements cause degradation of dilatancy and asperity which can modify the flow characteristics [Barton *et al.*, 1985, Bandis *et al.*, 1985]. Flow characteristics are also affected by alteration of morphology of the rock walls and the distribution of the void space [Hakami, 1988; Elsworth and Goodman, 1985; Billaux and Gentier, 1990]. Change of the distribution of the void space due to deformations lead to highly irregular preferential flow paths with widely varying velocities [Archambault *et al.*, 1997; Hakami, 1988]. Such big differences in velocities and very long exposure to the flow water (considering the lifetime of the dam) may result in the erosion process of the surfaces of the discontinuities and gouge material in it [Chen *et al.*, 2000; Momber, 2004], and gradual deterioration of the grout curtain.

To evaluate the foundation rock of the Håckren dam in term of deformations and possible evolvement of erosion a developed numerical model has been used. The monitoring of the rock mass, inflow into the inspection tunnel and velocity of the water flow around the tunnel has been carried outdone. Analyses are performed along ten idealized years for two cross-section A and B, oriented along and perpendicular to the river valley, respectively.

Numerical analyses of the Håckren dam foundation show that dam tends to slide along subhorizontal discontinuities on the downstream side after first filling of the reservoir. However the following cyclic loading caused by the variation of water in reservoir does not contribute to the development of this sliding, so the deformations do not progress (Figure 7.1). On other hand first filling and exploitation of the Håckrem dam along ten idealized years results in the shearing and opening of the discontinuities close to the surface on the upstream side (Figure 7.2). This effect is clearly observed in both cross-section A and B. The total inflow into the inspection tunnel is stabilized after the first year and keeps staying on the same level around 33-34 l/min, while the flow water velocity shows a slight rate increase which may raise a question about erosion in time. During analyses no preferable flow path for water flow along the discontinuities is observed. Analysis showed the stability of foundation rock of the Håckren dam in term of mechanical deformations and water flow into the inspection tunnel in evaluated period of time. However it should be kept in mind that water flow in rock mass may cause degradation of the strength properties of the rock mass in long-term perspective.

Max Shear Deformations in cross-section A

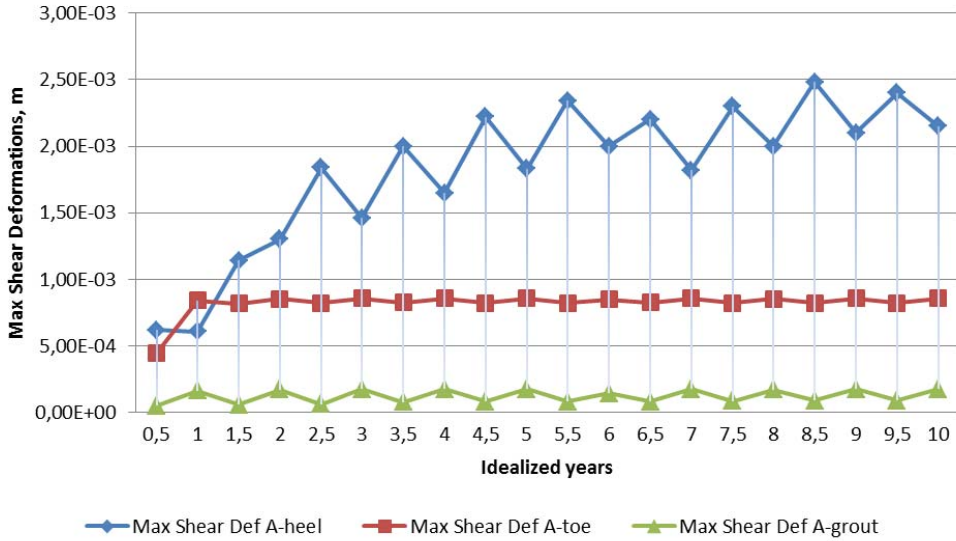


Figure 7.1 The variation of the max shear deformations within the foundation rock of cross-section A (A-heel, A-toe, A-grout)

Max Shear Deformations in cross-section B

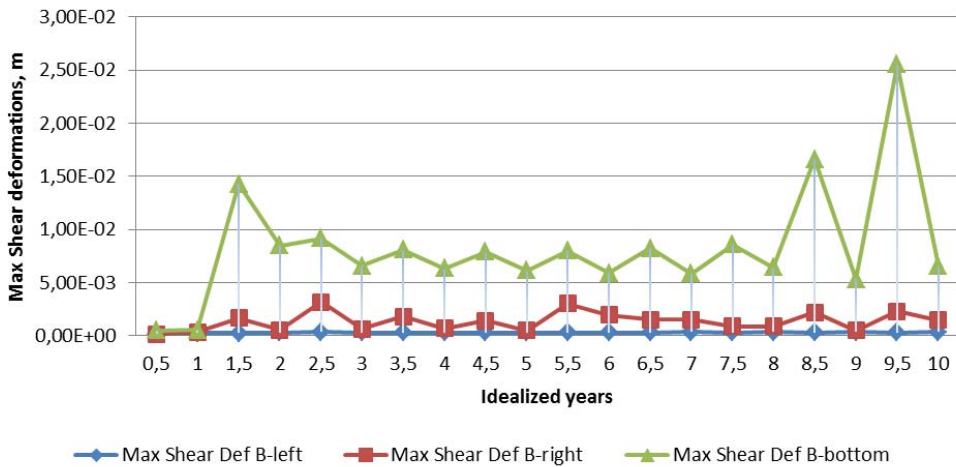


Figure 7.2 The variation of the max shear deformations within the foundation rock of cross-section B (A-left, B-right, B-toe)

8. CONCLUSIONS

In this thesis, the rock mass behavior after construction of an embankment dam, and its production, in terms of deformation and possible fracture erosion is at study. The initial analyses were made using the conceptual model developed by *Bondarchuk* [2008]. This model was subsequently modified and applied to the case study of the Håckren dam. The response of the rock mass under the Håckren dam has been investigated for a duration of ten idealized years.

The objective of this doctoral thesis has been to study the consequences on rock mass stability and fracture erosion induced by variations in loading conditions of a dam complex. The method in use is the coupled hydro-mechanical distinct-element method UDEC [*Itasca, 2005*]. The long-term developments of displacement along fractures, and distributions of pore pressure, leakage and flow velocity are studied in numerical models that are based on a real embankment dam in Sweden, the Håckren dam.

The conclusions regarding the rock mass response to static and cyclic loading based on the conceptual model are:

- Variations of the water table in the reservoir results in further deformation of the rock mass, either under the dam or in the reservoir. In general, deformations of all parameters included in the sensitivity analyses increase after one period of cyclic loading, though at different scale.
- The combined effect of high in-situ stresses and cyclic loading of water result in extensive shearing of discontinuities, followed by opening, with the change in shearing magnitude being more significant than that of normal opening.
- A small joint friction angles facilitates opening of discontinuities after the reservoir was filled with water the first time. The first period of cyclic loading of water has only resulted in small differences in shearing.
- Increase in frequency of subvertical discontinuities result in considerable opening of the discontinuities after the first impounding of the reservoir. The later variation of the water table have not resulted in further development, so this factor is critical for the first filling of the reservoir.
- Increased hydraulic aperture have not resulted in significant changes in shear and normal displacements in the rock mass, however significant influence on the conductivity of rock has been identified. In terms of amount of water passing through rock mass the increased hydraulic aperture is a critical parameter.

The conclusions regarding the validation of the developed conceptual model based on the case study of the Håckren dam are:

- The results show good agreement with available monitored data in terms of the pore pressure and water leakage into the inspection tunnel. The available results suggests that we have developed a realistic proper numerical model by using a combination of simple and low-cost (~10 kEUR) field- and laboratory tests and pre-existing data.
- With these limitations in mind, it remains apparent that we have developed reliable methodology for collecting data and evaluate of the condition of the rock mass under the dam and in the storage basin.

The conclusions regarding the application developed model for the evaluation of the rock mass response of the Håckren dam in long-term perspective are:

- Filling of the reservoir resulted in sliding of the dam in the downstream direction along subhorizontal discontinuities. However the following cyclic loadings caused by the variation of the water table in the reservoir do not contribute to the development of this sliding.
- First filling and exploitation of the Håckren dam results in the shearing and opening of the discontinuities close to the surface on the upstream side of the dam and in the reservoir floor.
- The total inflow into the inspection tunnel is stabilized after the first year and keeps staying on the same level. Possibly it is a result of low roughness of the discontinuities, which does not contribute to the dilation.
- Flow water velocity around the inspection tunnel shows a slight rate increase which may raise a question about erosion in long-term perspective.
- Analysis showed the stability of foundation rock of the Håckren dam in term of mechanical deformations and flow in evaluated period of time. However it should be kept in mind that water flow in rock mass may cause higher degradation of the strength properties of the rock mass in longer time perspective.

9. RECOMMENDATIONS

The development of this project gave ideas regarding what may improve this type of investigation.

First of all further investigation of different parameters of rock mass in simple 2D models e.g. presence of zones with different properties, and existence of faults should be implemented. A thorough investigation should be performed to identify how the weak zones as e.g. faults can be simulated properly with distinct element code, what parameters are required to describe their physical and hydraulic properties, how these parameters can be obtained using cost-efficient methods.

Another factor should be considered if more confident results are required from the analyses. The model should be a 3D with more complex joint pattern. Implementation of a 3D approach will help to consider the influence of the parameters, which is hard to consider in 2D approach. Application of more complex joint pattern will require better and thorough characterization of both fracture geometry and hydraulic properties. Additionally it will also require the application of the proper methodologies and the use of 3D joint generators, in order to realistically reproduce statistical description of the joint patterns. That way the numerical simulations can reflect the conditions of the rock mass with better accuracy.

A lot of analysis is carried out with implementation of the Mohr-Coulomb failure criteria. The reason behind that it is simple and therefore it is easier to obtain data for it. It is argued that application of more sophisticated models like Barton-Bandis or continuously yielding model would guarantee better results, but the question is how big advantage will be and what will be the price (laboratory and field tests) to obtain proper data for these models. Therefore it is recommended to perform a very thorough investigation and comparison of these different models based on the well studied case, where a lot of field, laboratory and research data are available.

A more thorough investigation is recommended to understand the best way to simulate the grout curtain. Should it be permeable or impermeable in distinct element method, what are the advantages and disadvantages of each approach.

During this research author found that there is a lack of information regarding the process of erosion within the rock mass under the dams. The reason for this might be that not that many failures are due to erosion process. However considering the expected lifetime of the dams and the level of danger they represent for the people and property it is recommended that a serious literature review, case study evaluations and establishment of the state of the art in this field should be done.

REFERENCES

- Archambault G, Gentier S, Riss J and Flamand R (1997) The evolution of void spaces (permeability) in relation with rock joint shear behavior *Int. J. Rock Mech. & Min. Sci.* 34, 3-4, paper No. 014
- Axheim, G. 2011. "Detta är SVC". Presentation at "SVC dagarna", meeting in Luleå, 4-5 May 2011. Available at <http://www.elforsk.se/SVC/Om-SVC/SVC-dagarna/SVC-dagarna-2011/> on 27 February 2012.
- Bandara, W.L.H.M.T., K.A.U.S. Imbulana (1996). Hydrological safety of dams, 2nd International Conference on Dam Safety Evaluation, Central Board of Irrigation and Power, India, pp. 171-183.
- Bandis S.C., Makurat A., Nik G (1985) Predicted and measured hydraulic conductivity of rock joints. *Proc. of the Int. Symp. on Fundamentals of Rock Joints* Björkliden, Norway
- Bandis S.C., Lumsden A.C., Barton N.R. (1983) Fundamentals of rock joint deformation *Int. J. Rock Mech. Min. Sci. & Geomech. Abstr.* 20, 6, pp. 249-268
- Barla, G., Bonini, M., Cammarata, G. (2004). Stress and seepage analyses for a gravity dam on a jointed granitic rock mass, Numerical modeling of Discrete Materials, pp. 263-268.
- Barton, N. (1973). Review of a new shear strength criterion for rock joints. *Engineering Geology*, 8, pp. 287-332.
- Barton, N. (1974). A review of the shear strength of filled discontinuities in rock, Norwegian Geotechnical Institute, 105, pp. 1-38.
- Barton, N. R., V. Choubey (1977). The shear strength of rock joints in theory and practice, *Rock Mech.* 10 (1-2), pp. 1-54.
- Barton N, Bandis S and Bakhtar K (1985) Strength Deformation and Conductivity of rock joints. *Int. J. Rock Mech. Min. Sci. & Geomech. Abstr.* 22, 3, pp. 121-140
- Billaux D and Gentier S (1990) Numerical and laboratory studies of flow in a fracture. *Proc. of the Int. Symp. on Rock Joints* Loen, Norway, Balkema ed. Rotterdam, The Netherlands, pp. 369-374
- Bondarchuk A (2008) Rock mass behavior under hydropower embankment dams. Results from numerical analyses, Licentiate Thesis, Luleå University of Technology ISSN:1402-1757
- Bondarchuk A., Ask M.V.S., Dahlström L-O., Nordlund E. (2011) Rock mass behavior under hydropower embankment dams: a two dimensional numerical study. *Rock Mechanics and Rock Engineering*, Springer, DOI 10.1007/s00603-011-0173-2
- Boulon MJ, Selvadurai APS, Benjelloun H and Feuga B (1993) Influence of rock joint degradation on hydraulic conductivity *Int. J. Rock Mech. Min. Sci. & Geomech. Abstr.*, 30, 7, pp. 1311-1317

- Cammarata G., Fidelibus C., Cravero M., Barla G. (2007) The hydro-mechanically coupled response of rock fractures. *Rock Mechanics and Rock Engineering*, 40, 1, pp. 41-61.
- Cheng, S-T. (1993) Statistics on dam failures, Reliability and Uncertainty Analyses in Hydraulic Design, pp. 97-105.
- Chen Z, Narayan SP, Yang Z and Rahman SS (2000) An experimental investigation of hydraulic behavior of fractures and joints in granitic rock *Int. J. Rock Mech. & Min. Sci.* 37, pp. 1061-1071
- Colback PSB and Wild BI (1965) Influence of moisture content on the compress strength of rock Proceedings of third Canadian rock mechanics symposium, University of Toronto, pp. 385-391
- Cook N.G.W (1992) Natural joints in rock: mechanical, hydraulic and seismic behavior and properties under normal stress. *Int. J. Rock Mech. Mining Sci. & Geomech. Abstr.* 29, 3, pp. 198-223.
- Duncan C.W. (1999). *Foundation on Rock*. Second Edition, E & FN Spon.
- Elsworth D and Goodman RE (1985) Hydro-mechanical characterization of rock fissures of idealized sawtooth or sinusoidal form *Proc. of the Int. Symp. on Fundamentals of Rock Joints* Björkliden, Norway
- Fell, R., MacGregor, P., Stapledon, D., and Bell, G. (2005). *Geotechnical engineering of dams*, Leiden A.A. Balkema.
- Foster M., Fell R., Spannagle M., (2000). The statistics of embankment dam failures and accidents. *Can. Geotech. J.* 37, pp. 1000-1024.
- Goldin A.L., Rasskazov L.N. (1992). *Design of Earth Dams*, Rotterdam : Balkema, 1992.
- Hakami. E. (1995). Aperture distribution of rock fractures, *Ph.D.*, Royal Institute of Technology, Stockholm, Sweden.
- Hakami E (1988) Water flow in single rock joints Licentiate thesis, Lulea University of Technology
- Hoek. E., J. W. Bray (1981). *Rock slope engineering*, London, Instn Min. & Metall.
- Hoek, E., P. K. Kaiser, W.F. Bawden (1997). *Support of underground excavations in hard rock*. Rotterdam: Balkema.
- Hoek. E., E. T. Brown (1997). Practical estimates of rock mass strength, *Int. Journal Rock Mechanics & Mining Science*, 34 (8), pp. 1165 - 1186.
- Hwang, N.H.C., R.J. Houghtalen (1996). *Fundamentals of hydraulic engineering systems*, 3rd edition, Prentice Hall, New Jersey.
- ICOLD (1974). *Lessons from Dam Incidents*.
- ICOLD (1983). *Deterioration of Dams and Reservoirs*.

- ICOLD (1995). Dam failures statistical analysis. Bulletin 99. Published by The International Commission on Large Dams.
- Idel, K. H. (1980). Seepage through jointed rock Sealing and drainage measures for earth-fill and masonry dams, Symposium on Problems and Practice of Dam Engineering, pp. 225 – 232.
- ISRM (1975). Suggested methods for determining shear strength: ISRM 9F, 1T ISRM Commission on Standard. Lab. Field Tests. Committee on Field Tests, Document, N1, FEB. 1974, 23P. International Journal of Rock Mechanics and Mining Science & Geomechanics Abstracts, 12(3): A3.5.
- ISRM (1978). Suggested methods for quantitative description of discontinuities in rock masses, *Int. J. Rock Mech. Mining Sci. & Geomechanics*, 15, pp. 319 – 368
- Itasca (2005). *UDEC* version 4.0. Manual. Minneapolis, ICG.
- Johansson S (2005) Seepage monitoring in embankment dams. Doctoral thesis, Royal Institute of Technology, Sweden ISBN 91-7170-792-1
- Johansson, F. (1997). Stability analyses of large structures founded on rock – an introductory study, Licentiate Thesis, Royal Institute of Technology, Stockholm, Sweden.
- Makurat A, Barton N, Rad NS, Bandis S (1990) Joint conductivity due to normal and shear deformation Rock Joints, Barton & Stephansson (eds.), Balkema, Rotterdam, pp. 535-540
- Vasconcelos Braga Farinha (2010) Hydro-mechanical behavior of concrete dam foundations. In-Situ tests and numerical modeling, Doctoral Thesis, Technical University of Lisbon
- Matsuoka H., L. Sihong, S. De'an, U. Nishikata (2001). Development of a new in-situ direct shear test. *ASTM geotechnical testing journal*, 24 (1), pp. 92-102.
- Momber AW (2004) Wear of rocks by water flow *Int. J. Rock Mech. Min. Sci.* 41, pp. 51-68
- McGrath, S. (2000). Study international practice and use of risk assessment in dam management, *Report*, Churchill Trust, Canberra, ACT, Australia.
- National Research Council (1983). Safety of Existing Dams, Evaluation and Improvement. National Academy Press.
- Patton, F. D. (1966). Multiple modes of shear failure in rock and related material, *Ph.D.* Thesis, University of Illinois.
- Pine R.J., Batchelor A.S. (1984) Downward migration of shearing in jointed rock during hydraulic injections, *Int. J. Rock Mech. Min. Sci. & Geomech. Abstr.* 21, 5, pp. 249-263
- Reinius (1988). Stresses and cracks in the rock foundation of an earthfill dam, *Water Power & Dam Construction*, 40, pp. 33-38.
- RIDAS (2002). Hydropower industry dam safety guidelines, Svensk Energi.

- RIDAS (2007). Gruvindustrins riktlinjer för dammsäkerhet, SweMin.
- Rutqvist J., Stephansson O. (2003) The role of hydro-mechanical coupling in fractured rock engineering. *Hydrogeology Journal*, 11, 1, pp. 7-40
- Rutqvist J. (1990) Modeling and field testing of coupled hydro-mechanical behavior of rock joints. Licentiate thesis, Lulea University of Technology.
- Samad, A.M., Bare, W.D., Taggart W.C., Pflaum J.M. (1987). Statistical analysis of embankment dam failures, *Hydraulic Engineering, Proceedings of the 1987 National Conference, Williamsburg, VA, USA*, pp. 582-587.
- Singh, B. (1995). *Engineering for embankment dams*, Rotterdam : Balkema.
- Swedenborg, S. (2001). Rock mechanical effects of cement grouting in hard rock. Doctoral thesis, Chalmers tekniska högskola. ISSN 0346-718X.
- Terzaghi, K. (1943). *Theoretical soil mechanics*, John Wiley & Sons, pp. 510.
- Thiel, K. (1989). *Rock Mechanics in hydroengineering*, Elsevier, Amsterdam.
- Varshney R.S. (1995). *Engineering for Embankment Dams*.
- Vasconcelos Braga Farinha, M.L.M.d (2010) Hydro-mechanical behavior of concrete dam foundations. In-Situ tests and numerical modeling, Doctoral Thesis, Technical University of Lisbon
- U.S, Army Corps of Engineers (2004). General design and construction considerations for earth and rock-fill dams, Engineering manual No. 1110-2-2300.
- Vattenfall (1988) *Vattenfalls handbok. Jord- och stenfyllningsdammar*. Happy Printing AB. Vattenfall, Sweden ISBN 91-7186-271-4
- Weaver, K. D, A.B. Bruce (2007). *Dam foundation grouting*. American Society of Civil Engineers (New York, N.Y.): 471pp.
- Wyllie, D. C., C. W. Mah (2004). *Rock Slope Engineering, Civil and Mining*, Spon Press, London & New York.

**ROCK MASS BEHAVIOR UNDER HYDROPOWER EMBANKMENT
DAMS: A TWO-DIMENSIONAL NUMERICAL STUDY**

Bondarchuk A, Ask M V S, Dahlström L-O and Nordlund E (2011).

Rock Mech. and Rock Eng., Springer

DOI 10.1007/s00603-011-0173-2

Rock Mass Behavior Under Hydropower Embankment Dams: A Two-Dimensional Numerical Study

A. Bondarchuk · M. V. S. Ask · L.-O. Dahlström · E. Nordlund

Received: 13 January 2011 / Accepted: 3 August 2011
© Springer-Verlag 2011

Abstract Sweden has more than 190 large hydropower dams, of which about 50 are pure embankment dams and over 100 are concrete/embankment dams. This paper presents results from conceptual analyses of the response of typical Swedish rock mass to the construction of a hydropower embankment dam and its first stages of operation. The aim is to identify locations and magnitudes of displacements that are occurring in the rock foundation and grout curtain after construction of the dam, the first filling of its water reservoir, and after one seasonal variation of the water table. Coupled hydro-mechanical analysis was conducted using the two-dimensional distinct element program UDEC. Series of the simulations have been performed and the results show that the first filling of the reservoir and variation of water table induce largest magnitudes of displacement, with the greatest values obtained from the two models with high differential horizontal stresses and smallest spacing of sub-vertical fractures. These results may help identifying the condition of the dam foundation and contribute to the development of proper maintenance measures, which guarantee the safety and functionality of the dam. Additionally, newly developed

dams may use these results for the estimation of the possible response of the rock foundation to the construction.

Keywords Homogeneous embankment dam · Numerical analysis · UDEC · Crystalline rock mass · Displacements

1 Introduction

The hydropower sector produces about 15% of the electricity worldwide. This source of electricity is flexible and instantaneous with little energy waste (Korsfelt et al. 2007). In Sweden, about 47% of the electricity in 2008 was produced by hydropower (Swedish Energy Agency 2009). This important source of electricity demands well-functioning hydropower dams. The stability of the dam body and its rock foundation (i.e. the underlying rock mass) is critical for both stable and high energy production and dam safety issues.

Many studies have addressed dam stability issues, with the majority focusing on the dam construction itself (Johansson 1997, 2005; Windelhed 2001), or on causes of failures and accidents (ICOLD 1974, 1983, 1995; Foster et al. 2000). A limited amount of studies have investigated the mechanical behavior of the rock foundation of hydropower dams, and the interaction between the dam construction and the rock foundation, using empirical (Reinius 1988) and numerical analyses (Barla et al. 2004; Dolezalova 2004; Bondarchuk 2008).

The majority of more than 190 large hydropower dams in Sweden were constructed between 1950 and 1980; hence, their age now ranges from 30 to 60 years old. A limited number of studies have proposed that problems in some dams may be caused by bedrock displacements and uneven foundation settlement (Bronner et al. 1988). In this study, a range of rock mass properties and their influence

A. Bondarchuk (✉) · M. V. S. Ask · L.-O. Dahlström · E. Nordlund
Mining and Geotechnical Engineering,
Luleå University of Technology,
971 87 Luleå, Sweden
e-mail: alexander.bondarchuk@ltu.se

L.-O. Dahlström
NCC Construction Sverige AB,
Gullberg Strandgata 2,
405 14 Gothenburg, Sweden

on the behavior of the foundation rock are investigated. Focus has been on the time interval from the construction of the dam through the early stages of energy production. The results contribute to the understanding of reasons behind existing problems.

Most, if not all hydropower dams in Sweden are founded on old Precambrian crystalline basement that was formed from 570 to 1,950 million years ago through igneous, sedimentary and metamorphic processes (Angelin et al. 1981). The general assumption of the Swedish hydropower dam owners is that the basement is stable. Therefore, it has not been investigated to what degree the load of the dam construction and the fluctuating water in reservoir influence the underlying foundation rock. The load from the dam construction may induce small-scale deformations along existing structures in the foundation rock, and the annual cyclic variation of water load may result in accumulation of irrecoverable deformations along these structures. The accumulation of subsequent small-scale deformation events may contribute to the erosion and settlement of the dam with time. At present, it is unclear what properties have the highest influence on the stability of the rock foundation under hydropower embankment dams in Sweden.

This paper presents results from numerical analyses of hydro-mechanical behavior of the foundation rock and the grout curtain under a conceptual hydropower embankment dam. Most deformation of the foundation rock is believed to occur along discontinuities (e.g. joints and faults; from now on referred to as joints). The simulations have been performed using the distinct element code UDEC that is suited to study potential modes of failure along discontinuous features. Analyses have been performed for two cross-sections of the river valley; one cross-section is oriented along the river valley, and second one is perpendicular. To simulate different condition of the rock mass under the dam, one parameter at the time was varied in the base case (BC) model, which represents the typical rock mass in Sweden. Achieved results are compared with a basic model and literature data.

The main objective of this study is to investigate how static load from the conceptual hydropower dam and cyclic load from the water reservoir affect the stability of the foundation rock and the grout curtain of the dam. This is achieved by determining location and magnitude of normal- and shear displacement in the foundation rock and the grout curtain during three important stages of the life time of the conceptual dam: (1) Construction of the dam, (2) The first filling of its reservoir, and (3) One cyclic water load to mimic a seasonal variation of precipitation. The subsequent variation of rock mass properties during the three stages are thought to reveal critical rock mass properties that lead to potential instability of the dam foundation and/or the grout curtain.

2 Methodology

2.1 Conceptual Analyses

A properly functioning dam complex requires a stable foundation rock and a competent grout curtain. This implies that the rock mass should withstand loads from the dam and its reservoir over short- and long-time perspectives. Several factors influence stability of the foundation rock, including state of stress, rock mass strength, rock mass deformability, geological structures, and hydraulic properties of the rock mass.

The primary, or in situ, stress field is the cumulative product of events in the geological history of a rock mass, e.g. gravitational (including topographic effects), tectonic, residual, and terrestrial stresses (Amadei and Stephansson 1997). Geological structures may result in redistribution of the stress field and possible stress relaxation in large blocks and zones. Residual, or locked-in stresses in a rock mass may create stress anomalies. The stress field at shallow depths is influenced by terrestrial stresses, e.g. stresses from temperature variations, moon pull, and Coriolis force (Amadei and Stephansson 1997). The construction of a dam and the filling of its reservoir disturb the stress state in the foundation rock. The stresses may increase in some areas of the foundation rock, but existing geological structures may also lead to stress relaxation in other areas of the foundation rock. To study effects from the stress state, three different stress fields have been applied in the base case (BC) model, Model 1 and Model 2 (Table 1).

Swedish rock mass generally consists of crystalline rock of good quality and high strength. The rock mass may be defined as intact rock blocks that are intersected by joints. The size of these blocks range from a few millimeters to several meters (Hoek et al. 1997). Because of the high strength of crystalline intact rock and the shallow depths of investigation, plastic deformation is not likely to occur within an intact rock block. On the contrary, all plastic deformation within the rock mass is believed to occur by displacing rock blocks along joints. The strength of joints is governed by friction angle, cohesion, dilation angle, and tensile strength (Duncan 1999). Cohesion usually is produced by the infilling material of joints, but all joints in the model are unfilled. The tensile strength of all joints is insignificant. The strength is only influenced by the friction and dilation angle of the joints. In addition to the BC Model, the role of the friction angle is investigated in Models 3–5, and that of the dilation angle is investigated in Model 6 (Table 1). Because the dilation angle influences the aperture of the joint, it also affects the hydraulic conductivity (Goodman 1980; Hoek et al. 1997). The hydraulic aperture is normally used to estimate volume of water flow through the rock mass; however, here we use hydraulic

Table 1 Model parameters and values for sensitivity analyses for cross-sections A and B

Model no.	Param.	σ_H (MPa)	σ_h (MPa)	σ_v (MPa)	φ_r (°)	φ_i (°)	ψ_B (°)	ψ_S (°)	x_{B0} (m)	x_{S0} (m)	α (mm)
BC	Base case	$\sigma_H(1)$	$\sigma_h(1)$	σ_v	35	9	-5	85	3	5	0.25
1	Stresses	$\sigma_H(2)$	$\sigma_h(2)$	σ_v	35	9	-5	85	3	5	0.25
2		$\sigma_H(3)$	$\sigma_h(3)$	σ_v	35	9	-5	85	3	5	0.25
3		Friction angle	$\sigma_H(1)$	$\sigma_h(1)$	σ_v	25	9	-5	85	3	5
4	$\sigma_H(1)$		$\sigma_h(1)$	σ_v	30	9	-5	85	3	5	0.25
5	Dilation angle	$\sigma_H(1)$	$\sigma_h(1)$	σ_v	40	9	-5	85	3	5	0.25
6		$\sigma_H(1)$	$\sigma_h(1)$	σ_v	35	0	-5	85	3	5	0.25
7	Dip of Joints	$\sigma_H(1)$	$\sigma_h(1)$	σ_v	35	9	-5	70	3	5	0.25
8		$\sigma_H(1)$	$\sigma_h(1)$	σ_v	35	9	-5	100	3	5	0.25
9		$\sigma_H(1)$	$\sigma_h(1)$	σ_v	35	9	-10	85	3	5	0.25
10	Spacing sub-vertical joints	$\sigma_H(1)$	$\sigma_h(1)$	σ_v	35	9	-5	85	3	1	0.25
11		$\sigma_H(1)$	$\sigma_h(1)$	σ_v	35	9	-5	85	3	9	0.25
12*	Aperture	$\sigma_H(1)$	$\sigma_h(1)$	σ_v	35	9	-5	85	3	5	0.50
13*		$\sigma_H(1)$	$\sigma_h(1)$	σ_v	35	9	-5	85	3	5	1.00
14*		$\sigma_H(1)$	$\sigma_h(1)$	σ_v	35	9	-5	85	3	5	2.50

Italics show what parameter has been analyzed

σ_H maximum horizontal stress [$\sigma_H(1) = 2.8 + 0.0399z$, $\sigma_H(2) = 6.7 + 0.0444z$, $\sigma_H(3) = 0.085z$], σ_h minimum horizontal stress [$\sigma_h(1) = 2.2 + 0.0240z$, $\sigma_h(2) = 0.8 + 0.0329z$, $\sigma_h(3) = 0.022z$], σ_v vertical stress ($\sigma_v = \rho gz$), φ_r joint friction angle, φ_i joint dilation angle, ψ_B dip of banking joints, ψ_S dip of subvertical joints, x_{B0} normal distance of banking joints, x_{S0} normal distance of subvertical joints, α hydraulic aperture, * models included only in cross-section A. Note that σ_H is oriented parallel to the river valley and σ_h is oriented out of plane in cross-section A, whereas σ_H is oriented out of plane and σ_h is oriented perpendicular to river valley in cross-section B

aperture for direct calculation of mechanical response in the model. The role of aperture is investigated in Models 12–14 (Table 1).

As argued by Amadei and Stephansson (1997) and others, geological structures plays a central role in stress distribution. To study the effects of joints, we have defined two joint sets in the rock mass, with subvertical and subhorizontal orientation. The subhorizontal joints are from now on referred to as sheeting joints. It is assumed that their most important characteristics are the dip angle and the joint spacing. Smaller joint spacing (e.g. crushed rock) reduces the overall strength of the rock mass (Hoek and Bray 1981). The roles of dip and spacing of joints are investigated in Models 7–9 and Models 10–11, respectively (Table 1).

2.2 Numerical Analyses

Although the problem is 3D in nature, the problem is analyzed in two dimensions (2D) using the Universal Distinct Elements Code (UDEC) of Itasca (2005). Most 3D aspects are covered by the 2D approach by performing the analyses along two cross-sections, A and B. Figure 1 shows the orientation of the two cross-sections, together with the model dimensions. Because the size of the reservoir exceeds that of the dam construction, the analyzed areas for cross-section A and cross-section B differs (cf.

red square in Fig. 1). For cross-section A, the area is 200×200 m, while it is 440×440 m for cross-section B. The size of the domains are chosen based on Dolezalova (2004), Barla et al. (2004), Mark Christianson (Itasca, pers. com. 2007), and from trial-and-error to minimize the boundary effects.

In cross-section A, the embankment dam is located in the central part of the free surface (ground surface) to allow observation of the behavior of the rock mass on the upstream and downstream sides of the dam. The grout curtain is situated directly under the dam and is represented by a 26×8 m sized rectangle (Fig. 1a). The dimension of dam and grout curtain as well the location of grout curtain is similar to several Swedish hydropower dams and fulfills construction recommendations (Fell et al. 2005; Vattenfall 1988). In cross-section B (Fig. 1b), the river valley is located in the central part to allow observations of the behavior of the rock mass in floor and banks of the reservoir. The set-up of cross-section B is similar to that of cross-section A, with two exceptions: (1) The area of investigation is expanded to mimic natural conditions where the reservoir is wider than the dam construction, and (2) The stress field is modified so the major horizontal stress is the out-of-plane stress and the minor horizontal stress is directed parallel to cross-section B.

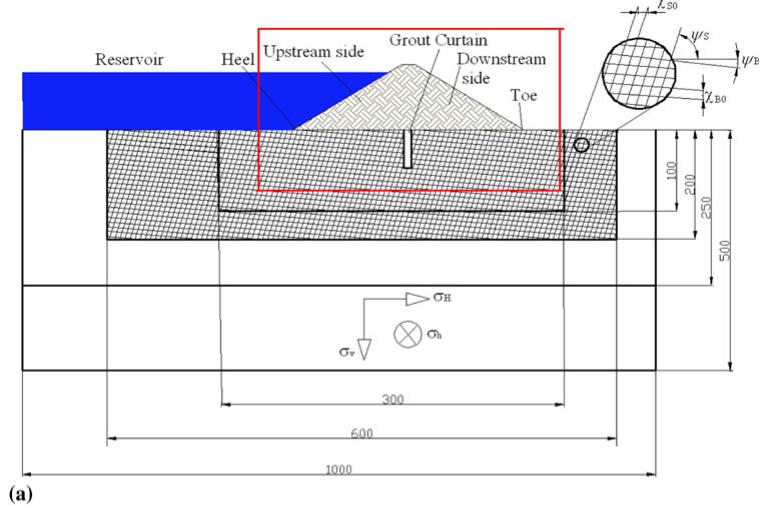
The rock mass has been discretized into deformable triangular finite-different zones (deformable material). To

Fig. 1 Overview of the UDEC models used in this study.

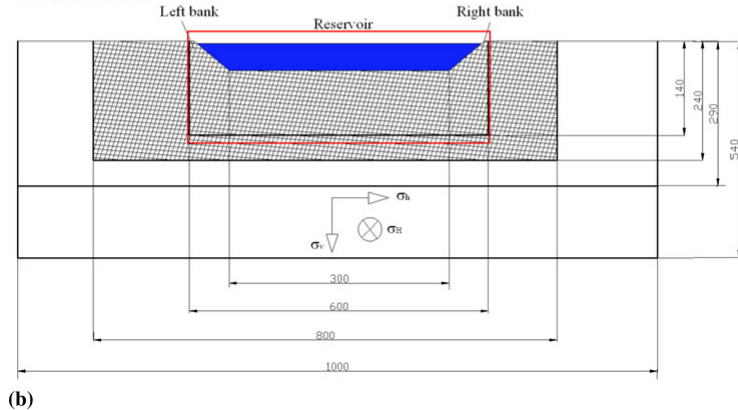
a Cross-section A is located parallel to the river axis. The toe of the dam is located to the left, on the upstream side towards the water reservoir. The heel of the dam is located to the right, on the downstream side. The foundation rock is subdivided in four zones with different element sizes: the element sizes of the first (depth 0–100 m, width 300 m), second (depth 100–200 m, width 600 m), third (depth 200–250 m, width 1,000 m), and fourth (depth 250–500 m, width 1,000 m) areas have element sizes of 2, 4, 6, and 18 m, respectively.

b Cross-section B is located perpendicular to the river valley on the upstream side of the dam, in vicinity of the dam. The foundation rock is divided in four zones with different sizes of elements: the element sizes of the first (depth 0–140 m, width 300 m), second (depth 140–240 m, width 600 m), third (depth 240–290 m, width 800 m), and fourth (depth 290–540 m, width 1,000 m) areas have element sizes of 2, 4, 6, and 18 m, respectively. The *red squares* show the plot area of Figs. 4, 5, 6. Geometrical parameters of the model are also shown in the figure (Table 1). Note that the dimensions in the cross-sections are not to scale. The permeability of the lateral and basal boundaries is zero in the model

Cross-Section A



Cross-Section B



achieve good resolution in the areas of interest while keeping the calculation time within reasonable limits, the models have been divided into four areas with different zone sizes—2, 4, 6, and 18 m (Fig. 1). The analyses use an elastic-perfectly plastic constitutive model for the blocks, and the Mohr–Coulomb failure criterion for the joints. The joint characteristics of the rock mass (Table 2) have been applied only into the first two areas with zone size of 2 and 4 m. All joints in the model are unfilled, and they have been assigned zero cohesion, except those in the grout curtain. These joints are assumed to be filled with grout, and they have been assigned a constant cohesion of 0.6 MPa (Table 2). The tensile strength of all joints is

approximated to be zero. The above implies that neither cohesion nor tensile strength is influencing the strength of joints in the model. All joints are permeable at the beginning of testing, with a hydraulic aperture value (Tables 1, 2). The minimum hydraulic aperture corresponds to a residual value, which is two times lower than the initial hydraulic value in all models. The maximum hydraulic aperture is ten times that of the residual value up to a maximum value of 6 mm.

The dam body is simulated as a solid impermeable block (Tables 3, 4) with linearly elastic and isotropic conditions that is thought to mimic a homogeneous embankment dam. Realistic values of the material for the dam body were

Table 2 Properties of discontinuities in rock mass and grout curtain, BC model

Name	Rock mass	Grout curtain
Joint normal stiffness (GPa/m)	10	12
Joint shear stiffness (GPa/m)	10	12
Aperture for zero normal stress (m)	0.25×10^{-3}	0.12×10^{-3}
Residual aperture (m)	0.125×10^{-3}	0.06×10^{-3}
Joint cohesion (MPa)	0	0.6
Joint residual cohesion (MPa)	0	0
Joint friction angle (°)	35	35
Joint residual friction angle (°)	30	25
Joint dilation angle (°)	9	9
Joint permeability constant (1/Pa s)	300	300
Joint tensile strength (MPa)	0	0
Joint residual tensile strength (MPa)	0	0
Distance between joints (m)	2 and 3	2 and 3

Table 3 Properties of intact blocks in rock mass and material in dam body

Parameter	Rock blocks	Material in dam
Density, ρ (kg/m ³)	2,700	2,100
Young's modulus, E (GPa)	61	6
Poisson's ratio, ν (-)	0.25	0.4
Friction angle, θ (°)	69	-
Cohesion, c (MPa)	5.142	-
Tensile strength, T (MPa)	1.21	-

Table 4 Dimension of the dam

Parameter	Value
Height (m)	40
Width of the crown (m)	8
Inclination of the walls, ratio	1:1.6
Freeboard (m)	5
Max level of water in reservoir (m)	35

obtained through verification models (see Sect. 2.3). The interface between the dam and the foundation rock has the same properties as the unfilled discontinuities within the rock mass (c.f. Assumption 3 of Table 5). Hydrostatic pressure corresponding to the level of water in the reservoir is applied on the interface between the dam and the rock foundation to simulate the pressure of the weight of the water within the dam body.

A total number of 34 input parameters are used to describe the rock mass properties (Tables 2, 3), stress field (Table 1), dam (Tables 3, 4) and grout curtain (Table 2). The values are chosen to represent typical Swedish rock mass conditions, and determined using the generalized Hoek and Brown failure criteria coupled with the rock mass characterization system GSI (Hoek et al. 2002;

Rocscience 2007) and existing literature (Swedenborg 2001; Mören 2005). The horizontal stress field is derived from Scandinavian stress data (Stephansson 1993; Sjöberg et al. 2005; Stephansson et al. 1987), whereas the vertical stress is assumed to be gravitational. The BC model and Models 3–14 use the same stress field, which was obtained from hydraulic fracturing data (Stephansson 1993), whereas those of Models 1 and 2 were obtained by over-coring stress data (Stephansson 1993; Sjöberg et al. 2005, respectively).

The influence of water is addressed by applying a fully coupled hydro-mechanical analysis, in which fracture conductivity is dependent on mechanical deformation, and joint water pressure affects the mechanical computations (Itasca 2005). Pore fluid pressure is assumed to be hydrostatic, and the ground water level coincides with the ground surface.

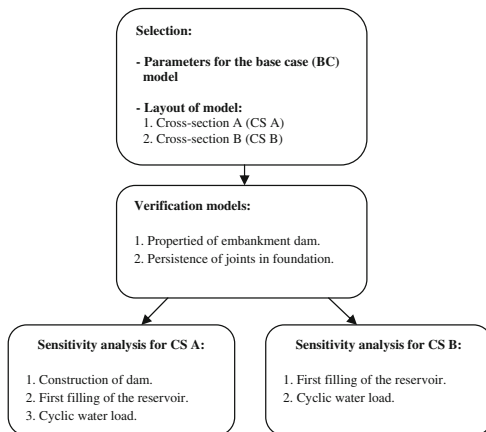
2.3 Calculation Sequence

Table 5 summarizes the limitations and assumptions of the numerical analyses. These analyses were made in three steps (Fig. 2). The first step comprised the selection of layout and parameters for the BC models for cross-sections A and B (Fig. 1; Tables 2, 3, 4). The BC model represents typical conditions for embankment dam and its foundation rock in Sweden. The second step consisted of execution of two verification models. The third step is composed of sensitivity analyses, in which the influence of individual parameters on rock mass behavior is evaluated during three stages of the life time of the dam (Stage 1, Construction of the dam; Stage 2, First water filling of the reservoir; and Stage 3, One cycle of variation in water load).

Two verification models were executed during the second step (Fig. 2). The first verification model was conducted to determine which length of joints gave the most

Table 5 Limitations and assumptions

No.
Limitations
1. Potential failure mechanisms within the dam itself are not considered
2. The model does not separate between zoned and homogeneous embankment dams
3. The models are limited to static and cyclic loading conditions from the dam and the water in the reservoir (no dynamic loading, caused by earthquakes or abrupt changes of the water level in the reservoir is considered)
4. The study is limited to Swedish conditions
Assumptions
1. The state of in situ stress is assumed to be unaffected by the construction sequence of the dam, e.g. by diverting the river from the former valley
2. Zoned and homogeneous embankment dams are assumed to produce identical loads on the underlying rock mass
3. The interface between the dam and the foundation rock is assumed to have identical properties to those of the rock discontinuities in the model
4. The grout curtain is assumed to be permeable
5. Dam damage is assumed to occur by break-down of the grout curtain, which is assumed to take place if the hydraulic aperture reaches a maximum value, and/or if large normal- and/or shear displacements occur close to the foundation
6. The presence of water in the dam body is assumed to generate hydraulic pressure on the dam foundation interface
7. The movement of water in the rock mass is assumed not to erode the rock mass, hence, the mechanical properties are constant in time
8. Total flow is calculated from the amount of water moving from the rock mass downstream side of the dam into free space by implementing a FISH function

**Fig. 2** Adopted model for analyses

realistic results. The response of joint sets that transected the entire rock mass in the model ($500 \times 1,000$ m and $540 \times 1,000$ m in cross-sections A and B, respectively; Fig. 1) was compared with those that only transected the upper part of the dam complex (200×600 m and 240×800 m in cross-sections A and B, respectively). Most reliable results were obtained for the second joint set, whereas joints transecting the entire rock mass revealed zones with extensive shear and normal displacements close to the lateral artificial boundaries of the model. Figure 1

shows that the chosen layout of joints is restricted to the inner two zones of the model. The second verification model was made to obtain realistic loading values of the dam body. An embankment dam is soft and generates a specific load pattern, with higher stresses under the dam center than at the upstream and downstream sides. Therefore, different physical properties of dam material (density, Young's modulus, and Poisson's ratio), and two approaches to simulate dam behavior (soft and rigid blocks) were evaluated. The use of the values in Table 3 resulted in the desired load pattern.

During the sensitivity analysis in step three, the rock mass response due to subsequent variation of rock mass properties is studied along cross-section A and B. Because the rock adjacent to the dam (on upstream side) is assumed not to be influenced by the construction of the dam, Stage 1 was only simulated along cross-section A. In total, 12 models were analyzed during this stage. The subsequent stages, 2 and 3 (first filling of the reservoir and one cyclic variation of the water load, respectively) are assumed to affect the rock foundation along both cross-sections. In total, 15 models were analyzed during these stages. The influence of the hydraulic aperture is only tested in Models 12–14 for Stages 2 and 3 (Table 1) along cross-section A, because the hydraulic aperture is assumed to reflect breakdown of the grout curtain (cf. Assumption 5 of Table 5). Consequently, these models are not included in the sensitivity analyses for Stage 1 along cross-section A, or in any of analyses along cross-section B. Each simulation in the sensitivity analysis followed the same calculation sequence. The first phase in the calculation sequence

predates the construction of the dam and its reservoir. The model is run to equilibrium in a “pre-excavation” state during which in situ stresses, load and boundary conditions are applied. The second phase includes the construction of the dam and the excavation of the reservoir along cross-sections A and B, respectively. The dam is constructed in two steps to prevent possible dynamic load on the foundation rock. The reservoir is excavated in several steps to prevent heaving caused by the ground water and stresses. The second phase corresponds to Stage 1 of the life time of the dam, and is only performed for cross-section A. The first filling of the reservoir (Stage 2) is immediately succeeding construction the dam (Stage 1). The water level is raised gradually to 35 m in two steps to prevent dynamic load on the rock surface. The first seasonal variation of the water level in the reservoir (Stage 3) is simulated through similar gradual changes in water table. First, the water table is reduced to a depth of 10 m, and then returned to a depth of 35 m. Steady state flow logic (Itasca 2005) is applied during these simulations to reflect water movements in the rock mass. Note that the reported displacements represent accumulative (total) values of displacements occurring along joints. Hence, they have not reset between different stages. For cross-section A, displacements recordings started in Stage 1 (construction of the dam). For cross-

section B, they started in Stage 2 (the first filling of the reservoir).

3 Results

Table 6 show the magnitude of maximum normal and shear displacements obtained during the sensitivity analysis. The results reveal that the displacements are concentrated to four areas along cross-section A and three areas along cross-section B. In the upper 27 m along cross-section A, normal- and shear displacements occur in three zones, A-heel, A-grout curtain, and A-toe (Fig. 3a). A fourth zone with displacements along cross-section A, A-deep is from 27 to 50 m depth. For cross-section B, concentrated displacements are occurring in the left and right banks (B-left and B-right, respectively), and near the reservoir floor (B-floor) (Fig. 3b). Figures 4, 5, 6 shows the location of maximum normal- and shear displacements in some simulations.

3.1 Constructing the Dam (Stage 1)

A total of 12 models have been run in Stage 1 to analyze the effect of the weight of the dam construction on the rock

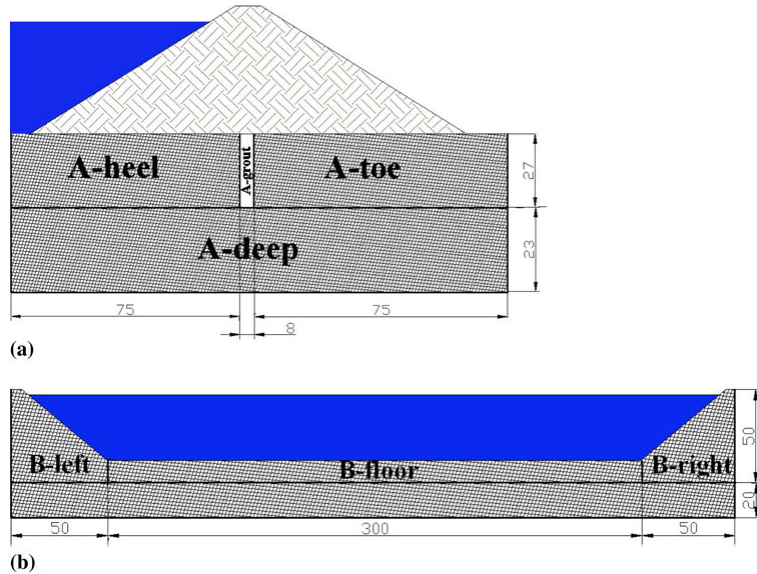
Table 6 Maximum values of shear and normal deformations in rock mass and grout curtain

Model no.	Param.	Rock mass deformation										Grout curtain deformation					
		Shear (mm)						Normal (mm)				Shear (mm)			Normal (mm)		
		A		B		A		B		A	B		A	B			
CS	Stage	1	2	3	2	3	1	2	3	2	3	1	2	3	1	2	3
BC	Base case	0.05	1.80	2.57	2.00	1.40	0.03	0.10	0.10	0.30	0.20	0	0.02	0.07	0	0.03	0.06
1	Stresses	0.12	3.00	6.01	0.90	0.96	0.07	0.31	1.00	0.20	0.20	0	0.30	0.97	0	0.04	0.04
2		0.06	0.23	0.51	1.00	4.00	0.01	0.03	0.06	0.90	0.10		0.01	0.02		0.03	0.03
3	Friction angle	0.23	2.10	3.72	1.00	3.13	0.05	2.17	0.07	0.20	0.20	0	2.14	2.80	0	0.03	0.04
4		0.04	1.75	2.72	2.00	1.96	0.03	1.03	0.09	0.30	0.30	0	0.09	2.55	0	0.06	0.04
5	Dilation angle	0.03	0.46	0.87	2.00	1.29	0.02	0.16	0.03	0.80	0.30	0	0.01	0.38	0	0.04	0.04
6		0.10	0.09	0.30	1.00	2.00	0.02	0.02	0.03	0.20	0.30	0	0.01	0.02	0	0.02	0.02
7	Dip of joints	0.02	1.34	2.26	0.76	0.95	0.01	0.11	0.10	0.10	0.30	0	0.02	0.04	0	0.05	0.03
8		0.22	2.10	2.82	1.00	2.34	0.04	0.16	0.11	0.20	0.60	0	0.03	0.07	0	0.03	0.04
9	Spacing sub-vertical joints	0.19	0.64	1.58	0.39	1.15	0.09	0.16	0.29	0.20	0.20	0	0.18	0.40	0	0.04	0.04
10		1.37	1.23	2.73	2.00	4.73	0.71	1.42	0.49	0.90	2.00	0.02	0.03	0.09	0.01	0.06	0.08
11	Aperture	0.03	0.71	1.97	1.42	1.43	0.01	0.04	0.09	0.20	0.20	0	0.01	0.04	0	0.04	0.03
12		-	1.21	2.10	-	-	-	0.07	0.11	-	-	-	0.02	0.07	-	0.04	0.06
13	-	0.73	1.84	-	-	-	0.05	0.12	-	-	-	0.02	0.06	-	0.04	0.07	
14	-	0.75	1.90	-	-	-	0.04	0.12	-	-	-	0.02	0.06	-	0.03	0.07	

Parameter column shows what value had been changed during sensitivity analyses. Stage 1 for cross-section B had not been simulated. Analyze of influence of Aperture (Models 12–14) had been done only for Stages 2 and 3 for cross-section A

BC base case, the numerical model with the most typical values for Swedish conditions, CS cross-section

Fig. 3 Areas of interest in foundation rock. **a** Areas of interest in Cross-section A are denoted as A-heel, A-grout, A-toe, and A-deep. **b** Areas of interest in Cross-section B are denoted as B-left, B-right, and B-floor



mass in cross-section A. No sensitivity analyses were made for cross-section B of this stage.

The BC model, simulating typical Swedish conditions reveals small shear- and normal displacements that are concentrated to the upper 5 m of zone A-heel, close to the interface between dam and foundation (Table 6; Fig. 4a, b). As expected, the shear displacements are concentrated to the subvertical joints whereas the normal displacement occurs along sheeting joints. The maximum shear- and normal displacement of 1.37 and 0.70 mm, respectively, are occurring within the upper 10 m of zone A-heel (Fig. 5a, b), along subvertical joints. These maximum displacements are obtained for Model 10, which has the smallest spacing (1 m) of subvertical joints (Table 1). The remaining simulations reveal smaller shear- and normal displacements than 0.23 and 0.09 mm, respectively (Table 6).

Significantly lower values of maximum shear- and normal displacement are recorded in the grout curtain (Table 6). The highest values of shear- and normal displacement (0.02 and 0.01 mm, respectively) in the grout curtain are comparable with the lowest recorded values in the rock mass. These high values are generated for by Model 10, with 1 m subvertical joint spacing.

3.2 First Filling of the Reservoir (Stage 2)

This Stage 2, simulate when the water level in the reservoir is raised to 35 m for the first time. The influence of this

additional load is analyzed in 15 models along cross-section A, and in 12 models along cross-section B (Tables 1, 6). In general, evident increases in both maximum shear- and normal displacements are observed. Note that the reported values of maximum displacements correspond to the accumulated displacements from Stages 1 and 2 in that location.

There is an evident increase from Stage 1 to Stage 2 in maximum shear displacement (1.80 mm) in the BC model (Table 6). This displacement occurs in the upper 5 m of zone A-toe near the dam-rock foundation interface (Fig. 4c). There is a more modest increase in maximum normal displacements (0.10 mm). However, these displacements are more widespread, and occur along sheeting joints down to ~ 20 m depth in A-grout curtain, A-heel, and (partially) A-toe zones (Fig. 4d). Maximum value of shear displacement (3.00 mm) is obtained for Model 1 with high differential stresses (Tables 1, 6). These displacements are concentrated to shallow sheeting joints in zone A-toe (Fig. 5c). Relatively high values of maximum shear displacements (1.75–2.10 mm) are obtained in three additional models (Table 6). These models had reversed dip of subvertical joints (Model 8) and reduced joint friction angle values (Models 3, 4). Most of the displacements in these models are restricted to the upper part of A-toe zone. The reduced joint friction values also result in highest and third highest values of maximum normal displacement (2.17 and 1.03 mm, respectively; Tables 1, 6). Second highest value of normal displacement (1.42 mm) is

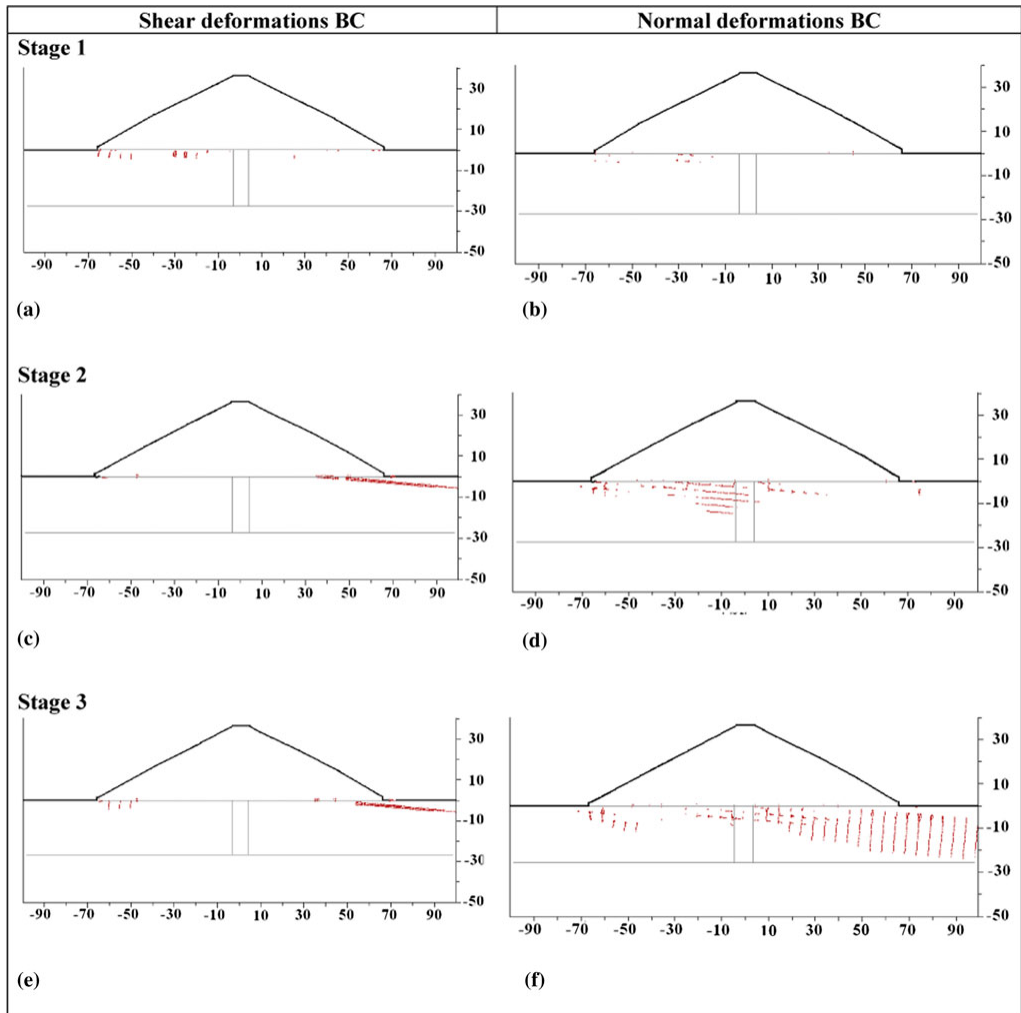


Fig. 4 Maximum shear and normal displacements along Cross-sections A for BC model, Stages 1–3. *Red dots* display the location of the displacements in the model. Axes are scaled in meters and show the depth and width of the evaluated area. **a** Max shear deformation at

Stage 1, **b** max normal deformation at Stage 1, **c** max shear deformation at Stage 2, **d** max normal deformation at Stage 2, **e** max shear deformation at Stage 3, **f** max normal deformation at Stage 3

obtained for Model 10 with small joint spacing. These recorded displacements all occur within distinct zones in the upper 2 m of the foundation rock, near the dam-foundation rock interface, mainly in the A-toe and A-heel zones (Fig. 5d).

The maximum shear displacement in the grout curtain is of the same order of magnitude as the top three highest displacements in the rock mass. A shear displacement of 2.14 mm is obtained for Model 3 with reduced joint

friction angle (Tables 1, 6). On the other hand, no anomalous values of normal displacements are observed. All values range from 0.02 to 0.06 mm, i.e., comparable to the lower values obtained in the rock mass.

Four models reach maximum shear displacements of 2.00 mm along cross-section B, namely the BC model, Models 4 and 5 with joint friction angles of 30° and 40°, respectively, and Model 10 with a joint spacing of 1 m (Tables 1, 6). In Model 10 displacements occur in the

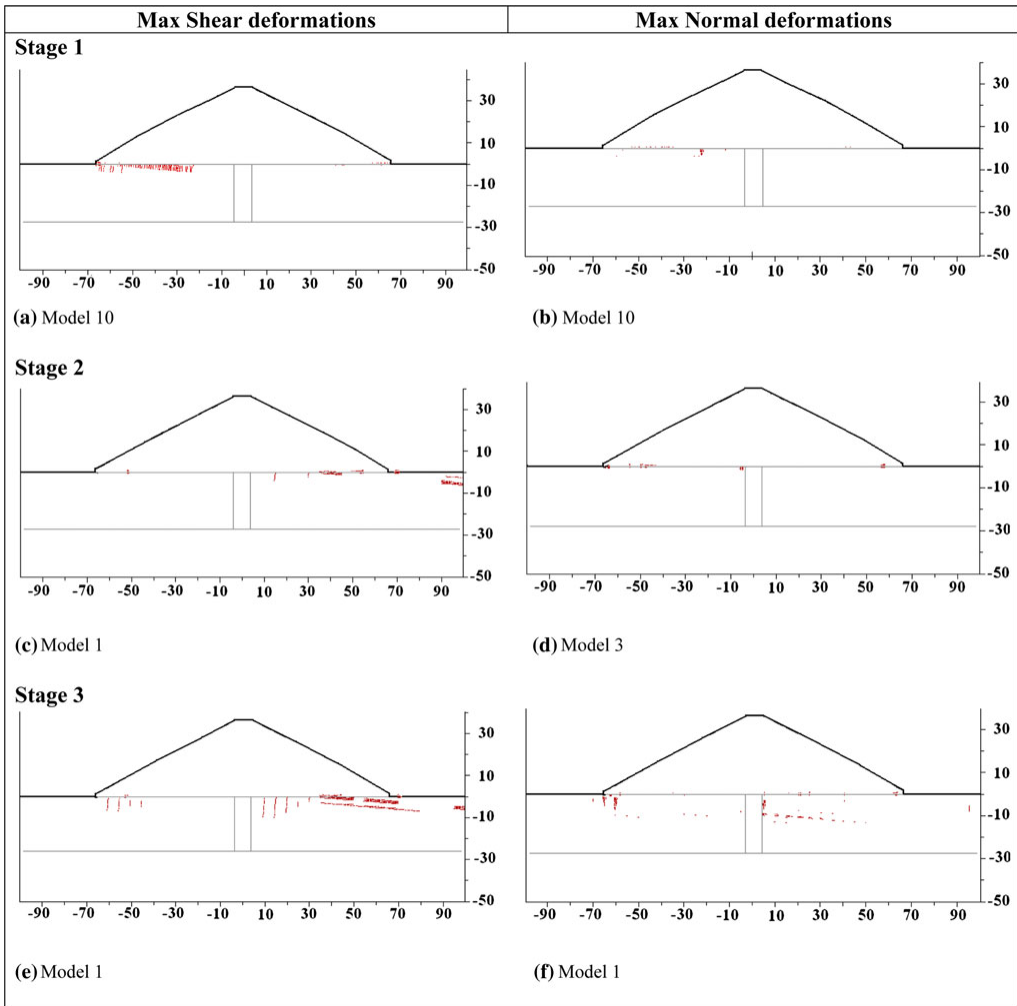


Fig. 5 Highest maximum shear and normal displacements, observed in the models along cross-sections A, Stages 1-3. *Red dots* display the location of the displacements in the model. Axes are scaled in meters and show the depth and width of the evaluated area. Number of model is specified for each case. **a** Max shear deformation at Stage 1, Model

10, **b** max normal deformation at Stage 1, Model 10, **c** max shear deformation at Stage 2, Model 1, **d** max normal deformation at Stage 2, Model 3, **e** max shear deformation at Stage 3, Model 1, **f** max normal deformation at Stage 3, Model 1

B-left zone (Fig. 6a), whereas shear displacements are concentrated to the B-floor zone in the BC Model and Model 5. In Model 4, shear displacements are observed near the intersection of the B-floor and B-right zones. Table 6 shows that elevated values of maximum normal displacements (0.80–0.90 mm) are observed in Model 2 with gravitational stresses, Model 5 with high joint friction angle, and Model 10 with 1 m spacing of subvertical joints

(Tables 1, 6). Figure 6b shows that displacements in Model 2 are concentrated to the B-floor zone, next to the right bank of the reservoir. In Models 10 and 5, they mainly occur in the B-left bank zone. Extensive shear- and normal displacements have been observed in many models close to the intersection between the B-floor zone with the B-left bank and the B-right bank zones. These displacements are attributed to be a corner effect in the model because of

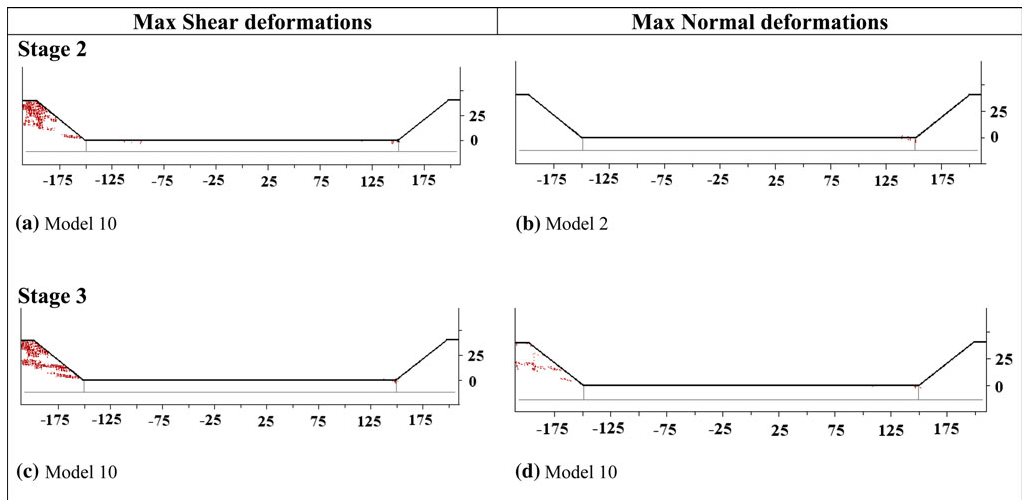


Fig. 6 Highest maximum shear and normal displacements, observed in the models along cross-sections B, Stages 2–3. *Red dots* display the location of the displacements in the model. Axes are scaled in meters and show the depth and width of the evaluated area. Number of model

is specified for each case. **a** Max shear deformation at Stage 2, Model 10, **b** max normal deformation at Stage 2, Model 2, **c** max shear deformation at Stage 3, Model 10, **d** max normal deformation at Stage 3, Model 10

stress concentration, and especially apparent in the B-right bank, where extensive displacement of sheeting joint occurs. This corner effect obscures to some extent the interpretation of the results along cross-section B. In two cases, there is a small decrease in shear displacements from Stages 1 to 2 (cf. Models 6, 10 in Table 6; Fig. 7a). This signals that directions of shear displacement are opposing those of Stage 1 in Stage 2 in these two models.

3.3 One Seasonal Variation in Water Level (Stage 3)

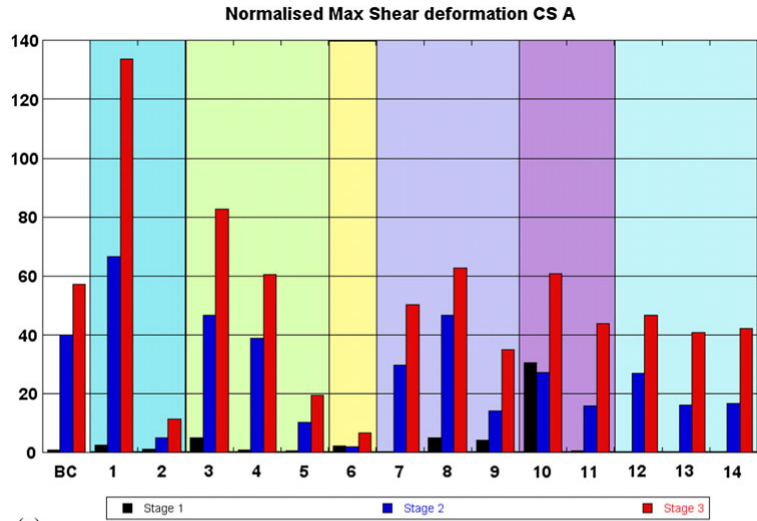
The analyzes of displacements during one seasonal variation in the water level of Stage 3 is obtained by first reducing the water level to 10 m, and then increase it to 35 m. The magnitudes and locations of displacements in the foundation rock and grout curtain are analyzed in 15 models along cross-section A, and 12 models along cross-section B (Tables 1, 6). The reported values correspond to the accumulated displacements from Stages 1 to 3 in that location. The variation in water level generally induces additional increases in maximum shear- and normal displacements in the rock mass and grout curtain (Table 6).

The maximum shear displacements in the BC model increases by more than 40% from Stage 2 to Stage 3. The maximum shear displacement is 2.57 mm in Stage 3, and is occurring in the A-toe zone of the dam (Fig. 4e). In contrast, there is no change in normal displacement in the BC model. It remains 0.10 mm during Stages 2 and 3 (Table 6). However, the area influenced by normal

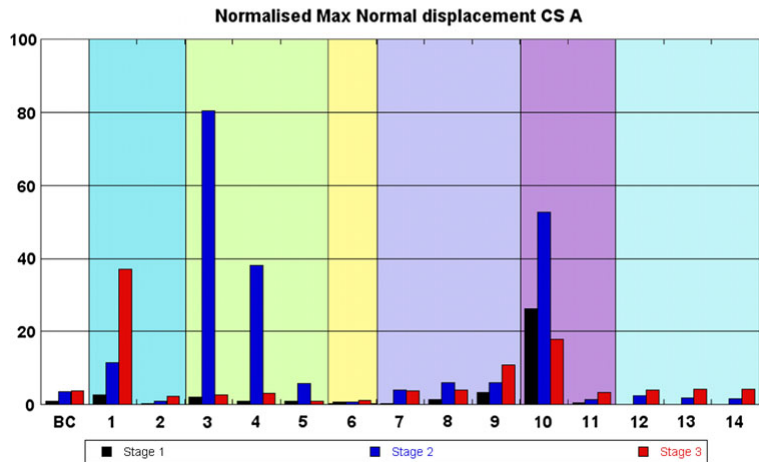
displacement increased in Stage 3 involves the upper part of zones A-heel and A-grout curtain, and the entire A-toe zone (Fig. 4f). Often, models that generate high values of maximum shear displacements during Stage 2 also reveal high values during Stage 3 along cross-section A.

Maximum shear displacement (6.01 mm) is induced in Model 1 with high differential stresses (Tables 1, 6). Figure 5e shows that deformations occur along subvertical- and sheeting joints in the A-toe zone, and mainly along subvertical- and sheeting joints in the A-heel zone. The reduced friction angle of Model 3 result in 3.72 mm of maximum shear displacement and displacement distributed along the entire length of the dam along subvertical- and sheeting joints in A-heel zone and mainly along sheeting joints in zones A-grout curtain and A-toe. Maximum shear displacement values from 2.57 to 2.82 mm are obtained for the BC Model and Models 4, 8, and 10 (Tables 1, 6). In all these models, shear displacements occur along sheeting joints in the A-toe zone to a maximum depth of ~ 10 m. In addition, most models reveal displacements in the A-heel zone (excluding Model 8), and shear displacements occurs in the A-grout curtain zone of Model 4. The magnitudes of maximum normal displacements generally are in the order of one magnitude lower than those of maximum shear displacements, and often the rate of increase is smaller in Stage 3 than in Stage 2 (Table 6; Fig. 7b). In fact, there are several models (e.g. Models 3, 4, 5, 7, 8 and 10, Table 6) that reveal a decrease in normal displacement from Stage 2 to Stage 3. This indicates a closure of joints due to

Fig. 7 Normalized values of maximum shear (a) and normal (b) displacements of Cross-section A against Stage 1 of BC model. *Black color* shows Stage 1, *blue* Stage 2, *red* Stage 3



(a)



(b)

variation of the water table in the reservoir. The highest value of maximum normal displacement (1.00 mm) is obtained for Model 1 with high differential stresses (Tables 1, 6). Displacements occur along subvertical joints in the A-toe and A-grout curtain zones, and along short segments down to over 10 m depth along sheeting joints under the entire length of the dam (Fig. 5f).

The magnitudes of maximum shear displacements in the grout curtain are lower than the two highest values in the rock mass, but comparable to the third highest values in the rock mass (Table 6). Models 3 and 4 with reduced joint

friction angles result in the highest magnitudes of shear displacement (2.55–2.80 mm). Relatively high shear displacements also were obtained by Model 1 with high differential stresses. Little variation in values of maximum normal displacements is observed. All values range from 0.02 to 0.08 mm, with the highest values obtained in Model 10 with 1 m joint subvertical spacing, and Models 13 and 14 with increased hydraulic aperture (Tables 1, 6).

Three models reveal increased values of maximum shear displacement along cross-section B (Table 6): (1) Model 10 with 1 m subvertical joint spacing has a value of

4.73 mm, and the displacements are focused to the B-left zone (Fig. 6c); (2) Model 2 with gravitational stresses has a value of 4.00 mm, and the displacements occur along subvertical joints to ~ 40 m depth near the intersections of the B-floor with the B-left and B-right zones; and (3) Model 3 with reduced joint friction angle has a value of 3.13 mm, and the displacements are mainly restricted to the B-left and B-right zones. Values of maximum normal displacement vary from 0.10 to 0.30 mm, with two exceptions (Table 6). First, Model 10 with 1 m subvertical joint spacing reaches a maximum of 2.00 mm normal displacement that is occurring in the B-left zone (Fig. 6d). Second, Model 8 with reversed dip of subvertical joints has a maximum normal displacement value of 0.60 mm (Tables 1, 6). The displacement is occurring near the base of the B-right zone.

4 Discussion

To estimate the scale of influence of different parameters on the response of the rock mass, the maximum shear and normal displacements have been normalized against the values obtained for BC model at Stage 1. Figure 7a, b show results for cross-section A.

Based on the results from this study, the construction of the dam in Stage 1 only induce little disturbances in the rock mass and the grout curtain. On the other hand, the first filling of the water reservoir in Stage 2 coincides with dramatic increases in displacements at relatively shallow depths in the rock mass and the grout curtain under the dam body and its reservoir. Additional displacements are occurring after the first seasonal variation of water level in the reservoir in Stage 3.

In this section, we will first discuss the effect of the most critical parameters for the rock mass revealed by this study, in situ stress state, joint friction, joint dip and joint spacing. We will then discuss implications for the grout curtain. Finally, the wider implications of this study will be discussed, i.e., how these findings may contribute to development of proper maintenance and monitoring measures for hydro-power dams.

4.1 Critical Rock Mass Parameters

4.1.1 In situ Stress State

It is difficult to select realistic state of in situ stress for shallow depths because the stresses at these depths are small, easily disturbed and discontinuous (Amadei and Stephansson 1997). Most stress measurements are made below 50 m and shallow depth stress estimations are most often obtained by extrapolation from deeper measurements (Töyrä 2006).

Some shallow stress measurements have been made using the overcoring method (Berg 2005). Like many other stress measurement methods, this method is associated with measurement related errors. Leijon (1989) showed that the overcoring method is associated with a random measuring error in the average normal stress corresponding to a standard deviation of ± 2 MPa, and that this error is most important at shallow depths where stresses are small. Ask (2003) investigated measurement-related uncertainties for two overcoring cells that commonly have been used in Sweden, and he found that temperature-related errors during overcoring reduces horizontal stresses by up to 3 MPa. Hence, both these authors identify errors that are in the same order of magnitude as the average stress at shallow depths.

We selected three different stress fields that have been reported in the literature in Scandinavia. The chosen stress fields represents an average case (the BC model), and two extreme cases (Models 1, 2) so that a maximum difference in magnitude is obtained at shallow depths (Table 1). The BC model has the best guess of an average stress state. The stress field in Model 1 mimics a tectonic stress field with high differential stresses near surface. The stress field in Model 2 represents a gravitational stress field with small differential stresses near surface. The three stress fields have different stress gradients; the consequence is that the internal relationship in magnitudes between the three stress fields varies with depth. Since our evaluation focus on displacements occurring at depths less than 50 m we expect small influence from gradients on final results.

Our results show that the state of stress has little importance on the rock mass response during the construction of the dam (Stage 1; Table 6). However, the situation under the A-toe zone is changed abruptly when the reservoir is filled at the first time (Stage 2) and under the A-heel and A-toe zones after one seasonal variation of water level (Stage 3) if the stress state is one with high differential stresses (Model 1) (Table 6; Fig. 5c, e). The size of normal displacements is smaller than the maximum shear displacements. During Stage 2, they occur in A-heel zone, adjacent to the grout curtain. We will discuss the implications for grout curtain of these displacements in Sect. 4.2. The seasonal variation of water level in reservoir in Stage 3 results in further development of shear- and normal displacements in foundation rock (Table 6), with most noticeable values are again observed for the high differential stresses. Such an increase of displacements for the model with high in situ stress field is a result of increased load on the downstream side of the dam (Reinius 1988), which results in increasing of shear stresses. The high differential stresses are greater than the shear resistance of joints. The available results strongly suggest that the occurrence of high differential stresses induce extensive shear displacements in the rock mass. Because the stress field in Scandinavia even at shallow depths is

characterized by high differential stresses, (e.g. Amadei and Stephansson 1997), it is important to have a good understanding of the stress field for the dam owner.

4.1.2 Joint Friction

Our results show that some values of joint friction- and dilation angles result in higher shear- and normal displacements in the rock mass compare to BC model, but others seem to have little influence on these displacements (Fig. 7a, b). In general, higher displacements are obtained for small joint friction angles in cross-section A (Table 6).

Only one simulation was made to test the influence of the joint dilation angle. The results show that largest shear displacements were induced for the higher joint dilation angle during Stages 2 and 3. Such abnormal behavior may be explained how the UDEC treat dilation angle. It does not affect the shear strength directly, instead the dilation angle is included in the effective friction angle for the joint where it can be added or subtracted from friction angle depending on the direction of shearing (Itasca 2005). The exception is cross-section B during Stage 3, where the lowest shear displacement is obtained for the high joint dilation angle (Table 6).

The magnitudes of joint friction- and dilation angles seem to have a smaller influence on normal displacements in the rock mass along cross-sections A and B (Fig. 7b; Table 6). The outstanding exception from this trend is observed in cross-section A during Stage 2, where decreasing joint friction angles result in dramatically increasing normal displacements.

The shear displacements in cross-section A are occurring in the rock mass in A-toe area, on the downstream side of the dam. These observations supports those of Reinius (1988), who proposed that impounding of reservoir causes a change of the location and inclination of the resultant force, and consequently a change of vertical and horizontal tension stresses below the downstream part of the dam. Observed shear displacement is considered to be a combination of increased shear stresses (Reinius 1988) and low friction angle. The increase of the frictional angle of joints results in reduction of magnitude of shearing. At the same time horizontal tension stresses causes substantial normal displacements in the foundation rock, close to the grouting.

4.1.3 Structures and Hydraulic Aperture: Joint Dip, Joint Spacing

The 1-m joint spacing model shows the highest magnitudes of shear and normal displacement in cross-section A (Fig. 7a, b; Table 6) after construction of the dam (Stage 1). These results are in agreement with Hoek and Bray (1981), who stated that a fractures rock mass has lower

strength than a non-fractured rock. Normal displacements are located close to the grout curtain, in A-grout curtain area, in the area where the dam has the highest load on the foundation rock. The first filling of reservoir results in further opening of joints in highly fractured rock (Table 6). However, the fluctuation of the water table in the reservoir during Stage 3 result in a reduction of the magnitude of normal displacements. Evaluation other structural parameters such as dip of subhorizontal- and subvertical joints, and hydraulic aperture show that only small normal and shear displacements are occurring during all stages.

In cross-section B, highly fractured rock results in extensive development of shear and normal displacement in B-left area at Stage 2. Probably first filling of the reservoir causes a reduction in effective normal stress by build-up of pore pressure. Maximum normal displacement from Stage 3 reveals the same pattern as after Stage 2.

4.2 Degradation of the Grout Curtain

Because the grout curtain cannot easily be accessed after the construction of the dam, all grout curtain operations are normally completed before the dam body is constructed on the foundation rock (Water Resources Commission of NSW 1980). This approach is not ideal, because the additional weight of the dam body on the grout curtain may lead to the development of displacements of grouted joints. Results from Stage 1 show that the range of parameters investigated here generally have little influence on normal- and shear displacement of joints in the grout curtain. This small effect is also observed during first impounding of the reservoir in Stage 2 and after the first seasonal variation in water level in Stage 3. However, the joints with reduced friction angle have higher chance to start the degradation process of integrity of the grout curtain because of increased shear displacements, as it is observed in Model 3 during Stage 2 and Models 3, 4 during Stage 3 (Table 6).

In addition, this study shows that certain models, such as the model with high differential stresses (Model 1), low friction angle (Models 3–4) and small joint spacing (Model 10) results in shearing and opening of joints close to the grout curtain. In time, these displacements may develop further and intersect grout curtain. Hence, these conditions may affect the integrity of grout curtain, so it becomes dissolved and eroded by percolating leakage water with time (Reinius 1988).

4.3 Wider Implication

4.3.1 Long-Term Monitoring Program

Evaluation of rock mass behavior at shallow depths using numerical analyses is superior to analytical methods in

several aspects. A major advantage is that a large number of parameters simultaneously can be analyzed with numerical methods, and then results can be compared with analytical ones. The outcome of numerical analyses depends on the amount, accuracy and quality of the input data and, to some degree, how the model has been calibrated (Itasca 2005).

In this study, we have focused on the first stages of the life time of an embankment dam. It is demonstrated that low displacements in the rock mass are induced under low friction angle of joints, high differential stresses and high density of joints. These displacements may not have so negative influence at the early stages of the life time of the dam, but the long term consequences of seasonal variations in water level may be degradation of the stability of the foundation rock. For risk evaluation, it is essential to collect data from critical areas of the foundation rock of the dam. Different geological conditions and properties of rock may influence the location of these critical areas. This approach may provide important information on potential instability areas and therefore provide guidance in the design of monitoring programs for a dam.

4.3.2 Application of Results to Other Types of Embankment Dams

This study uses a homogeneous embankment dam in analyses for simplicity. The results show that shear- and normal displacements occur in the foundation rock near the grout curtain, see above. However, most of embankment dams in Sweden are zoned with central core (Angelin et al. 1981). Zoned embankment dams are more sensitive to foundation displacements than homogeneous ones; therefore, they require a stable foundation rock. The foundation rock of the upstream and downstream side of zoned dam (outer shells, the area outside the core) should be resistant against sliding and major settlements, whereas minor foundation settlements may be tolerated without any damage to the construction of the dam (Singh 1995). The contact area between the impermeable core and the foundation rock is the most critical in terms of integrity of the core (Singh 1995). Reinius (1988) analyzed analytically process of construction and first filling of reservoir of embankment dam on foundation rock. He stated that construction develops tension stresses in rock and if tensional stresses result in opening (normal displacement) in the order of 1 mm close to the core, this displacement may lead in material transport from the core to the rock foundation. Singh (1995) supported Reinius's statement. Our study suggest that the first filling of reservoir in Stage 2 causes development of tension stresses in foundation rock, which result in normal displacements of joints (Table 6). To guarantee the integrity of that contact area, the

foundation rock should consist of hard rock with few joints and fault plains (Goldin and Rasskazov 1992; Singh 1995).

Homogeneous and zoned embankment dams with vertical core are similar in two at least aspects: First, the load pattern on the foundation rock is similar. The highest load is located to the middle part of the interface between the dam and the foundation rock. Second, the grout curtain may be placed in the same location. These similarities allow applying of received results from numerical analysis for the zoned embankment dams. On the other hand, several zoned embankment dams in Sweden have a tilted core, e.g. Grundsjön and Trängslet dams (Angelin et al. 1981). For these dam types, the grout curtain is located under the upstream side of the dam. In analyses, we have placed the grout curtain under the middle part of the dam, which results in different redistribution of pore pressure than for the tilted core (Angelin et al. 1981) and therefore different locations and magnitudes of displacements. As a result, our results cannot not be approximated and evaluated to dams with a tilted core.

5 Conclusions

In this study, we have studied the rock mass behavior under a homogeneous embankment dam complex along the two orthogonal cross-sections A and B, during their early stages of life time, including the construction of the dam (Stage 1), the first filling of the reservoir (Stage 2), and the first seasonal variation of the water level (Stages 3). We have investigated the response of a suite of parameters and their values to identify conditions that influence the rock mass stability.

The construction of the dam (Stage 1) generally induces limited shear and normal displacements in the rock mass, with the exception for the model with 1-m joint spacing (i.e. highly fractured rock). This model results in the formation of noticeable normal displacements in the vicinity of the grout curtain at the interface of between dam and foundation rock.

The first filling of reservoir (Stage 2) results in further development of displacements for the model with 1-m joint spacing. At the same time, parameters such as high differential stress field and low joint friction angle also show significant displacements. All shear displacements occur at the downstream side of the dam, while normal displacements located close to the grout curtain at the interface between dam and foundation.

Variations of the water table in the reservoir (Stage 3) results in additional displacements of the rock mass. The models with high differential stress, low friction angle and small joint spacing show the most significant displacements. Resulted shear displacements occur downstream of

the dam, in the same area as in Stage 2. Significant normal displacement is observed only for case with high differential stress, and the location of it is the same as in Stage 2, in the vicinity of the grout curtain at the interface between the dam and the foundation rock.

Our results reveal that high differential stresses, friction angles and small joint spacing result in the most adverse effect on the stability of the rock mass. Remaining parameters poses little, if any interest in terms of rock mass displacements. However this does not mean that these parameters are unimportant, rather that evaluated range of these parameters has little significance on rock mass stability in this study.

Significant displacements in the grout curtain are induced by the same models as for the rest of the rock mass in the foundation. However, the scale of their displacements is significantly lower. This implies that the range of study parameters does not have significant affect on the integrity of the grout curtain at the early stages of the life time of the dam. However, these ranges may become significant along the exploitation of the dam.

Evaluation of cross-section B identifies that most displacement occur at the banks during first filling (Stage 2) and variation of the water table (Stage 3). The same parameters, which are significant for cross-section A are also important for cross-section B, in term of displacements.

Acknowledgments The research has been supported by VINNOVA, NCC via SBUF and Svensk Vattenkraft (SVC). SVC has been established by the Swedish Energy Agency, Elforsk and Svenska Kraftnät together with Luleå University of Technology, The Royal Institute of Technology, Chalmers University of Technology and Uppsala University (<http://www.svc.nu>) Their contribution is thankfully acknowledged. We would like thank the project reference group, Anders Isander (E-On), Erik Nordström and Peter Viklander (Vattenfall), Fredrik Johansson (KTH), and Staffan Swedenborg (NCC AB). We finally thank Mark Christianson (Itasca) for his advice concerning UDEC.

References

- Amadei B, Stephansson O (1997) Rock stress and its measurement. Chapman & Hall, London
- Angelin S, Brännfors S, Lasu S, Rosenström S, Flodén AK (1981) Hydro power in Sweden. The Swedish Power Association and The Swedish State Power Board, Sweden
- Ask D (2003) Evaluation of measurement-related uncertainties in the analysis of overcoring rock stress data from Äspö HRL, Sweden: a case study. *Int J Rock Mech Min Sci* 40:1173–1187
- Barla G, Bonini M, Cammarata G (2004) Stress and seepage analyses for a gravity dam on a jointed granitic rock mass. In: Konietzky H (ed) Numerical modeling of discrete materials in geotechnical engineering, civil engineering & earth sciences (1st International UDEC/3DEC Symposium, Bochum, Germany, September 2004), Leiden, Balkema, pp 263–268
- Berg S (2005) Bergspänningsmätningar på litet djup. Civilingenjörsexamen, Väg- och vattenbyggnadsteknik, Lulea University of Technology, 2005:246
- Bondarchuk A (2008) Rock mass behavior under hydropower embankment dams: Results from numerical analyses. Licentiate thesis, Lulea University of Technology, 2008:03
- Bronner N, Fagerström H, Stille H (1988) Bedrock cracks as a possible cause of leakage in two Swedish dams. *Transactions of 16th international congress large dams*, San Francisco, vol 2, pp 1029–1052
- Dolezalova M (2004) Numerical analysis of an old masonry dam using UDEC. In: Numerical modeling of discrete materials in geotechnical engineering, civil engineering & earth sciences (1st International UDEC/3DEC Symposium, Bochum, Germany, September 2004), pp 269–277, H. Konietzky, Ed. Leiden, Balkema
- Duncan CW (1999) Foundation on rock, 2nd edn. E & FN Spon
- Energy in Sweden (2009) Swedish energy agency. <http://www.energimyndigheten.se>
- Fell R, MacGregor P, Stapledon D, Bell G (2005) Geotechnical engineering of dams. Taylor & Francis Ltd, UK
- Foster M, Fell R, Spannagle M (2000) The statistics of embankment dam failures and accidents. *Can Geotech J* 37:1000–1024
- Goldin AL, Rasskazov LN (1992) Design of earth dams. Balkema, Rotterdam
- Goodman RE (1980) Introduction to rock mechanics. Wiley, New York
- Hoek E, Bray JW (1981) Rock slope engineering. Institution of mining and metallurgy, 3rd edn, London
- Hoek E, Kaiser PK, Bawden WF (1997) Support of underground excavations in hard rock. Balkema, Rotterdam
- Hoek E, Carranza-Torres C, Corkum B (2002) Hoek–Brown failure criterion-2002 edition. In: Proceedings of the 5th North American rock mech symposium and 17th tunnelling association of Canada conference: NARMS-TAC 2002, July 7–10, University of Toronto, pp 267–271 Updated version (October 2, 2002). <http://www.roscience.com>
- ICOLD (1974) Lessons from dam incidents. International Commission on Large Dams (ICOLD), Paris
- ICOLD (1983) Deterioration of dams and reservoirs. International Commission on Large Dams (ICOLD), Paris
- ICOLD (1995) Dam failures statistical analysis. Bulletin 99. International Commission on Large Dams (ICOLD), Paris
- Itasca (2005) UDEC version 4.0. Manual. ICG, Minneapolis
- Johansson S (1997) Seepage monitoring in embankment dams. Doctoral thesis, Royal Institute of Technology, Sweden. ISBN 91-7170-792-1
- Johansson F (2005) Stability analyses of large structures founded on rock—an introductory study. Licentiate Thesis, Royal Institute of Technology, Sweden. ISSN 1650-951X
- Korsfelt T, Lublin Z, Lagerquist M, Persson A, Andersson A, Lindberg C, Andersson DG, Waluszewski D, Veibäck E, Cato J, Petersson K (2007) Energiläget 2007. Svensk energimyndigheten, Sweden. <http://www.energimyndigheten.se>
- Leijon BA (1989) Relevance of point wise rocks stress measurements—analysis of overcoring data. *Int J Rock Mech Min Sci Geomech Abstr* 26:61–68
- Mörén L (2005) Bergerosion i utskovskanaler. Rock Scour in Spillway Channels. Master Thesis, Uppsala University, Sweden. ISSN 1401–5765
- Reinius E (1988) Stresses and cracks in the rock foundation of an earthfill dam. *Water Power Dam Constr* 40: 33–38
- Rocscience (2007) RocLab. Ver. 1.031. Freeware. <http://www.roscience.com/products/RocLab.asp>
- Singh B (1995) Engineering for embankment dams. Balkema, Rotterdam
- Sjöberg J, Lindfors U, Perman F, Ask D (2005) Evaluation of the state of stress at the Forsmark site. Preliminary site investigation Forsmark area-version 1.2. SwedPower AB, SKB R-05-35

- Stephansson O (1993) Rock stress in the Fennoscandian shield. *Comprehensive rock engineering—principles, practice and projects*, vol 3. Pergman Press, Oxford, pp 445–459
- Stephansson O, Dahlström L-O, Bergström K et al (1987) Fennoscandian rock stress data base—FRSDB. Research report, Luleå 1987:06
- Swedenborg S (2001) Rock mechanical effects of cement grouting in hard rock. Doctoral thesis, Chalmers University of Technology. ISSN 0346-718X
- Töyrä J (2006) Behavior and stability of shallow underground constructions. Licentiate thesis, Lulea University of Technology, 2006:76
- Vattenfall (1988) Vattenfalls handbok. Jord- och stenfyllningsdammar. Happy Printing AB. Vattenfall, Sweden. ISBN 91-7186-271-4
- Water Resources Commission of NSW (1980) Grouting manual, 3rd edn. Australis
- Windelhed K (2001) Dammsäkerhet, Jetinjektering, en intressant reparationsmetod för jorddammar—förstudie. Elforsk AB, Sweden, Elforsk Rapport 01:10

**HYDROMECHANICAL NUMERICAL ANALYSIS OF ROCK MASS BEHAVIOUR
UNDER S SWEDISH EMBANKMENT HYDROPOWER DAM**

Bondarchuk A, Ask M, Dahlström L, Nordlund E and Knutsson S (2009).
Long Term Behaviour of Dams. Bauer, E., Semprich, S. & Zenz, G. (eds.).
p. 113-118.

Hydro-mechanical numerical analyses of rock mass behavior under a Swedish embankment hydropower dam

Bondarchuk A.¹, Ask M.¹, Dahlström L-O.^{1,2}, Nordlund E.¹ and Knutsson S.¹

¹Luleå University of Technology, SE-971 87, Luleå, Sweden

²NCC Construction Sverige AB, Gullberg Strandgata 2, 405 14 Göteborg

E-mail: alebon@ltu.se

Abstract

The behavior of the rock mass under a hydropower dam is important for the functionality and safety of the dam. In addition to the static load of the dam complex itself, the foundation rock is exposed to different cyclic water loads that vary with time from the very first filling of the reservoir throughout the life time of the dam. These varying loads induce deformations in the foundation rock that may lead to different processes such as erosion and reduction of bearing capacity of the dam. With time these deformations develop in the exposed rock mass, which in turn facilitate degradation of the properties of bed rock. Most existing dams in Sweden have been in operation over the last 30 - 60 years, which makes it important to study the potential rock mass deformation over longer times. The objective of this paper is to show how the developed conceptual model has been adopted for the investigation of foundation rock of Häckren dam. For that purpose a coupled hydro-mechanical two-dimensional discrete element method with the program UDEC was used. This program allows the study of deformation along existing discontinuities, which is thought to occur in the rock mass under existing embankment dams in Sweden. The problem was first studied using conceptual models, with the results indicating that the first filling of the reservoir and one seasonal variation of the water table cause substantial shear- and normal deformation of the underlying rock mass and the grout curtain. Parameters that induce higher deformations are closely spaced discontinuities, low friction angles of discontinuities, and high differential stresses. In this paper, we will present the preliminary results from converting the conceptual numerical model to a Häckren dam, Sweden.

Keywords: embankment dam, foundation rock, Häckren dam, Sweden, numerical analyses, UDEC.

Introduction

The mechanical behavior of the rock mass under a dam complex has received relatively little attention in the

literature. The seasonal variation of the water level in the reservoir may induce displacement along discontinuities. Even small displacement may have unfavorable influence on the integrity of a grout curtain. Cyclic variations of load also may result in break-down of filled fractures. This could enhance the amount of erosion along fractures. A few studies of rock mass in terms of stability of dam have been carried out using analytical [1] or numerical methods [3], [4], [6].

The peak of dam construction in Sweden occurred from 1950 to 1980. Hydropower is an important source of energy in Sweden that is relying on safe dam conditions. The concerns regarding the potential of a degraded grout curtain and enhanced fracture erosion has resulted in the start of this study, which is executed as a PhD project in three steps. 1) construction of a conceptual model in 2D; 2) the adaptation of the conceptual model to a real case in 2D; and 3) the expansion of the 2D model to a 3D model.

Bondarchuk [2008] has analyzed the response of the bed rock to the construction and initial exploitation of a dam in a conceptual numerical model. The Universal Distinct Element Code, UDEC [5] was selected for the analyses, because the code is suited to study displacements along discontinuities in a blocky rock mass, i.e. the conditions that are thought to prevail under a dam. Bondarchuk [2008] constructed two conceptual models using typical Swedish rock mass conditions, and a dam of the homogeneous embankment type. The major findings were that highly fractured bed rock, rock mass with large differential stresses, and/or joints with low friction angles result in the largest magnitudes of shear- and/or normal displacements along the joints and total flow through the bedrock.

The second step has been initiated, to adopt the conceptual model to a real dam in a case study. The Häckren dam has been chosen as the real case dam for the following reasons: It is a zoned embankment dam, mostly founded on rock, it has a high regulation surface, and, for Swedish conditions, an unusual amount of data had been collected. The annual amplitude of regulation is 27 m, which will allow us to test the hypothesis that substantial variation of the water table has a negative influence on the stability of rock foundation [9]. Figure 1 shows the location of the Häckren dam.

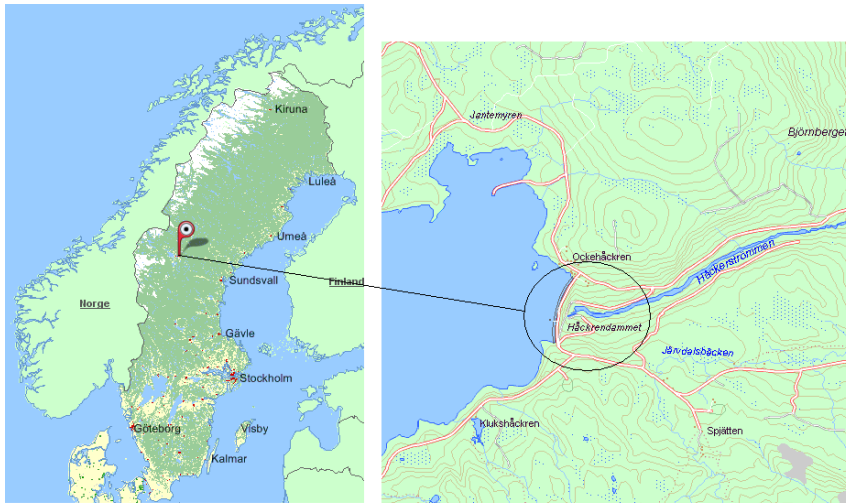


Figure 1: Location of the Häckren dam, Sweden

The Häckren dam is a Class 1A dam where loss of life and serious injury and damage may follow if dam failure may occur [7], [8]. In 2008, it was examined by the international Review Panel of “Svenska Kraftnät” and Swedenergy to ensure that the safety of dam comply with best international practice and standards [8]. “Svenska Kraftnät” is considered to be the authority that provides guidance on issues of supervision of dam safety in Sweden.

This work aims at modeling the dam performance by fitting results obtained from numerical models to the measured results of hydraulic pressure in foundation rock. A calibrated model will be used for analyzing potential bed rock deformation with focus on dam stability and fracture erosion. Description of the conceptual model and dam with more detailed geology, simplification / assumptions and selected results focusing on deformation and pore pressure in the foundation bedrock are presented in this paper.

Conceptual numerical analyses

Model description

The initial step of this study was to analyze the behavior of the rock mass using 2D conceptual model [6]. The investigation were performed along two cross-sections: Cross-Section A (CS-A) which is normal to the axis of the dam, and Cross-Section B (CS-B), which is parallel to the axis (Figure 2). The rock mass has been discretized into deformable triangular finite-difference zones in the UDEC mesh for two conceptual models (CS-A and-B). The models

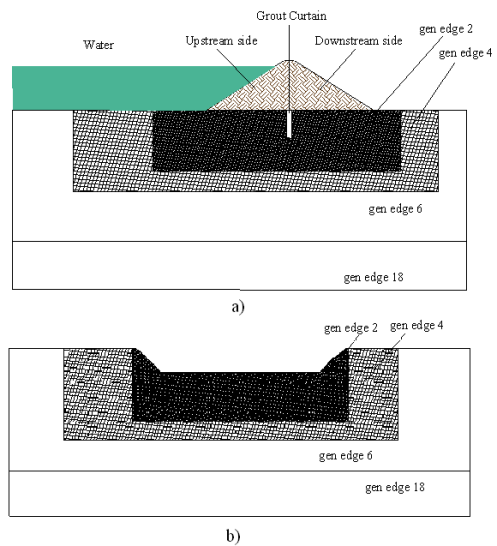


Figure 2: Distinct element mesh of conceptual model for two cross-sections A (a) and B (b)

were subdivided into four areas of different zone size to obtain good resolution in the areas of interest and to optimize the calculation time. The linear elastic-perfectly plastic (Mohr-Coulomb) model has been applied for blocks and discontinuities in the analyses. A total number of 34 input parameters describe the properties of the rock mass (Table 1 and Table 2), grout curtain (Table 2), dam body, and stress field.

TABLE 1: ROCK BLOCK PROPERTIES

Parameter	Value
Density, ρ [kg/m ³]	2700
Young's modulus, E [GPa]	61
Poisson's ratio, ν [-]	0.25
Friction angle, θ [°]	69
Cohesion, c [MPa]	5.142
Tensile strength, T [MPa]	1.21

TABLE 2: PROPERTIES OF DISCONTINUITIES

Name	Value	Value
	ungROUTED	grouted
Joint normal stiffness [GPa/m]	10	12
Joint shear stiffness [GPa/m]	10	12
Aperture for zero normal stress [m]	$0.25 \cdot 10^{-3}$	$0.12 \cdot 10^{-3}$
Residual aperture [m]	$0.125 \cdot 10^{-3}$	$0.06 \cdot 10^{-3}$
Joint cohesion [MPa]	0	0.6
Joint residual cohesion [MPa]	0	0
Joint friction angle [°]	35	35
Joint residual friction angle [°]	30	25
Joint dilation angle [°]	9	9
Joint permeability constant [1/Pa s]	300	300
Joint tensile strength [MPa]	0	0
Joint residual tensile strength [MPa]	0	0
Distance between joints [m]	2 and 3	2 and 3

The sensitivity analyses included the study of six parameters: the first parameter characterize the stress state, whereas the remaining five parameters describe the joint behavior (Table 3). The influence of individual parameters, expressed in terms of magnitude and location of shear / normal displacement and total leakage through the bedrock, was estimated during three stages of the life time of the dam:

- Stage 1 Static loading from the constructing of the dam facility;
- Stage 2 Impounding the reservoir; and
- Stage 3 Cyclic loading from water in the reservoir

During the sensitivity analyses, one parameter (Table 3) was

varied at a time from the base case model (BC). During each of these stages, between 11 and 14 simulations were run.

Results of conceptual model

The magnitudes and locations of maximum shear and normal deformation along discontinuities (i.e. joints), and the total water flow through the rock mass were studied in a total number of 61 sensitivity analyses. Figure 3 shows an example of where deformations occurred in the models. The location and value of maximum shear and normal deformation in each model was determined using the curtain commands of UDEC that only plots a certain range of values: The upper limit of the plotted range is the maximum deformation found in the model, while the lower limit is calculated by dividing the maximum values by 5. Figure 5 compares the variation of deformation of the maximum deformation of individual parameters with respect to shear and normal deformation in the rock mass and grout curtain during the three stages of the dam life. The magnitudes of deformation for the three stages and for normal and shear deformation in the rock mass and grout curtain vary from 0 to 6010 μm . In general, the smallest deformations are obtained in the normal direction in the grout curtain, and the largest deformations are obtained as shear deformations in the rock mass.

TABLE 3: ALTERED PARAMETERS

Model No.	C-S	Parameters	BC Model
1,2	A & B	Stress magnitudes [MPa]	$\sigma_H = 2.8 + 0.0399z$ $\sigma_h = 2.2 + 0.0240z$
3, 4, 5	A & B	Joint friction angle [°]	35
6	A & B	Joint dilation angle [°]	9
7, 8, 9	A & B	Dip of joints [°]	subhorizontal: 5 subvertical: 85
10, 11	A & B	Normal subvertical joint distance [m]	5
12, 13	A	Hydraulic aperture [mm]	0.25
14			

KEYS: σ_H , maximum horizontal stress; σ_h , minimum horizontal stress; σ_v , vertical stress; B, subhorizontal (banking) joints; SVJ, subvertical joints.

It was estimated that construction of the dam facility (Stage 1) causes usually insignificant shear and normal deformations in the bedrock, however presence of areas with high joint frequency may results in noticeable normal deformation of joints.

The first filling of the reservoir (Stage 2) results in noticeable development of displacements in the rock mass. It causes

dangerous opening of joints when the joint frequency is high and the friction angle is low. The importance is emphasized by the location of deformation. Grout curtain shows a stable condition in general. However within the group (grouted joints) low friction angle identifies the most noticeable influence on shear deformation.

Variation of the water table causes cyclic loading of the bedrock and dam (Stage 3) and it results in further development of displacement in the rock, with most noticeable magnitudes for high differential stress and low friction angle. Normal deformations are not influenced significantly, except for the case where the rock mass is under high differential stress. Grout curtain shows the same condition as in previous stage.

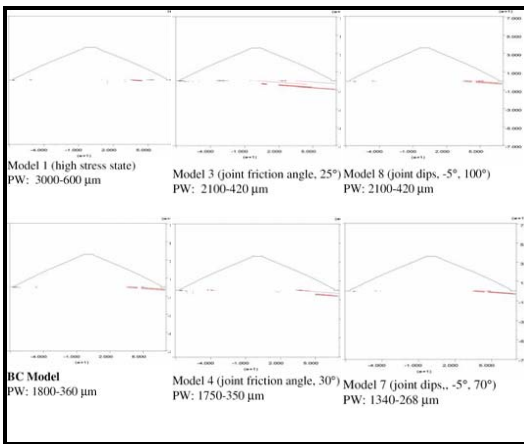


Figure 3: Calculated shear deformations during Stage 2

Case study: Håckren dam

The Håckren dam is a zoned regulation dam with a height of 67 m, length of 860 m, storage capacity of $700 \cdot 10^6 \text{ m}^3$, and an allowed amplitude of regulation of 30 m. The dam was constructed from 1962 - 1965, followed by the first filling of the reservoir that took about one year. The cross-section of dam and its foundation rock mass is shown in Figure 4.

The bedrock is composed of metamorphosed sedimentary deposits, i.e. clayey slate interbedded with greywacke [2]. The strata sequence is generally greywacke in layers 10 - 20 cm thick, alternating with thinner layers of clayey slate and counter wise. The bedrock strata within the dam area have a fairly flat dip towards the upstream direction of the dam. However, because the rock locally is folded, the dip of beds varies, up to near vertical in places [2].

Folded sequences are resulting from ductile deformation. In addition, brittle crack formation is also extensively observed. Investigations in the area suggest that two main discontinuity

systems exist within the dam area [2]. One discontinuity set is fairly regularly oriented in relation to the folding direction, and runs across the valley with a steep downstream slope. Sideways the extension, as a rule, small and the discontinuities are generally filled with quartz and calcite. The second system is less regularly oriented. The discontinuities, have a considerably longer extension in the longitudinal direction of the valley. They cross the dam axis in the form of local fissure zones. In addition, one of these zones is located under the river bed and it consisted of badly crushed rock. The width of this zone is, comparatively small. Cleft existed in the zone, one meter wide at the rock surface, and filled with fine fragments of rock; it crossed the core area at an angle of about 45° .

The tightening core of the dam, the supporting fill, as well as the rock-fill members at the upstream and downstream toes of the slope, are founded on rock. The remaining parts of the supporting fill are founded on natural soil with the exception of those areas where the ground consisted of fine-grained or loosely compacted strata that are susceptible to erosion.

Below the impermeable core, sections with intensely fractured rock were carefully blasted off at the time of construction [2]. Steep rock slopes and overhanging parts of more than half a meter were blasted or leveled off using concrete. The crushed-zone under the river bed was excavated to a depth of about 1 m and refilled with concrete. At the upstream edge of the tightening core, concrete was moulded out to a somewhat greater depth.

Extensive grouting was carried out within the zone of impervious soil. Concrete was been poured or sprayed onto the surface rock of poor quality, and it has been stabilized by grouting down to a depth of 1.6 m across a width of 10-30 m. It has been subsequently grouted to a depth of 6.4 m across the width of 6 m. A grout curtain was placed under the impervious core and propagated to different depths, depending on the height of the dam. It runs along the complete length of the impervious core [9].

An additional inspection tunnel was blasted out downstream of the impervious zone and it propagates along the greater part of the dam length. It is used for investigation, inspection and drainage purposes (Figure 4).

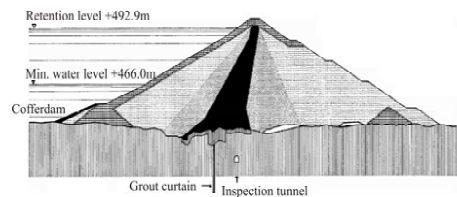


Figure 4: Layout of Håckrent embankment dam

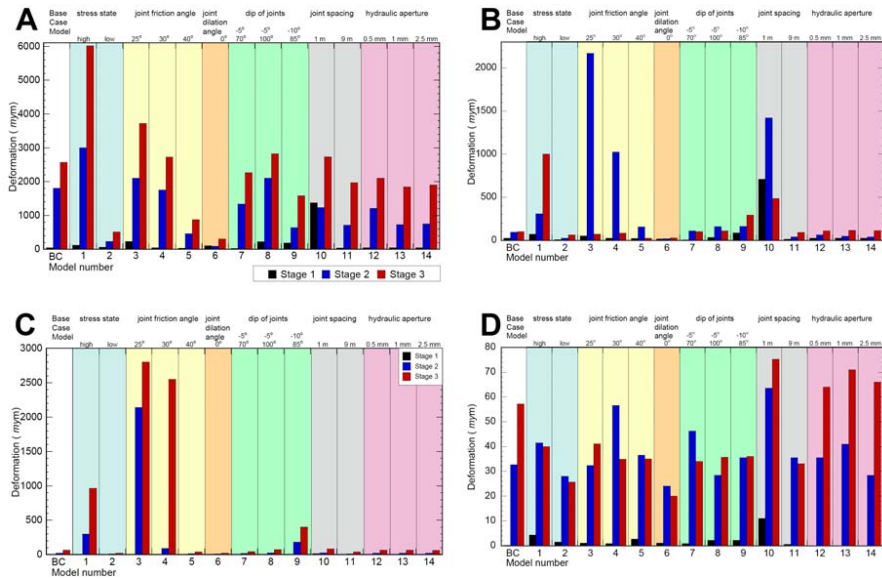


Figure 5: Comparison of calculated values of maximum deformation obtained during Stage 1 to 3. Shear (A, C) and normal deformations (B, D) of the rock mass (A, B) and the grout curtain (C, D)

Preliminary UDEC model of the Håckren dam

The work on adapting the conceptual model to the real case has started. To better account for the water pressure in the dam on the interface between the dam and foundation rock, several simplified models have been developed. These models help determining properties of material and discontinuities for supporting fill and core, which will introduce more realistic values of water pressure and weight on the interface between dam and foundation.

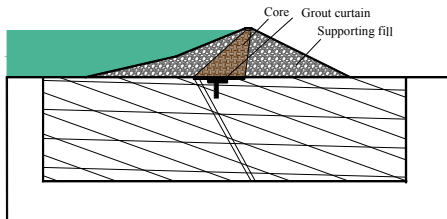


Figure 6: Håckren dam jointed rock mass hydro-mechanical model

The dimension of model has been modified slightly. In horizontal plane model extends up to 500 m from upstream of the heel and downstream of the toe. The foundation rock was simulated to a depth of 200 m. As the rock foundation consists of two rock types, we are currently using the properties of the weaker rock type for building material of the rock mass in the model.

The characteristics of existing discontinuities in the rock mass (joints and lithological boundaries) are introduced into a restricted zone of the model only (Figure 6). The discontinuities correspond to three major geological structures, namely fissure zone, joint system, and lithological boundaries. The fissure zone extends along the axis of the embankment dam from right abutment, at widths up to 2 m. The joint system runs across the valley with a steep downstream slope. The altering lithological layers of clayey slate and greywacke in the rock mass are introduced into the model as horizontal discontinuities.

The grout curtain is simulated in three parts: (1) The area-grouting was performed to the depth up to 1.6 m, which extends along the whole foundation of the core; (2) Part of this area was subsequently grouted to the depth of 6.4 m; and (3) The depth of the main grout curtain was performed to the depth of 25 m in the area of investigation. All the

discontinuities in these areas are assigned properties of grouted joints.

To account for the inspection tunnel, which works also as a drainage tunnel, a zero pore pressure is assumed in the area of the tunnel in the rock mass.

A simplified approach has been chosen for the early steps of simulations. The rock blocks are simulated as isotropic elastic material, based on the assumption that the stress state at shallow depth is small and no plastic deformation occurs. The elastic properties of blocks in fissured zone are slightly lower to account for the crushed rock. Joints are assumed to be relatively permeable, with stress-dependent permeability characterized by their stiffness and initial hydraulic aperture. The permeability of joints in fissure zone was even higher compared to surrounding discontinuities.

Concluding remarks

The investigation of case studies with numerical code is a complicated process. The accuracy of the results of the analysis is depending on available information, its quality and how well it describes the rock mass. Nevertheless, numerical analyses are useful for studying complex problems and understanding the impact of individual parameters. Such investigations are important for predicting the long term behavior of the Håckren dam.

Currently, we focus on calibrating our models with existing pore pressure measurements in bedrock and core. We anticipate to have progressed in time for the conference.

Acknowledgements

We are very grateful for the opportunity to study the Håckren dam, and would like to thank Vattenregleringsföretagen, and especially Gunnar Sjödin, Birgitta Rådman and Svante Andersson for their generous help in locating data for our project. We also thank Anders Isander (E-On) for his help in identifying the Håckren dam for the case study, and the members of the reference group: Staffan Swedenborg, Fredrik Johansson and Peter Viklander. The research presented was carried out as a part of "Swedish Hydropower Centre - SVC". SVC has been established by the Swedish Energy Agency, Elforsk and Svenska Kraftnät together with Luleå University of Technology, The Royal Institute of Technology, Chalmers University of Technology and Uppsala University.
www.svc.nu

References

- [1] Reinius E. (1988). *Stresses and cracks in the rock foundation of an earthfill dam*. Water Power & Dam Construction Vol. 40, pp. 33-38.
- [2] Abrahamson R., Edlund L. (1967). *Foundation grouting at the Håckren dam*. Proc. Of the 9th International Congress on Large Dams, Istanbul, 1967, pp. 353-366
- [3] Barla G., Bonini M., Cammarata G. (2004). *Stress and seepage*

- analyses for a gravity dam on a jointed granitic rock mass*. In: Konieczky, H. (eds), Proc. of the 1st Int. UDEC/3DEC Symposium: Numerical Modeling of Discrete Materials in Geotechnical Engineering, Civil Engineering, and Earth Sciences, Bochum, Germany, 2004, pp. 263-268.
- [4] Dolezalova M. (2004). *Numerical analysis of an old masonry dam using UDEC*. In: Konieczky, H. (eds), Proc. of the 1st Int. UDEC/3DEC Symposium: Numerical Modeling of Discrete Materials in Geotechnical Engineering, Civil Engineering, and Earth Sciences, Bochum, Germany, 2004, pp. 269-277.
 - [5] Itasca (2005). *UDEC version 4.0. Manual*. Minneapolis, ICG.
 - [6] Bondarchuk A. (2008). *Rock mass behaviour under hydropower embankment dams: results from numerical analysis*. Lic. Thesis, Luleå University of Technology, Luleå, Sweden.
 - [7] *Rating of dam safety defects*. Svensk Energi & Svenska Kraftnät, 2004
 - [8] Höeg K., Viotti C., Engström Å., Aufleger M. (2008). *Håckren dam safety review*. Svensk Energi & Svenska Kraftnät, Sweden.
 - [9] Dath J., Lindgren S., Rytters K., Yngland D., Heiner A., Pettersson B., Jonsson B. (2002). *Comprehensive dam safety evaluation of the facilities at Håckren*. SWECO VBB VIAK, Sweden.

**ROCK MASS STABILITY OF THE HÅCKREN HYDROPOWER
EMBANKMENT DAM IN CENTRAL SWEDEN: PART I – DEVELOPING
AND VALIDATING 2D UDEC NUMERICAL MODELS**

Bondarchuk A, Ask M V S, Dahlström L-O and Nordlund E (2012).

Submitted for publication in the
Rock Mechanics and Mining Science

Rock mass stability of the Håckren hydropower embankment dam in central Sweden: Part I — Developing and validating 2D UDEC numerical models

Abstract

The stability of the rock mass under a hydropower dam is important for the functionality and safety of the dam. The static load of the dam complex itself and the annually varying water loads induce deformations in the foundation rock that may lead to different processes such as erosion and reduction of bearing capacity of the dam. The long-term effect from accumulating loads is fairly little known for most existing hydropower dams in Sweden. Considering that at this moment a big number of old dams (constructed in 60-70s) are in operation in Sweden. Majority of them were built at early stages of rock mechanics engineering, and were designed based only on good engineering sense and experience. Presently dam owners in Sweden are trying to guarantee high levels of safety of dams in an international perspective, with priority for dams where the consequences of failure would be particularly severe. In connection with the review of the structural safety of existing dams, it is necessary to perform extensive field and laboratory works both in dams and foundation rock. Examination of foundation rock is troublesome due to its inaccessibility. Such conditions can raise the price of investigation work significantly. Combination of numerical code with simple field and laboratory tests data for preliminary appraisal of the rock mass allows understand the processes in the basement and locate the “weak points” for further thorough examination with more sophisticated approach and equipment.

This work presents a methodology for analyzing fracture erosion and rock mass stability under hydropower embankment dam complexes using the numerical distinct-element code UDEC. The Håckren dam is one of largest embankment dams in Sweden and it is classified as a high consequence dam (1A) in case of dam failure therefore it was chosen for the case study. The first paper (Part I) develops the numerical model by populating it with existing and new geological and rock mechanical data, conducts sensitivity analyses, and validate the results with existing monitoring data from the dam. We have aimed at keeping the new site investigation costs at a minimum by using robust and commonly used engineering geology field investigation methods for collecting data. Additionally this paper (Part I) investigates if this approach for collecting new data is satisfactory, or if more cost-intense investigation methods are needed. The second paper (Part II) simulates a decade of cyclic variations in water load within the storage basin. By this approach it

investigates the relationships between shear- and normal- displacements, and hydraulic conductivity of the discontinuities. The aim of this work is to forward the understanding of, and to relate the observed displacements with the fracture erosion process within the discontinuities.

The results of Paper I show a good agreement with available monitored data in terms of the pore pressure and water leakage into the inspection tunnel. The available results suggests that we have developed a realistic proper numerical model by using a combination of simple and low-cost (~10 kEUR) field- and laboratory tests and pre-existing data. The implications for fracture erosion and bedrock stability due to cyclic variation in water load is discussed in Paper II.

1 Introduction

The stability of the rock mass under a hydropower dam is important for the functionality and safety of the dam. Dam safety in Sweden is handled by Svenska Kraftnät and Svensk Energi, which are representing the authorities and the dam owners, respectively [e.g. 1]. A pilot study was initiated in 2005 to investigate dam safety, and this resulted in a review that included five class 1A hydropower dams [2]. The dams investigated were selected to allow a wide geographic and owner spread, and included the Höljes, Håckren, Hällby, Ajaure, and Suorva hydropower dams.

Process of erosion has a significant influence on rock mass strength [3]. It may result in loose of strength and reduction of shear resistance along weak planes. If this occurs in unfavorable direction it may have a significant impact on the stability of the dam. Most studies on fracture erosion within the dam body have been a long focus of investigation [e.g. 4; 5; 6; 7]. Fracture erosion may be induced by small deformations along pre-existing discontinuities in the rock mass under the dam. Such small displacements are influencing the integrity of the grout curtain, and thus the permeability and the stability of the entire rock mass under the dam complex.

The static load of the dam complex itself and the annually varying water loads induce deformations in the foundation rock that may lead to different processes such as erosion and reduction of bearing capacity of the dam. The long-term effect from accumulating loads is fairly little known for most existing hydropower dams in Sweden. The seasonal variation of the water level in the water storage basin may induce displacement along discontinuities. Even small displacement may have unfavorable influence on the integrity of a grout curtain. Cyclic variations of load may also lead to break-down of filled fractures. This could enhance the amount of erosion along fractures. A few studies of rock mass in term of stability of dam have been carried out using analytical [8; 9] or numerical methods [10; 11; 12].

Bondarchuk et al [12] were the first to conduct a large-scale parametric numerical study on the bedrock stability under a hydropower embankment dam complex in Sweden. They used a conceptual model using the two-dimensional numeric code UDEC that simulates deformations along discontinuities [13]. In the conceptual numerical study, they propose that seasonal variations (also referred as cyclic variations) in load from the water in the storage basin may induce substantial shear- and normal deformation of the rock mass under certain conditions [12]. The three most important conditions were stress state, fracture frequency, and fracture friction angle. It appears that deformations along pre-existing discontinuities due to cyclic variations in load from the storage

basin may be substantial enough to facilitate the fracture erosion. However, the results must be validated by running a model based on a real dam.

The overarching objective of this study, which consists of two parts, is to develop a methodology for analyzing fracture erosion and rock mass stability under hydropower embankment dam complexes using the numerical distinct-element code UDEC [13]. The Håckren dam is one of largest embankment dams in Sweden and it is classified as a high consequence dam (1A) in case of dam failure [e.g. 2]. In the first paper (Part I), we are developing the numerical model by populating it with existing and new geological and rock mechanical data, conducting sensitivity analyses, and validating the results with existing monitoring data from the dam. We have aimed at keeping the new site investigation costs at a minimum by using robust and commonly used engineering geology field investigation methods for collecting data. A second objective of this first paper (Part I) is to investigate if this approach for collecting new data is satisfactory, or if more cost-intensive investigation methods are needed. In the second paper (Part II), we are simulating a decade of cyclic variations in water load within the storage basin. We are investigating the relationships between shear- and normal- displacements, and hydraulic conductivity of the discontinuities. The aim of this work is to forward the understanding of, and to relate the observed displacements with the fracture erosion process within the discontinuities. This work forms the base for the evaluation of the rock mass response of the Håckren dam in long-term perspective.

This paper (Part I) is divided into three parts: the first reviews the approach, rationale and background for the analyses; the second describes the development of the numerical model and how input data parameters were acquired; and the third validates and discusses the obtained model and our approach.

2 Håckren embankment dam

The Håckren embankment dam was selected as the real case dam because of the following characteristics: (1) It is a zoned embankment dam; (2) To the greatest extent, it is founded on rock; (3) It has a high regulation amplitude (27 m); (4) For Swedish conditions, the amount of data available is unusual large; and (5) It has an inspection tunnel. The large amplitude of regulation will allow us to test the hypothesis that substantial cyclic variation of the water table has a negative influence on the stability of rock foundation [12; 14]. It is classified as a class 1A facility, which implies that there is a high probability for many lives and very serious damages on infrastructure and property in case of dam failure [e.g. 1].

The Håckren dam is located in the tributary Storån that feeds into the river Indalsälven, 80 km west of the city of Östersund in central Sweden (Figure 1). The storage basin has a volume of 700 Mm³, and a design flood of 470 m³/s [e.g. 15]. The dam is owned by Vattenregleringsföretagen.

Construction of the dam complex started in 1962, and the first filling of the storage basin was completed in 1965 [16]. This means that the dam will have been in operation in 50 years in 2015. Together with four other 1A class dams (Höljes, Hällby, Ajaure, and Suorva), the Håckren was selected for a special evaluation of dam safety by Svenska Kraftnät [2; 15]. The NNE-SSW striking dam crest is 860 m – long and 67 m high, and the maximum regulation amplitude is 26.9 m [16]. The dam body consists of a tight core of moraine that is surrounded by layers of sand and gravelly sand (Figure 2). The outer parts of the dam consist of gravel and rock.

The dam is founded directly on the bedrock over most parts of its length, with the exception of a minor part that is founded on natural soil [16]. The natural soil is composed of fine-grained or loosely compacted strata. The sedimentary bedrock generally consists of 10-20 cm thick layers of clayey slate or greywacke that is interbedded with thinner layers of greywacke or clayey slate [16]. A large number of diamond drill-holes revealed that the quality of the bedrock rapidly improved below surface. Extensive grouting had been applied to guarantee the stabilization of foundation and make a leakage barrier. Stabilization grouting had been performed down to a depth of 1.6 m across the width of 10-30 m. It had been subsequently grouted to a depth of 6.4 m across the width of 6 m. A grout curtain was placed under the complete length of impervious core, and the depth of it was dependent on the height of the dam.

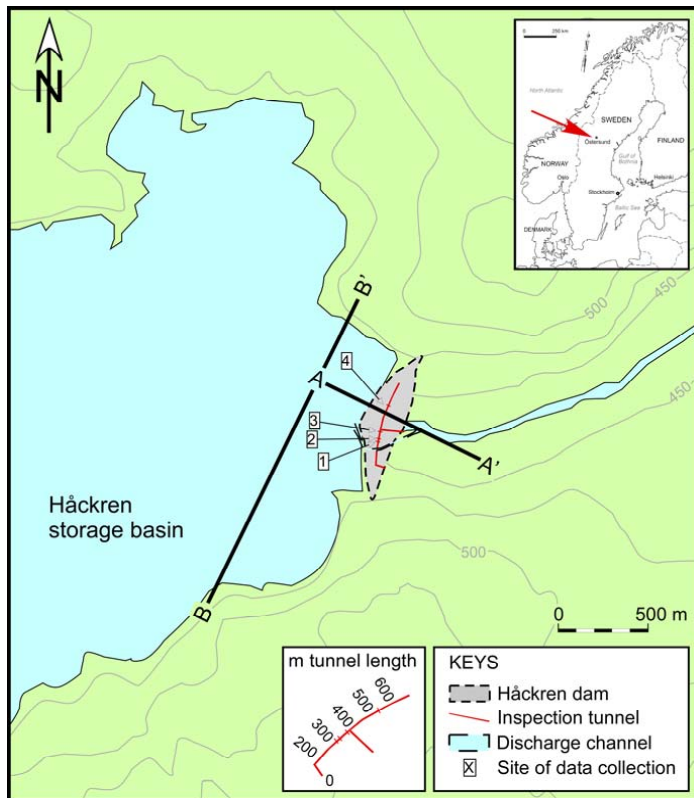


Figure 1. Map of the Håckren dam and the eastern most part of the Håckren storage basin. The red arrow in the inserted map shows the study area. The location of the inspection tunnel and the sites of data collection in the tunnel are marked, and the insert of the inspection tunnel shows the approximate location of the length coordinates in the tunnel that also is shown in Figure 3. Profiles A-A' and B-B' shows the location of UDEC Models A and B, respectively.

An inspection tunnel has been built at about 20 m depth in the rock mass downstream of the grout curtain (Figure 1). A total of 16 vertical drainage holes of 10 m each were drilled into the floor of the inspection tunnel, and four 10-m long inclined drainage holes were drilled into the tunnel roof towards the upstream direction [15]. The inspection tunnel acts as a large drain, and because it is easy accessed, it allows direct monitoring of the hydraulic conditions in the rock mass under the dam. A dozen pipes for monitoring the pore pressure were installed in the foundation rock in the inspection tunnel. The pore pressure was monitored from 1966 to 1975, after which no measurements have been collected [15].

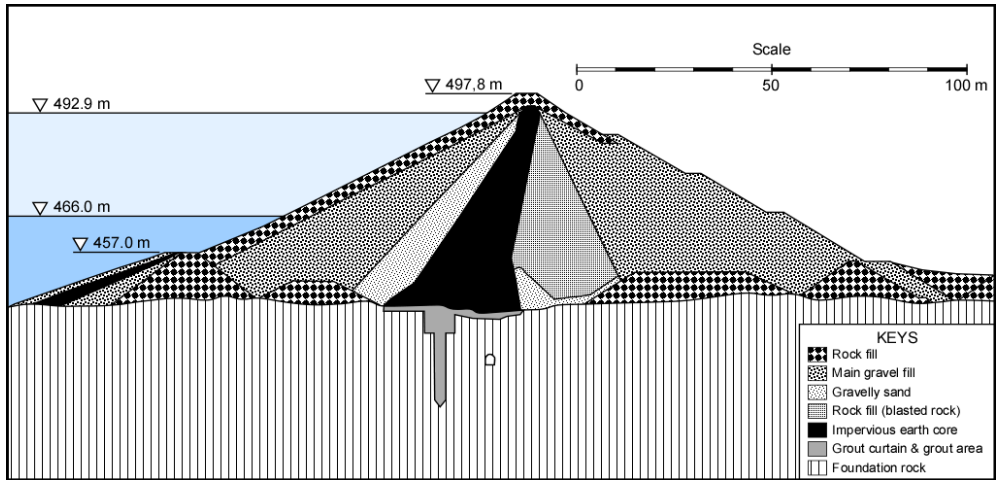


Figure 2. Layout of the Håckren dam after Abrahmsén and Edlund [16]. Profile A-A' shows the location of this profile in map view in Figure 1.

3 Method

3.1 Discontinuum modeling

We are using the distinct-element code UDEC [13] to model coupled hydro-mechanical processes acting along a pre-defined discontinuity network in terms of normal- and shear displacement, pore pressure, and water flow. Although our problem is 3D in nature, we analyze it in 2D. To some extent, we cover 3D aspects in the 2D approach by performing the analyses along two orthogonal UDEC models cross-sections (c.f. profiles A-A' and B-B' in Figure 1).

A major task for the analyses is to develop a well-responding computational mesh with proper properties. The UDEC computational mesh consists of the dam body, its underlying rock mass, and the interface between the two. The input parameters needed for the UDEC mesh is included in Table 1. In addition, an in situ stress field is applied using three stress gradients in two horizontal and one vertical direction. The influence of water is addressed by applying a fully coupled hydro-mechanical analysis, in which fracture conductivity is dependent on mechanical deformation, and joint water pressure affects the mechanical computations [13]. Pore fluid pressure is assumed to be hydrostatic, and the ground water level coincides with the ground surface.

3.2 In data for the UDEC numerical mesh

Pre-existing data from the Håckren dam allows us to construct a realistic numerical model with respect to the dimensions and properties of the embankment dam, and main geological structures.

About a dozen pipes were installed in the inspection tunnel and measured the pore pressure from 1966 to 1975 [15]. Four of the pipes measured the pore pressure upstream of the grout curtain, and eight pipes measured the pore pressure downstream of the grout curtain. Furthermore, the water level and the leakage through the inspection tunnel have been regularly monitored [15]; we have access to data from 1966 to 2009.

We were not able to locate any engineering geology data, for example on the rock mechanical properties of the rock mass, intact rock, and rock fractures, as well as on the in-situ state of stress. Because the data are needed for the UDEC models, we needed to acquire new data. The limited budget of the project influenced the extent of the field campaign: We collected basic engineering geological parameters of the intact rock, discontinuities and rock mass in the inspection tunnel, using methods that commonly are applied in the field of civil engineering.

Table 1. Input data parameters for the UDEC computational mesh

Parameter	Dam body		Interface between dam body and rock mass		Rock mass			
	Support	Core	Under support	Under core	Intact rock	Discontinuities		
						Open 0-25 m*	>25 m*	Grouted 0-25 m*
CHARACTERISTICS OF INTACT ROCK								
Bulk density, ρ [kg/m ³]	2100	2100	–	–	2700	–	–	–
Bulk modulus, K [GPa]	1	1	–	–	14	–	–	–
Shear modulus, G [GPa]	0,1	0,1	–	–	8,4	–	–	–
CHARACTERISTICS OF DISCONTINUITIES								
Normal stiffness, K_n [GPa/m]	1	1	1	1	–	14,27	93,81	14,27
Shear stiffness, K_s [GPa/m]	1	1	1	1	–	0,6	1,1	0,6
Friction angle, ϕ [°]	85	85	45	45	–	26	26	26
Residual friction angle, ϕ_r [°]	–	–	–	–	–	26	26	21
Cohesion, c [MPa]	1e14	1e14	0	0	–	0	0	0,6
Tensile strength, T [MPa]	1e14	1e14	0	0	–	0	0	0,6
Aperture, α [mm]	1,5	0	1,5	0	–	0,152	0,05	0,05
Residual aperture, α_r [mm]	–	–	–	–	–	0,05	0,05	0,05

*0-25 m and >25 m refers to depth

3.2.1. Pre-existing data

The dam owners provided detailed information on the original design and construction of the dam, including the drawings of the dam, topographic maps, amount and densities of the material that constructs the dam (sand to gravel grain sizes). Site investigation data include information about lithology and the strike and dip of main structures. We also have access to information as to how the dam was constructed.

3.2.2. Acquisition of new engineering geological data

Table 2 summarizes the types of field- and laboratory measurements that have been conducted, and the anticipated use of the data. Below follows a brief presentation of methods used and how the parameters of interest are determined.

Parameters of rock blocks

We are interested in the parameters for describing the parameters of the intact rock blocks (Table 1). Of these parameters, only the bulk density may be directly measured in the laboratory using the new data acquired during the field campaign. The bulk- and dry density (ρ and ρ_d , respectively), and water content (w) may be calculated from the weight- and volume of wet samples (M and V , respectively), and the weight of dry samples (M_s) [17]:

$$\rho = M / V \quad [\text{Eq. 1a}]$$

$$\rho_d = M_s / V \quad [\text{Eq. 1b}]$$

$$w = \frac{M_w}{M_s} \cdot 100 = \frac{M - M_s}{M_s} \cdot 100 \quad [\text{Eq. 1c}]$$

The Bulk- and Shear Modulus (K and G , respectively) are calculated from the different estimated of Young's Modulus (E , E_m and E_i) and Poisson's ratio (ν) [e.g. 18]:

$$K = \frac{E}{3 \cdot (1 - 2 \cdot \nu)} \quad [\text{Eq. 2a}]$$

$$G = \frac{E}{2 \cdot (1 + \nu)} \quad [\text{Eq. 2b}]$$

Values of E and ν are normally obtained from uniaxial compressive strength tests on intact core samples [19]. Unfortunately, the core quality did not allow us to conduct these tests on the available cores. Below, we summarize the different methods that were used to assess the Young's Modulus.

Four rock classification systems are used to first estimate the Young's modulus (E_m) of the rock mass from the field data: Rock Quality Designation index (RQD) [20]; Rock Mass Rating (RMR) [21]; rock mass Quality system (Q) [22]; and Geological Strength Index (GSI) [23].

The RQD value is included in the three other systems, and because no cores were available, RQD is obtained using mean discontinuity frequency per meter (λ) [20]:

$$RQD = 100 \cdot e^{-0.1 \cdot \lambda} \cdot (0.1 \cdot \lambda + 1) \quad [\text{Eq. 3}]$$

Table 2. Investigations and results of field- and laboratory measurements

Type of investigation	Anticipated results
FIELD MEASUREMENTS	
Fracture mapping	Available discontinuities in the tunnel were mapped to determine strike, dip, aperture, fracture filling, hardness of joint surfaces, presence of water.
Schmidt hammer testing	The uniaxial strength of the rock mass was obtained from the rebound number (R) and the dry density of samples
Joint roughness mapping	The roughness of joint surfaces were compared to roughness profiles to obtain a quick estimate of the Joint Roughness Coefficient (JRC)
Rock mass classification	The data collected in the tunnel was used for constraining the quality of the rock mass using three rock mass classification systems: Rock quality designation (RQD), Rock mass rating (RMR), Rock tunneling quality index (Q), and Geological strength Index (GSI)
Coring	A portable drill was used to collect drill 24-mm-diameter core samples. These intact rock samples are later used for laboratory measurements.
Collecting samples	Loose or easy accessed larger samples are collected using a hammer
LABORATORY TESTS	
Index properties	Index properties including bulk- and dry- density, and water content were determined from the weight and volume of the wet samples and the dry weight of the samples.
Point load index testing	Point load index can be used to estimate the uniaxial strength of rock
Tilt test	The basic friction angle was determined on larger rock samples collected in the tunnel

In the RMR classification scheme, the sum of six parameters yields a RMR value [21]. The six parameters are the uniaxial strength of intact rock, RQD , discontinuity spacing, joint condition, ground water condition, and joint orientation. For $RMR > 58$, E_m is estimated from [21]:

$$E_m = 2 \cdot RMR - 100 \quad [\text{Eq. 4}]$$

Romana [24] discussed the application of the RMR classification system to dam foundations, and identified several problems; for example, how the water pressure is accounted for; how the joint orientation is quantified; how the ground water condition is addressed. Romana [24] suggests: (1) The Young's modulus of the rock mass (E_m) depends on the anisotropy and maximum stress direction. For anisotropic rock masses, the stress effect results in a minimum Young's Modulus ($E_{\min} = E_m - 16$), and a maximum Young's Modulus ($E_{\max} = E_m + 8$); and (2) The pore pressure

influences E_m . Most of authors use the same value of E_m before and after the first filling of the water storage basin. Romana [24] suggests to subtract 10 from RMR value to get E_m saturated. The Q -system classifies the rock mass using six parameters [22]:

$$Q = \frac{RQD}{J_n} \cdot \frac{J_r}{J_a} \cdot \frac{J_w}{SRF} \quad [\text{Eq. 5a}]$$

Besides RQD , Q consider the number of the fracture sets (J_n); the roughness (J_r) and alteration (J_a), the water pressure (J_w), and the stress reduction factor (SRF). The Young's Modulus for rock mass (E_m) is obtained from [22]:

$$E_m = 25 \cdot \log(Q) \quad [\text{Eq. 5b}]$$

The reduction in rock mass strength in various geological settings is assessed in the GSI system [23]. In this system, the Young's modulus of intact rock (E_i) and the rock mass (E_m) may be estimated from the modulus ratio (MR), uniaxial compressive strength of intact rock (σ_{ci}) and the disturbance factor (D) using:

$$E_i = MR \cdot \sigma_{ci} \quad [\text{Eq. 6a}]$$

$$E_m = E_i \cdot \left(0.02 + \frac{1 - D/2}{1 + e^{\left(\frac{60 + 15 \cdot D - GSI}{11}\right)}} \right) \quad [\text{Eq. 6b}]$$

The disturbance factor has a significant influence on the rock mass modulus of deformation, but no precise guidelines exists on how to select MR and D , because it varies for each application [25]. In a case study on Canadian dams, D was set to zero for dam foundation rock [25]. The values of σ_{ci} may be obtained from Schmidt hammer tests, $I_{s(50)}$, and uniaxial compressive strength tests.

During Schmidt hammer testing, a spring-loaded piston is first pressed and then released against a rock surface, providing a rebound value (R). To allow statistical analyses, at least 20 measurements are made at each location. The obtained rebound values are subsequently normalized with respect to the horizontal impact direction, and the type of Schmidt hammer used. The unconfined compressive strength (σ_c) is subsequently obtained from R and dry density (ρ_d) [e.g. 26; 27]:

$$\log(\sigma_c) = 0.00088 \cdot \rho_d \cdot R + 1.01 \quad [\text{Eq. 7}]$$

The point load strength index ($I_{s(50)}$) is determined from the failure strength (P) and the equivalent diameter of the sample (D_e) [28]:

$$I_{s(50)} = \sqrt{(D_e/50)^{0.45}} \cdot \frac{P}{D_e^2} \quad [\text{Eq. 8a}]$$

Various shapes of samples may be tested, which is reflected in the determination of D_e . For diametric core samples, the effective diameter (D_e) is equal to the diameter of the core sample (D). For axial core samples and irregularly shaped lumps, D_e corresponds to the minimum cross sectional area of the plane through the platen contact points [c.f. 28]. There is an approximate correlation between $I_{s(50)}$ and σ_c , that is site specific. On average, σ_c is 20-25 times the $I_{s(50)}$, but this ratio may vary in the range of 15-50, and higher for anisotropic rocks [28; 29]. We have estimated σ_c from [30]:

$$\sigma_c \approx 24 \cdot I_{s(50)} \quad [\text{Eq. 8b}]$$

The Poisson's ratio (ν) could not be measured in the field or in the laboratory. We consult available literature and also obtain a measure of ν from the stress gradients of the average horizontal- and vertical stress (σ_{hh} and σ_v , respectively) and the stress ratio (k) [e.g. 18]:

$$k = \frac{\Delta\sigma_{hh}}{\Delta\sigma_v} = \frac{1-\nu}{\nu} \quad [\text{Eq. 9}]$$

Discontinuities

Eight parameters are needed for describing the rock mechanic response of discontinuities (Table 1). In addition, we also need to know the strike and dip of the major fracture groups, which subsequently, is converted to apparent strike and dip along the two profiles A-A' and B-B' (Figure 1).

The basic friction angle (ϕ_b) of rock sample is directly measured in tilt tests. The upper- and lower parts of a sawed rock sample are placed on a tilt table, which is gradually raised until the upper part of the sample starts to slide. The self-weight of the upper sample is providing the normal- and shear stress that is acting on the surface, and the angle of onset of sliding corresponds to ϕ_b . The test is repeated to account for the normal distribution. The residual friction angle (ϕ_r) may be obtained

from the basic friction angle and Schmidt rebound values of dry unweathered surfaces (R) and wet joint surfaces (r), respectively [26]:

$$\phi_r = (\phi_b - 20) + 20 \cdot (r/R) \quad [\text{Eq. 10}]$$

Values of normal stiffness (K_n) and shear stiffness (K_s) are obtained from review of the test on the same type of rock. Joint deformation may be expressed in terms of K_n and K_s , and they correspond to the rate of change of normal stress with respect to normal displacement, and the rate of change of shear stress with respect to shear displacement, respectively [31]. It is difficult to determine the magnitudes of normal- and shear stiffness for discontinuities because of the dependencies on magnitudes of normal- and shear stresses (σ_n , τ) [32]. Each stress increment corresponds to a unique stiffness value. For mated fractures, Goodman et al [31] describe the relationship between stress and stiffness by an empirical hyperbolic fracture closure law. Bandis et al [32] use a semi-logarithmic closure law to describe the relationship between stress and stiffness for non-mated fractured. The Håckren fractures are considered to be mated; hence, a hyperbolic fracture closure law has been adopted.

The initial normal stiffness (K_{ni}) and the initial aperture (a_i) of a joint under self weight ($\cong 1$ kPa) is obtained from [32]:

$$K_{ni} = -7.15 + 1.75 \cdot JRC + 0.02 \cdot \left(\frac{JCS}{a_i} \right) \quad [\text{Eq. 11a}]$$

The joint roughness coefficient (JRC) is obtained from comparing roughness measurements on fractures surfaces in the inspection tunnel with joint roughness profiled [e.g. 26], the joint compressive strength (JCS) is obtained from Schmidt hammer rebound tests, and the initial aperture is obtained from [32]:

$$a_i = \frac{JRC}{5} \cdot \left(0.2 \cdot \frac{\sigma_c}{JCS} - 0.1 \right) \quad [\text{Eq. 11b}]$$

The relationships in Equations (11a) and (11b) are only valid for very near surface rocks (i.e. less than 0.1 m depth for a horizontal discontinuity and a rock bulk density of 2700 kg/m³). For rocks at greater depths, the normal stiffness (K_n) is obtained from K_{ni} , σ_n and the average maximum closure (V_m) [32]:

$$K_n = K_{ni} \cdot \left(1 - \frac{\sigma_n}{V_m \cdot K_{ni} + \sigma_n}\right)^{-2} \quad [\text{Eq. 11c}]$$

The shear stiffness may be estimated from [26]:

$$K_s = \frac{100}{L} \cdot \sigma_n \cdot \tan\left(JRC \cdot \log\left(\frac{JCS}{\sigma_n}\right) + \phi_r\right) \quad [\text{Eq. 12}]$$

where L is the joint length. Bandit et al [32] propose that the joint stiffness is much lower in the tangential than in the normal direction and that the ratio of normal- to peak shear stiffness is not constant value that depends on the magnitude of normal stress. Bandis et al [32] presented a significant experimental work on rock joint deformation.

The two parameters (cohesion and tensile strength) could not be determined directly or indirectly from the field measurements. Cohesion and tensile strength are generally depended on the joint infilling material. Swedenborg [33] argued that because rock joints correspond to rock mass discontinuities, the cohesion and tensile strength are zero. Barton and Choubey [26] argue that if the critical joints are clay filled or planar then it is advisable to use residual friction angle in the design. At such conditions the dilation angle is assumed to be zero for all practical purposes.

4 Model input data

4.1 Populating the UDEC model (Field and laboratory results)

4.1.1. Intact rock

Subsamples with a diameter of 24 mm were cored from four locations in the inspection tunnel (Figure 1). Abrahmsén and Edlund [16] reported that the rock in the southern part of the foundation (from 210 to 370 m of the inspection tunnel) is worse quality than in the northern part. Three of the four sample locations within the inspection tunnel focused on the presumed weaker rocks (c.f. locations 1 to 3 of Figure 1), whereas location 4 is supposedly sampling better quality rocks. After coring, the samples were wrapped in plastic foil and stored in closed boxes to preserve the natural water content. Before testing, the samples were stored in a tank with distilled water for at least 3 days prior to testing. Measurements of the wet- and dry mass and wet volume were used to measure the index properties in accordance with ISRM [17]. Sample mass was measured using an electronic balance (A&D EK-600G), which has a 600 g weighing capacity and an accuracy of 0.1 g. The volume was calculated from measurements with a digital caliper with an accuracy of 0.1 mm.

The height of the sample was measured twice, and the diameter of sample was measured in three locations: Near the base-, middle- and top height of the sample, the diameter was measured in two orthogonal directions.

In total, bulk density and water content was measured on 91 core samples, dry density was measured on 41 samples, and point load strength index was measured on 51 samples. At each location within the inspection tunnel, the number of subsamples varies from 6 to 13. The bulk density from the 91 samples varies from 2.57 to 2.82 t/m³, and the average bulk density is 2.70±0.04 t/m³ (Figure 3A). We use the value of average bulk density ($\rho_b = 2.70 \text{ t/m}^3$) for the UDEC model (Table 1).

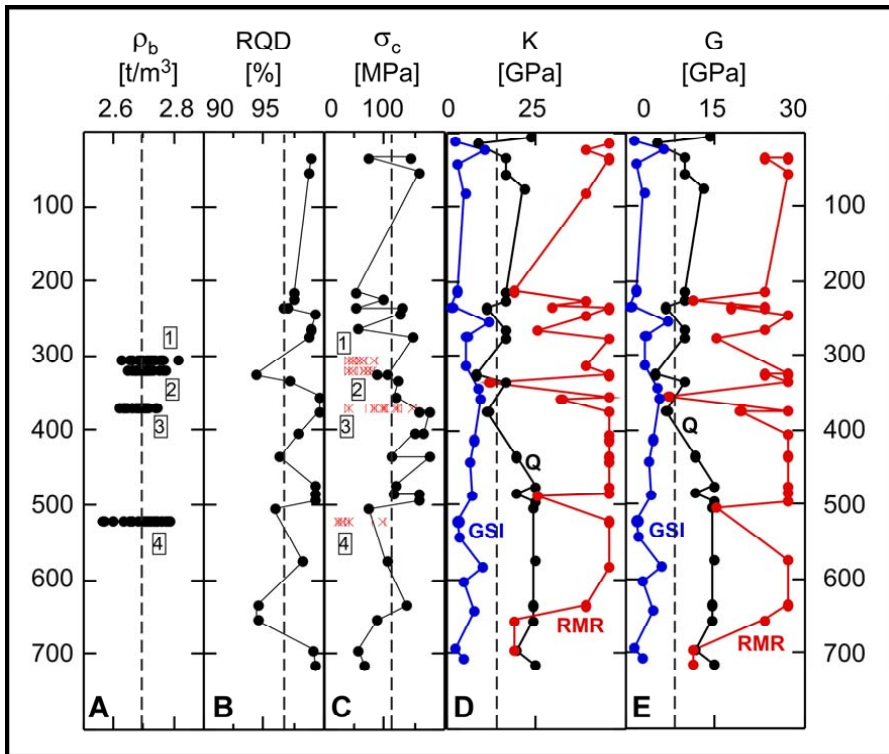


Figure 3. Results on intact rock data from field- and laboratory measurements plotted against tunnel length (c.f. Figure 1 for the length position within the inspection tunnel). A, Bulk density; B, RQD; C, Uniaxial compressive strength calculated from Schmidt hammer tests (black filled circles) and point load strength index tests (red crosses, red vertical bars). The red vertical bars show $\sigma_c = 20 \cdot I_{s(50)}$ and $\sigma_c = 25 \cdot I_{s(50)}$, and the red crosses show $\sigma_c = 24 \cdot I_{s(50)}$; D, Bulk modulus, based on the Young's modulus obtained from RMR, Q and GSI systems; E, Shear modulus based on the Young's modulus obtained from RMR, Q and GSI.

The corresponding variation for the water content is 0.3 to 0.7 %, and $0.5\pm 0.3\%$, respectively. The dry density is slightly lower than the bulk density. For the 41 samples, values of dry density range from $2.59 - 2.77 \text{ t/m}^3$, with an average dry density of $2.68\pm 0.04 \text{ t/m}^3$. In general, we obtain similar results from the four locations, with the exception that there is a tendency for a larger scatter in values at location 4 than at the three other locations.

Shear- and bulk modulus is determined from E and ν (Eq. 2). Because no uniaxial compressive strength tests were conducted, we estimate Young's Modulus from three rock mass classification systems (RMR , Q and GSI). These systems consider several parameters, and RQD commonly is included. The inspection tunnel is characterized by RQD values greater than 94%, and the average RQD value is $98\pm 2\%$, suggesting excellent rock quality (Figure 3B).

The three rock classification systems also provide an estimate of the Young's Modulus of the rock mass (E_m), rather than the intact rock (E); hence, values of E_m is anticipated to be smaller than those of E . However, because the block size is large (up to $4 \times 2 \text{ m}$) and the rock mass at the site is very anisotropic due to foliation and numerous small joints and fractures, E_m is probably reflecting the in situ rock properties better than E . The results from rock mass classification show that the RMR system provides the highest and most scattered estimates of E_m (Table 3; Figure 3), with RMR varying from 59 – 84 and an average of 78 ± 8 , which corresponds to good quality rock. The average E_m is $57\pm 15 \text{ GPa}$, and the average E_{\min} is $41\pm 15 \text{ GPa}$. The RMR compilation also includes a term of rock strength. Figure 3B shows the variation of the unconfined compressive strength obtained from Schmidt hammer tests and point load strength index tests on core samples. In total, σ_c varies from 53–176 MPa, with an average of $116\pm 39 \text{ MPa}$. These values are slightly higher than those obtained from point load strength index tests. Figure 3C, shows the combined results from the Schmidt hammer tests and the point load strength index tests. In general, the Schmidt hammer tests results in a higher σ_c than the corresponding estimates from point load strength index, assuming that σ_c is 20 to 25 times greater than $I_{s(50)}$.

Table 3. Ranges of rock mass parameters used in estimation of RMR and Young's modulus

	σ_c [MPa]	P_1	RQD [%]	P_2	P_3	P_4	P_5	P_6	RMR	E_m [GPa]	E_{min} [GPa]
Maximum	176	12	99.7	20	20	25	7	0	84	68.0	52
Minimum	52.9	7	94.3	20	5	10	7	0	59	18.0	2
Average	116	10	98	20	17	25	7	0	78	57	41
Standard deviation	39	2	2	0	6	3	0	0	8	15	15

Keys: P1. Uniaxial compressive strength; P2. Rock quality; P3. Discontinuity spacing; P4. Condition of discontinuity; P5. Ground water condition; P6. Fracture orientation. σ_c is calculated from (Eq. 6).

Intermediate magnitudes of E_m (28±8 GPa) was obtained using the Q system for which Q values vary from 3 to 30, with an average of 16±10 (Table 4). The average value also corresponds to good quality rock, although Q values from 4-10 are classified as fair, and those from 1-4 are classified as poor in quality. Lowest E_m values are obtained using the GSI system, which suggest an average E_m of 9±5 GPa (Table 5). The GSI values range from 35 to 55, with an average of 45±6.

Table 4. Ranges of rock mass parameters used in estimation of Q and Young's modulus

	RQD [%]	J_n	J_r	J_a	J_w	SRF	Q	E_m [GPa]
Maximum	99.7	6	2	2	1	2.5	30	37
Minimum	94.3	2	1.5	1	0.7	2.5	3	13
Average	98	3	2	1	1	3	16	28
Standard deviation	2	1	0	1	0	0	10	8

Key: Parameters are explained in (Eq. 4a).

Table 5. Ranges of GSI and estimated Young's modulus

	GSI	E_m [GPa]	θ_{rock} [°]	C_{rock} [MPa]
Maximum	55	18	66	1
Minimum	35	2	59	0.24
Average	45	9	64	0.55
Standard deviation	6	5	2.1	0.21

The Poisson's ratio has not been measured in the field or in the laboratory, but often varies from 0.20 to 0.30 in many rocks. The calculation of ν from the stress gradients result in $\nu = 0.24$ if the maximum horizontal stress gradient is taken into account, and in $\nu = 0.34$ if the average maximum horizontal stress gradient is considered. Reported values of Poisson's ratio of slate varies from $\nu = 0.21$ to $\nu = 0.30$ [e.g. 34]. From uniaxial reloading tests on greywacke, Ask [unpublished

results] obtained values $\nu = 0.24$ and $\nu = 0.25$. We select a value of $\nu = 0.25$ for the further calculation of the shear- and bulk modulus.

Figures 3D and 3E shows the variation in Bulk- and Shear Modulus along the length of the tunnel for the three rock classification systems. The trend with lowest values obtained with *GSI*, intermediate values produced by *Q*, and highest values produced by the *RMR* system. Romana [24] discussed various problems with the *RMR* classification system in hydropower dams. Even using the E_{\min} results in significantly higher values.

4.1.2. Discontinuities

Abrahmsén and Edlund [16] report that sedimentary sequences consisting of greywacke interbedded with slate are also folded, which result in wide variations in bedding dips, from sub-horizontal to subvertical. Two dominate fracture systems are associated with the folding. The first fracture system dips steeply to the downstream direction, and strikes perpendicular to the river valley. These fractures are often filled with quartz and calcite. The second fracture system generally strikes parallel to the river. One crush-zone, about 1 m-wide at the surface, was found to strike along the river valley to the east with a dip of 45° . Two additional weak zones strikes along the river valley have steeper dip, in the order of $70-75^\circ$. Complementary measurements of dip and strike of major joints were conducted in the inspection tunnel during the field campaign (Figure 4). The results were analyzed using the program DIPS, which allows graphical and statistical analysis of orientation data [35].

The new data (Figure 4) supports the pre-existing data. The reported fairly flat dip of the rock mass in the upstream direction is presented here by $257^\circ\text{N} / 12^\circ$ discontinuity. Three fracture sets with high dips were observed, which may correspond to the steeply dipping folded strata. Their strikes and dips are $140^\circ\text{N} / 80^\circ$; $018^\circ\text{N} / 89^\circ$, and $229^\circ\text{N} / 89^\circ$. The new measurements indicate the another fracture group, with strike and dip of $179^\circ\text{N} / 48^\circ$ (Figure 4). On the other hand, this fracture group may be associated with the folded strata. We have incorporated thee major geological structures in UDEC Model A, with dip angles 12° , 50° , and -85° . Transformation of discontinuities into UDEC Model B results in two fracture groups, with dip angles of 12° and 85° .

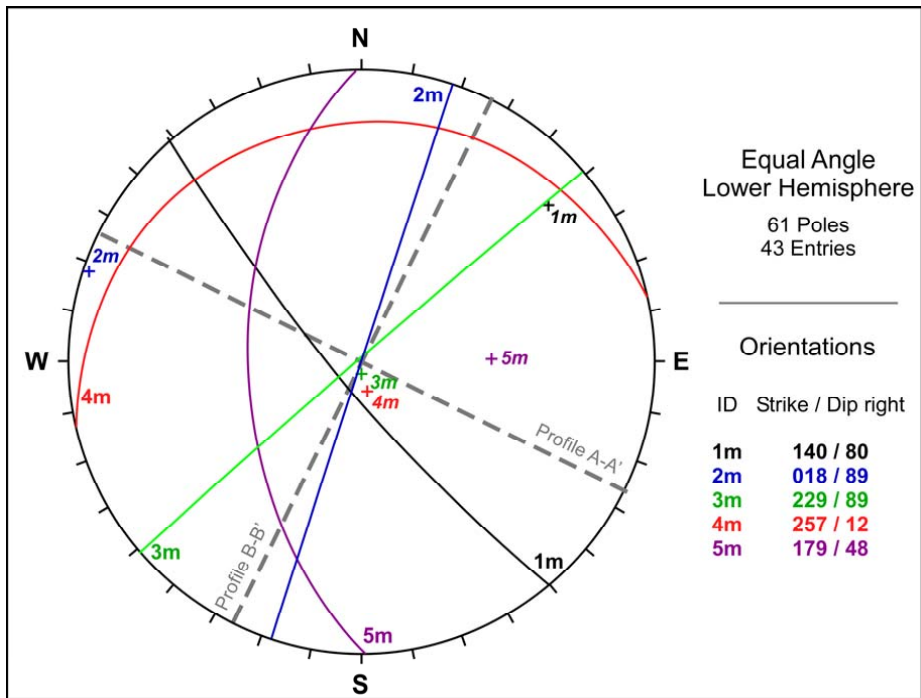


Figure 4. Results from complementary measurements of brittle deformation structures in the inspection tunnel (see location in Figure 1). The orientation of profiles A-A' and B-B' is indicated by the dotted grey line.

Several samples of the rock were delivered from the site of the Håckren dam. They were prepared in the laboratory for the tilt test by sawing them in half. Afterwards each sample was tested by using the tilt table. The basic friction angle varied from 24° to 34° with average of $29^{\circ} \pm 3$. The value of 29° has been used as a basic friction angle for the numerical model, however Barton and Choubey [26] argue that if the critical joints are clay filled or planar then it is advisable to use residual friction angle in the design. The estimation of the residual friction angle was not possible because the samples were destroyed during estimation Schmidt rebound value on dry unweathered sawn surfaces. Therefore the residual friction angle was calculated by a reduction of basic friction angle by 3° (the lowest mean value). The filling of the discontinuities with cement suspension has not effect on the basic friction angle, however during the shearing it may act as a lubricant. Swedenborg [33] performed a series of shear tests on grouted and ungrouted joints and showed that a drop of shear resistance, up to approximately 8° - 10° compared to identical ungrouted samples, therefore the grouted discontinuities have lower residual friction angle (Table 1)

The information regarding the normal and shear stiffnesses of the discontinuities is not available. Using Eq. 11a and 11c it was possible to approximate the normal stiffness of the discontinuities lying above and below 25 m depth (Table 1). Shear stiffness has been estimated based on the presented results of the experimental work by Bandis et al. [32]

Using the field and laboratory data and Eq. 11b the approximation of the aperture at the surface rock mass, 0.152 mm, has been identified. This value is in good agreement with the data presented by Barton et al [36]. According their numerous borehole pumping tests performed at US dam sites in the depth range 0-60 m most conducting apertures were in the range of 0.05-0.15 mm at this shallow depth. Neither the high normal stress nor the filling of the discontinuities with cement suspension is capable complete seal the aperture, therefore the residual value has been established on the level 0,05 mm which is the limit for passing the cement suspension within the discontinuity. The maximum aperture was set to 2 mm. It is more based on numerical approach then on field and laboratory tests. This magnitude is a good indicator of adverse condition of the discontinuities, at the same time it keeps the calculation time within the reasonable limits.

4.2 Rock stress

It is generally agreed that the in-situ stress field in the upper most crust (down to 4 – 5 km depth) is caused by gravity, deformation (tectonic forces), and temperature gradients, and that rock property contrasts, topography, stress relaxation, rock strength, and pore fluids influences the stress field [e.g. 37; 38]. The stress field in this part of the crust is often assumed to be linearly elastic and taking account for gravitational and tectonic stresses [e.g. 38]. Stress gradients are often used to describe the variation of the three principal (or two horizontal and one vertical) stresses with depth, but this requires that the concept of continuum is fulfilled. The in situ stress field in the uppermost part of Earth's crust is characterized by a large scatter in situ stress magnitudes, because the stress field is not continuous at these depths [e.g. 18; 39; 40; 41]. In Scandinavia, topography, discontinuities and variation in rock properties result in scattered in situ stress measurements down to ~400 m depth [42]. Below this depth, the stress field is characterized by high horizontal stresses, with a NW-SE mean orientation of the maximum horizontal stress [e.g. 43].

No stress measurements has yet been made in the area of the Håckren dam. Based on the deformation history and information from exploration drilling and grouting [16], we assume that the extensive jointing significant reduce the magnitudes of near-surface in-situ stress (0-25 m depth). We are aware drawbacks of applying stress gradients at shallow levels in the rock mass. However, the application of stress gradients even at shallow depths in UDEC result in the same result as only

gravitational stresses are applied. Furthermore, the application of stress gradients is more time effective than applying gravitational and topographic stress fields (see further Section “Sensitivity analyses”). All stress gradients, the vertical- and maximum and minimum horizontal stress gradients (σ_v , $\sigma_{H \max}$ and $\sigma_{h \min}$, respectively) increase linearly with depth, with $\sigma_{h \min}$ being slightly smaller than that of the vertical stress (σ_v), and $\sigma_{H \max}$ is taken from Sjöberg et al [44]:

$$\sigma_{H \max} = 0.085 \cdot z \quad [\text{Eq. 13a}]$$

$$\sigma_{h \min} = 0.022 \cdot z \quad [\text{Eq. 13b}]$$

$$\sigma_v = \rho \cdot g \cdot z \quad [\text{Eq. 13c}]$$

4.3 Construction of UDEC Models A and B

We have constructed two UDEC models along profiles A – A’ and B – B’, respectively (Figures 1 and 3). In both models, the intact rock blocks have been discretized into deformable triangular finite-different zones. To achieve good resolution in the areas of interest while keeping the calculation time within reasonable limits, the models have been subdivided into three areas with three different zone sizes: 2, 6 and 18 m, in which the area with discontinuities lying close to the dam has the lowest size, while the area at the bottom has the highest size (Figure 2). The elastic-plastic with Coulomb slip failure and residual values constitutive model has been used for discontinuities, and pure elastic model for the blocks (Table 1). Low normal stress level governing the problem justified the use of linear failure envelope [11]. The characteristics of discontinuities in the rock mass have only been applied into the first area with zone size of 2 m. The hydrostatic pressure on the interface is applied through the distribution of the water in the upstream part of the supporting fill.

In UDEC Model A, the dam body is located in the central part of the free surface (ground surface) to allow observation of the behavior of the rock mass on the both sides of the dam. The dam body is simulated as a two layered block (Table 1 and Figure 5A) with linearly elastic and isotropic conditions. The outer block corresponds to the supporting fill and is permeable for water, whereas the inner block corresponds to the core, which is impermeable for water. The interface between the dam and the foundation rock has zero cohesion and tensile strength, but the friction angle is high to prevent sliding of the dam [12; 44; 45].

The main purpose of the grout curtain is to prevent the extensive movement of the water in the upper foundation rock. Based on the assumption that grouting work has been performed thoroughly at the moment of the construction of the dam the hydraulic aperture of the grouted discontinuities

had been set to low values (Table 1). Introduction of the grout material into the discontinuity gives also a slight reinforcing effect in term of cohesion bond [33]. Additionally Swedenborg [33] performed a series of shear tests on grouted and ungrouted joints and showed that a drop of shear resistance, up to approximately $8 - 10^\circ$ compared to identical ungrouted samples.

In UDEC Model B, the storage basin is located in the center of the model, as reflected by the topography of the upstream side of the dam (Figure 5B). This model will allow us to analyze the response of the rock mass under the floor of the storage basin, and along its banks.

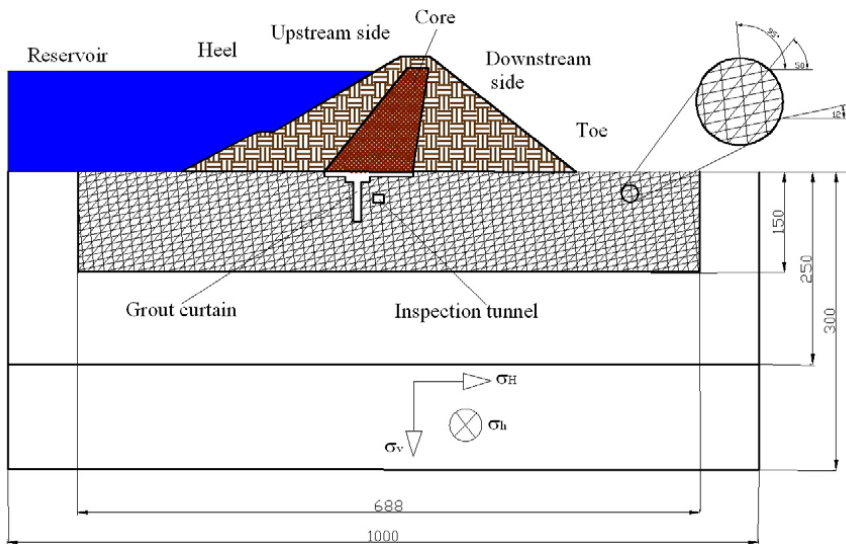
We have subdivided the properties of the discontinuities into two categories: The first group regards the upper bedrock (0 – 25 m), whereas the second group regards the lower bedrock (26 – 300 m) in UDEC Model A. In case of UDEC Model B the upper bedrock is 0 – 83 m and the lower bedrock is 83 – 300 m. The depth of the grout curtain is up to 25 m in the Håckren dam [16]. In general, the grout curtain is extending over depths with fractured rocks and poor rock condition. Hence, groups 1 and 2 of Model A–A' reflect poor and good rock conditions, respectively. In Model B–B', the height of water in the storage basin is taken in account. Hence, the boundary between groups 1 and 2 occurs 26 m below the floor of the storage basin, which corresponds to 83 m in the model. The stress gradients $\sigma_{H \max}$ and $\sigma_{h \min}$ are oriented out-of-plane and in-plane, respectively, in UDEC Model B.

4.4 Calculation sequence

The numerical analyses are made in three steps. The first step comprises the selection of the layout and the parameters of the rock mass, grout curtain for UDEC Models A and B (Figure 2; Table 1). The second step consists of execution of the verification model. The third step is composed of running and monitoring the developed models for UDEC Models A and B for the shear and normal deformations, the inflow into the inspection tunnel and the pore pressure redistribution in the foundation rock

The verification model was executed during the second step. It was conducted to determine the constitutive model of the intact blocks in the model. For that reason the blocks were assigned the elastic perfectly plastic constitutive model. The close observation showed that loads caused by the dam and the water in the storage basin and in-situ stress field were not enough to cause significant plastic deformations within the intact blocks. Therefore in further simulations the linearly elastic, isotropic constitutive model was adopted.

A



B

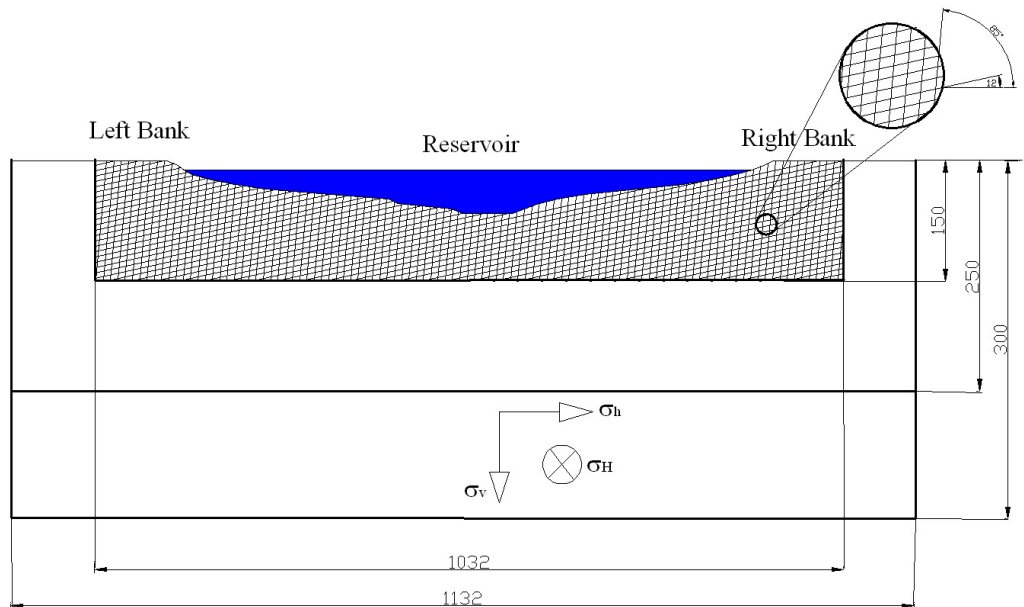


Figure 5. Layout of the UDEC models of the Håckren dam. A, UDEC Model A. The maximum horizontal stress is oriented in-plane (and strikes in the WNW – ESE direction) and the minimum horizontal stress is oriented out-of-plane; B, UDEC Model B. The maximum horizontal stress is oriented out-of-plane and the minimum horizontal stress is oriented in-plane. Figure 1 shows the location of profiles A–A’ and B–B’.

In step three, the rock mass response from dam operations is studied along UDEC Models A and B. The registered inflow into the inspection tunnel and redistributed pore pressure in the rock mass has been compared with the monitoring field data [15; 46]. The shear and normal deformations were registered for both cross-sections and compared with literature data. Each simulation in analysis followed the same calculation sequence as described by Bondarchuk et al. [12]. The first phase in the calculation sequence predates the construction of the dam and its storage basin representing the undisturbed area. The model is run to equilibrium in a “pre-excavation” state during which in situ stresses, load and boundary conditions are applied. The second phase includes the construction of the Håckren dam and the excavation of the storage basin along UDEC Models A and B, respectively. The dam construction is performed in two steps to prevent possible dynamic loads on the foundation rock. The storage basin is excavated in seven steps to prevent heaving caused by the ground water and stresses. The first filling of the storage basin is immediately succeeding construction the dam. The water level is raised to 50 m in two steps to prevent dynamic load on the rock surface. The seasonal variation of the water level in the storage basin is simulated through similar gradual changes in water table 2 times 25 m, which represents the critical levels. First, the water table is reduced to a level of 25 m, and then returned to a level of 50 m. Steady state flow logic [13] is applied during these simulations to reflect water movements in the rock mass. The reported displacements along the discontinuities are total displacements (accumulative), therefore they have not reset between different stages. For UDEC Model A, recording of displacements started from the moment of construction of the dam. In case of UDEC Model B, recording started at the first filling of the storage basin.

5 Validation of model during sensitivity analyses

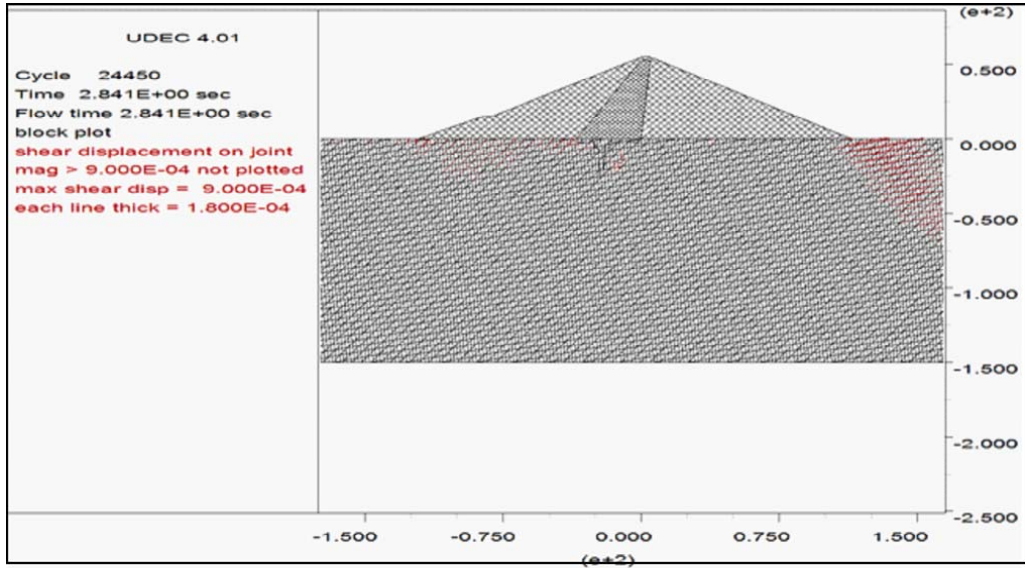
We are validating the new UDEC models in three ways: First, we observe the location and order of shear- and normal displacements that are generated along UDEC models A and B in the sensitivity analyses when the water level in the storage basin is varied. The results are compared with literature. Second, we compare leakage data that have been monitored in the inspection tunnel with values obtained from UDEC Model A [46]. Third, we compare data from pore pressure measurements in the inspection tunnel with pore pressure redistribution in UDEC Model A in the rock mass [15]. Finally, we are giving a brief comment on the quality of the indata to the numerical model.

5.1 Shear- and normal displacements

The first filling of the storage basin resulted in development of shear displacements under the heel and toe of the dam in UDEC Model A (Figures 6). The magnitudes of the shear displacements were less than 1 mm, but they occurred along different type of discontinuities. Under the heel, displacements are concentrated along the discontinuity with a dip angle of 50°, whereas most shear displacements under the toe of the dam on the downstream side occur along sub-horizontal discontinuities. The latter is interpreted to be induced by induced by a push effect of the water in the storage basin. The normal displacements in the foundation rock have localized manner and are less than 0, 1 mm. Small opening of discontinuities during shearing is related to the quite smooth surfaces of the discontinuities at the Håckren dam site, which has been applied to the model by using 0 dilation angle.

The first filling of the storage basin with water in UDEC Model B results in development of the localized shear displacement area along the sub-horizontal discontinuities located close to the surface in the B-floor area (Figure 7). However the magnitude is very small, less than 0,5 mm. The more important is the opening of the same discontinuities, with magnitude up to 2 mm. This behavior is expectable because of the more significant reduction of the effective stresses on these discontinuities.

A



B

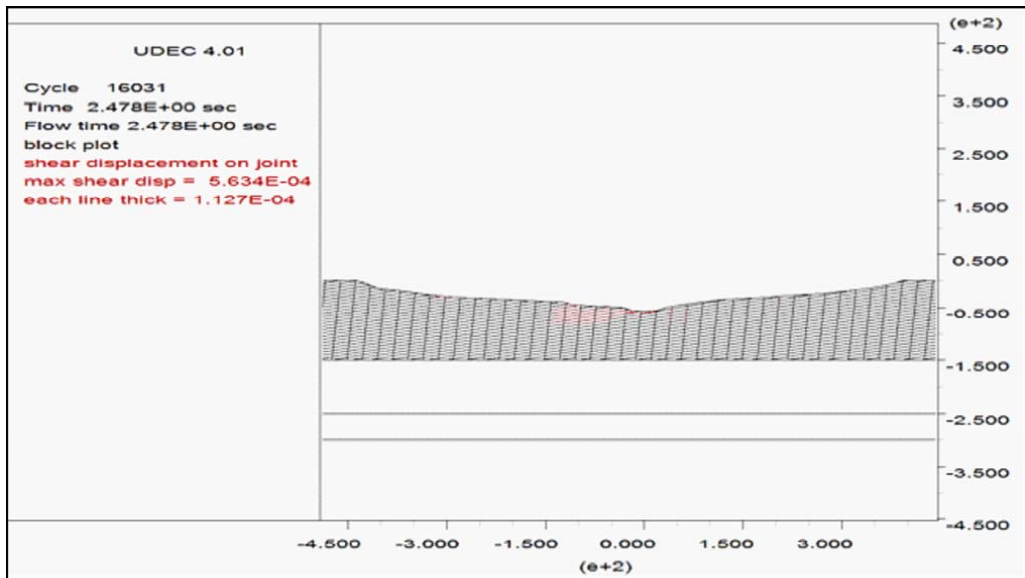


Figure 6. Shear displacements observed after the first filling of the storage basin. A, UDEC model A; B, UDEC model B. Deformations, up to 0.9 mm and up 0.56 mm, respectively. Figure 1 shows the location of profiles A-A' and B-B', respectively.

5.2 Leakage monitoring

Data on leakage into the inspection tunnel has been regularly collected since the construction of the dam. Sjödin [46] provided digital data from January 1966 to March 2009. The inspection tunnel is located downstream of the grout curtain (Figures 2, 3A), and leakage water is pumped out from a shaft situated at the beginning of the access tunnel [15]. About 16 10-m-long vertical drainage holes were originally drilled into the floor of the inspection tunnel. Later, four 10-m-long inclined drainage holes were drilled into the tunnel roof in the upstream direction. Figure 7 shows the variation in leakage from the first ten years of dam operation as a function of the depth of the water table [46].

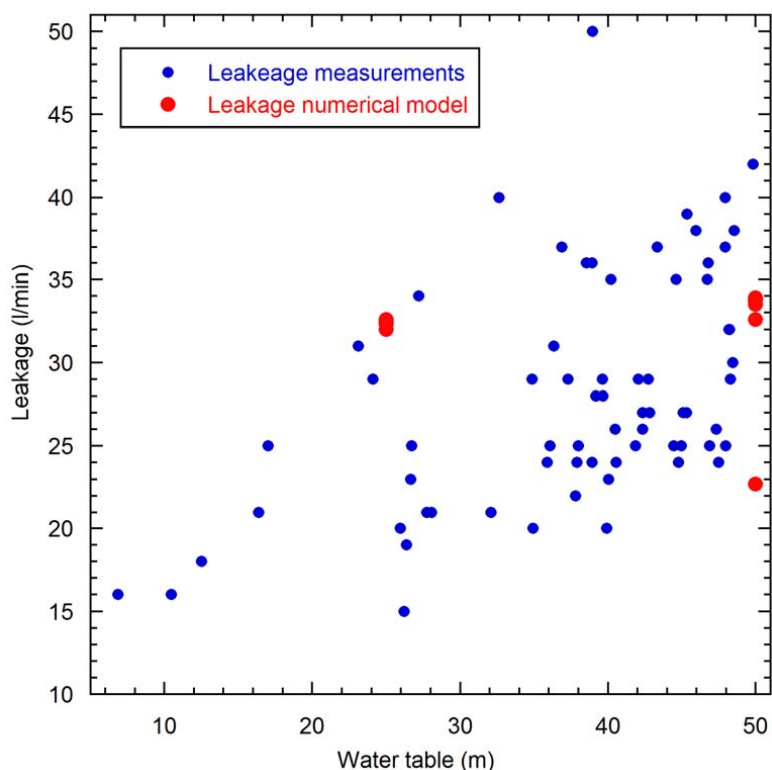


Figure 7. Leakage plotted against the depth of the water table in the inspection tunnel for real leakage measurements (blue filled circles) from 1966 to 1976, and numerical modeling data (red filled circles).

The depth of the water table varies from ~8 to 50 m for the real data. The leakage data is rather scattered and varies from ~15 to 42 l/min, following a general trend with increasing leakage as a

function of the level of the water table. Leakage data from the numerical sensitivity analyses can only be compared with real data when the numerical model is in equilibrium, which only occur at 25 and 50 m water table. At 25 m water table, the numerical leakage is 32-33 l/min. At 50 m water table, somewhat higher numerical leakage is obtained (33-34 l/min), but also a value of ~23 l/min. Figure 8 shows that the variation of the numerical leakage is within the variation of the real leakage data.

5.3 Pore pressure distribution

About 12 pipes for pore pressure measurements installed in the inspection tunnel [15]. Eight pipes monitored the pore pressure on the downstream side of the grout curtain, and four monitored the pore pressure on the upstream side of the grout curtain. Pore pressure measurements were carried out from 1972 to 1975 [15]. The highest pore pressures were observed at a water level of 492.2 m above sea level (masl). At this time, the pore pressure ranged from 478.8 to 483.9 masl on the upstream side of the grout curtain, and from 430.8 to 462.8 masl on the downstream side of the grout curtain [15]. Hence, the water pressure on the upstream side was ~16-53 masl higher than on the downstream side. This corresponds to a water pressure of 0.16 – 0.53 MPa. Figure 8 shows the pore pressure distribution over UDEC Model A after the first filling of the storage basin / 5 cycles of water loading.

The results from the numerical modeling show that the grout curtain effectively redistributes the pore pressure gradients towards depth downstream of the grout curtain. The pressure differs by ~0.3 MPa across the grout curtain, which is the same order of magnitude as the real data [15].

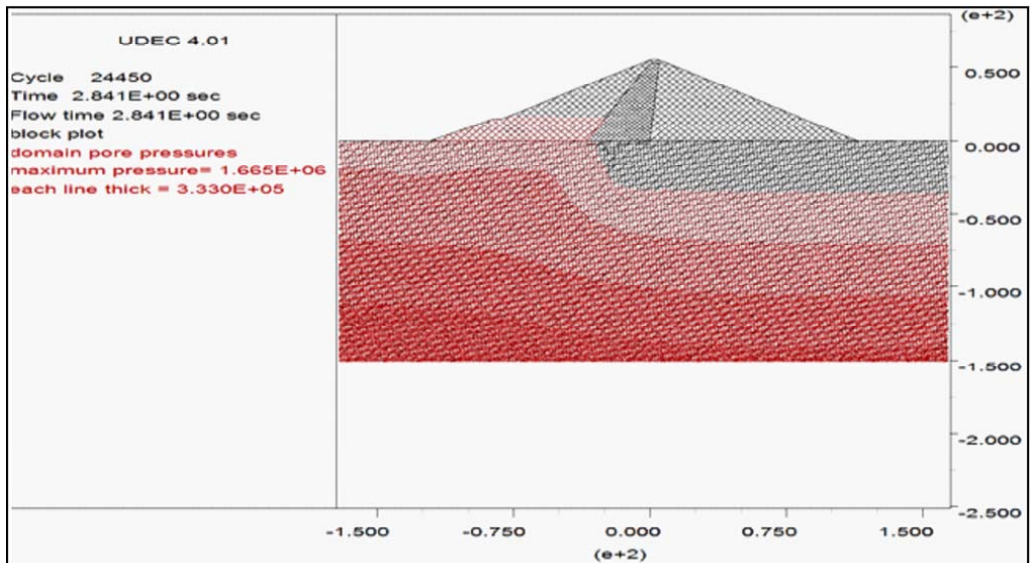


Figure 8. Pore pressure distribution along UDEC model A from the first filling of the storage basing from 0 to 150 m depth. The maximum pore pressure in the model is 1.66 MPa, and countours are given each 0.33 MPa.

5.4 Quality of in data

The validation of data above indicates that we have populated a numerical model that agrees well with the real conditions in Håckren. The field- and laboratory campaigns amounted to about 10 k€. However, the quality of the input data to the numerical models might have improved if we would have achieved better quality cores. We used a hand-held field drill for drilling paleomagnetic cores. This drill was not optimal for drilling cores in the horizontal and inclined orientations. The available core quality was sufficient for index properties and point load strength index tests. However, a wall-mounted drill would have allowed collection of better quality cores, which could have been used for uniaxial compressive strength tests. Such tests provide information on the uniaxial compressive strength, Poisson's ratio, Young's Modulus, and the friction angle.

We have adopted three stress gradients that are believed to fairly well represent the stress field in the region at shallow depths (well above 400 m depth). Because the stress field may be major player in inducing large deformations in the rock mass under a dam complex [12], we suggest to include more than one stress field in the sensitivity analyses in the future. If the stress field is suspected to induce critical displacements, the UDEC models may provide incentive to conduct carefully planned in situ stress measurements.

6 Conclusions

The overall aim of this study is to develop a methodology for analyzing fracture erosion and rock mass stability under an existing hydropower embankment dam complex. We are using the numerical code the distinct-element code UDEC [13]. We have developed two UDEC models for analysis the stability of the rock mass under the Håckren dam complex, in central Sweden. The models have been populated with commonly used cost-effective engineering geology methods that were collected in the field and laboratory. In addition, review of existing data of the dam owners have provided with important insights on details from when the dam was constructed, geological and structural data, as well as some monitoring data. Due to lack of local stress data, we have made informed assumptions based on stress data from Scandinavia [e.g. 42; 43; 47], and information on stress distribution at shallow depths [e.g. 38; 39]. As a result we have applied three stress gradients. The objective of this first paper out of two is to investigate if this approach for collecting new data is satisfactory, or if more cost-intensive investigation methods are needed.

We have validated our numerical models by comparing magnitudes and location of shear- and normal displacement with literature information [8; 48]. The results show good agreement with available monitored data in terms of the pore pressure and water leakage into the inspection tunnel. The available results suggests that we have developed a realistic proper numerical model by using a combination of simple and low-cost (~10 kEUR) field- and laboratory tests and pre-existing data. However, we recommend to improve the core collection so that uniaxial strength tests can be performed, and the model incorporates site data on uniaxial compressive strength, Poisson's ratio, Young's Modulus, and Friction angle. In addition, we also recommend to include two contrasting stress fields into the sensitivity analyses in order to improve the understanding of the role of in situ stresses. With these limitations in mind, it remains apparent that we have developed reliable methodology for collecting data and evaluate of the condition of the rock mass under the dam and in the storage basin. The implications for fracture erosion and bedrock stability due to cyclic variation in water load will be further discussed in part II of this study [12].

7 Acknowledgements

The research presented was carried out as a part of "Swedish Hydropower Centre - SVC". SVC has been established by the Swedish Energy Agency, Elforsk and Svenska Kraftnät together with Luleå University of Technology, The Royal Institute of Technology, Chalmers University of Technology and Uppsala University. www.svc.nu

8 References

- [1] Svenska Kraftnät. Review of Swedish System for Dam Safety: A report to the government. Svenska Kraftnät 2010; Reg. Nr. 2010/877, 46 pp. Available at [www.svk.se/Om-oss/Var-verksamhet/Dammsakerhet/Rapporter on 25 February 2012](http://www.svk.se/Om-oss/Var-verksamhet/Dammsakerhet/Rapporter%20on%2025%20February%202012).
- [2] Bartsch M, Mill O, Birkedahl J, Brandesten C-O, Hammar L, Norstedt U, et al. Peer Review of Swedish High Consequence Dams. Test of a model for “special examination” of dam safety – A compilation of facts and experiences from 5 reviews performed in 2006 – 2008. Svenska kraftnät 2009; PM 17 June 2009, 19 pp. Available at [www.svk.se/Om-oss/Var-verksamhet/Dammsakerhet/Rapporter on 25 February 2012](http://www.svk.se/Om-oss/Var-verksamhet/Dammsakerhet/Rapporter%20on%2025%20February%202012).
- [3] Colback PSB, Wild BI. Influence of moisture content on the compress strength of rock. Proceedings of third Canadian rock mechanics symposium, University of Toronto, 1965, pp. 385-391
- [4] Fell R, MacGregor P, Stapledon D, and Bell G. Geotechnical engineering of dams, Leiden A.A. Balkema; 2005.
- [5] Lee J-Y, Kim H-S, Choi Y-K, Kim J-W, Cheon J-Y and Yi M-J. Sequential tracer tests for determining water seepage paths in a large rockfill dam, Nakdong River basin, Korea. *Engineering geology*, 89, 2007, pp. 300-315
- [6] Mattsson H, Hellström JGI and Lundström TS. On internal erosion in embankment dams. A literature survey of the phenomenon and the prospect to model in numerically. Research report, Luleå University of Technology, 2008.
- [7] Sjö Dahl P, Dahlin T, Johansson S and Loke MH. Resistivity monitoring for leakage and internal erosion detection at Hällby embankment dam. *Journal of applied geophysics*, 65, 2008, pp. 155-164
- [8] Reinius. Stresses and cracks in the rock foundation of an earthfill dam, *Water Power & Dam Construction*, 40, 1988, pp. 33-38
- [9] Johansson F. Shear strength of unfilled and rough rock joints in sliding stability analyses of concrete dams. Doctoral Thesis, Royal Institute of Technology, Stockholm, Sweden; 2009.
- [10] Barla G, Bonini M, Cammarata G. Stress and seepage analyses for a gravity dam on a jointed granitic rock mass, *Numerical modeling of Discrete Materials*, 2004, pp. 263-268
- [11] Dolezalova M. Numerical analysis of an old masonry dam using UDEC, *Numerical modeling of Discrete Materials*, 2004, pp. 269-277

- [12] Bondarchuk A, Ask MVS, Dahlström L-O, Nordlund E. Rock mass behavior under hydropower embankment dams: a two dimensional numerical study. *Rock Mechanics and Rock Engineering*, Springer, 2011. DOI 10.1007/s00603-011-0173-2
- [13] Itasca. *UDEC* version 4.0. Manual. Minneapolis, ICG; 2005.
- [14] Dath J, Lindgren S, Rytters K, Ygland D, Heiner A, Pettersson B, Jonsson B. *Comprehensive dam safety evaluation of the facilities at Håckren*. SWECO VBB VIAK, Sweden; 2002.
- [15] Höeg K, Viotti C, Engström Å, Aufleger M. Håckren dam safety review. Review panel report 2008-12-05. Svenska Kraftnät 2008: 28 pp.
- [16] Abrahmsen R, Edlund L. *Foundation grouting at the Hackren dam*. Proc. Of the 9th International Congress on Large Dams, Istanbul, 1967, pp. 353-366
- [17] ISRM. Suggested methods for determining water content, porosity, density, absorption and related properties and swelling and slake-durability index properties: Part 1: Suggested methods for determining water content, porosity, density, absorption and related properties, *International Journal of Rock Mechanics and Mining Sciences & Geomechanics Abstracts* 1979; 16: 143-51.
- [18] Brady BHG, Brown ET. *Rock Mechanics for underground mining*. 3rd edition. Dordrecht: Springer; 2004.
- [19] Fairhurst CE, Hudson JA. Draft ISRM suggested method for the complete stress-strain curve for intact rock in uniaxial compression. *International Journal of Rock Mechanics and Mining Sciences* 1999; 36: 279-89.
- [20] Priest SD, Hudson JA. Discontinuity Spacings in Rock. *Int. J. Rock Mech. Min. Sci. & Geomech. Abstr* 1976; 13: 135-48.
- [21] Bieniawski ZT. *Engineering rock mass classifications*. New York: Wiley; 1989.
- [22] Barton NR, Lien R, Lunde J. Engineering classification of rock masses for the design of tunnel support. *Rock Mech.* 1974; 6: 189-239.
- [23] Hoek E, Carranza-Torres C, Corkum B. Hoek–Brown failure criterion – 2002 ed. In: *Proceedings of the 5th North American Rock Mechanics Symposium and 17th Tunnelling Association of Canada Conference: NARMS-TAC 2002, July 7–10, University of Toronto*, pp. 267–271. Updated version (October 2, 2002). Available from: www.rocsience.com.
- [24] Romana M. DMR (an adaptation of RMR), a new geomechanics classification for use in dam foundation. 9^o Congresso Luso de Geotecnia, Aveiro, 2004.

- [25] Hoek E, Diederichs M. Empirical estimates of rock mass modulus. *Int. J Rock Mech. Min. Sci.*, 43, 2006, pp. 203–215
- [26] Barton N, Choubey V. The shear strength of rock joints in theory and practice. *Rock Mechanics* 1977; 10: 1-54.
- [27] Aydin A. ISRM Suggested method for determination of the Schmidt hammer rebound hardness: Revised version. *International Journal of Rock Mechanics and Mining Sciences* 2009; 46: 627-34.
- [28] Franklin JA, et al. Suggested method for determining point load strength. *International Journal of Rock Mechanics and Mining Sciences & Geomechanics Abstracts* 1985; 22: 51-60.
- [29] ASTM D5731. Standard Test Method for Determination of the Point Load Strength Index of Rock and Application to Rock Strength Classifications. ASTM 2008; D5731-08.
- [30] Broch E, Franklin JA. The point-load strength test. *Int. J. Rock Mech. Min. Sci.*, 9, 1972, pp.669-697
- [31] Goodman RE, Taylor RL, Brekke TA. A model for the mechanics of jointed rock. *J. Soil Mech. Fdns. Div., Proc. Am. Soc. Civ Engrs*, 94, 1968, pp. 637-659
- [32] Bandis SC, Lumsden AC, Barton NR. Fundamentals of rock joint deformation *Int. J. Rock Mech. Min. Sci. & Geomech. Abstr.* 20, 6, 1983, pp. 249-268
- [33] Swedenborg S. Rock mechanical effects of cement grouting in hard rock. Doctoral thesis, Chalmers tekniska högskola; 2001. ISSN 0346-718X.
- [34] Takahashi N, Kodair S, Nakanishi A, Park J-O, Miura S, Tsuru T, et al. Seismic structure of western end of the Nankai trough seismogenic zone. *Journal of Geophysical research* 2002; 107 DOI:10.1029/2000JB000121
- [35] Rocscience. Graphical and statistical analysis of orientation data. Available on <http://www.rocsience.com/products/1/Dips>; 2012.
- [36] Barton N, Bandis S, Bakhtar K. Strength Deformation and Conductivity of rock joints. *Int. J. Rock Mech. Min. Sci. & Geomech. Abstr.* 22, 3, 1985, pp. 121-140
- [37] Amadei B, Stephansson O. *Rock stress and its measurement*. London: Chapman and Hall; 1997.
- [38] Savage WZ, Swolfs, HS Amadei B. On the state of Stress in the Near-surface of the Earth's Crust. *Pure and applied Geophysics* 1992; 138: 207-28.
- [39] Plumb R, Engelder T, Sbar M. Near-surface in situ stress. A comparison with stress directions inferred from earthquakes, joints, and topography near Blue Mountain lake, New York. *Journal of Geophysical Research*, 89, 1984, pp. 9333-9349

- [40] Hudson JA, Cooling CM. In situ rock stresses and their measurement in the UK—Part I. The current state of knowledge. *International Journal of Rock Mechanics and Mining Sciences & Geomechanics*, 25 (6), 1988, pp. 363–370
- [41] Clement C, Merrien-Soukatchoff V, Dunner C, Gunzburger Y. Stress measurement by overcoring at shallow depths in a rock slope: the scattering of input data and results. *Rock Mech. Rock Eng.*, 42, 2009, pp. 585-609
- [42] Stephansson O, Ljunggren C, Jing L. Stress measurements and tectonic implications for Fennoscandia. *Tectonophysics*, 189, 1991, pp.317-322
- [43] Müller B, Zoback ML, Fuchs K, Mastin L, Gregersen S Pavoni N, et al. 1992. Regional patterns of tectonic stress in Europe. *Journal of geophysical research* 1992; 97: 11783-803.
- [44] Sjöberg J. Personal Communication 2011.
- [45] Johansson F. Personal Communication 2011.
- [46] Sjödin G. Personal communication 2009. Sammanställning Håckren.xls. Leakage data from 1966.01-24 to 2009 -03-10.
- [47] Sjöberg J, Lindfors U, Perman F, Ask D. Evaluation of the state of stress at the Forsmark site. Preliminary site investigation Forsmark area - version 1.2., 2005, SKB R-05-35.
- [48] Singh B. *Engineering for embankment dams*, Rotterdam : Balkema; 1995.

**ROCK MASS STABILITY OF THE HÅCKREN HYDROPOWER
EMBANKMENT DAM IN CENTRAL SWEDEN: PART II —
INVESTIGATING FRACTURE EROSION**

Bondarchuk A, Ask M V S, Dahlström L-O and Nordlund E (2012).

Submitted for publication in the
Rock Mechanics and Mining Science

Rock mass stability of the Håckren hydropower embankment dam in central Sweden: Part II — Investigating fracture erosion

Abstract

The stability of the rock mass under a hydropower dam is important for the functionality and safety of the dam. The static load of the dam complex itself and the annually varying water loads induce deformations in the foundation rock that may lead to different processes such as erosion and reduction of bearing capacity of the dam. The long-term effect from accumulating loads is fairly little known for most existing hydropower dams in Sweden. Considering that at this moment a big number of old dams (constructed in 60-70s) are in operation in Sweden. Presently dam owners in Sweden are trying to guarantee high levels of safety of dams in an international perspective, with priority for dams where the consequences of failure would be particularly severe. In connection with the review of the structural safety of existing dams, it is necessary to perform extensive field and laboratory works both in dams and foundation rock. Examination of foundation rock is troublesome due to its inaccessibility. Such conditions can raise the price of investigation work significantly. Combination of numerical code with simple field and laboratory tests data for preliminary appraisal of the rock mass allows understand the processes in the basement and locate the “weak points” for further thorough examination with more sophisticated approach and equipment.

This paper (Part II) simulates a decade of cyclic variations in water load within the storage basin. By this approach it investigates the relationships between shear- and normal- displacements, and hydraulic conductivity of the discontinuities. The aim of this paper is to forward the understanding of, and to relate the observed displacements with the fracture erosion process within the discontinuities.

The results show that dam tends to slide along subhorizontal discontinuities on the downstream side after first filling of the storage basin. However the following cyclic loading caused by the water in storage basin does not contribute to the development of this sliding. On other hand first filling and exploitation of the Håckrem dam results in the shearing and opening of the discontinuities close to the surface on the upstream side. The total inflow into the inspection tunnel is stabilized after the first year and keeps staying on the same level, while the flow water velocity shows a slight rate increase which may raise a question about erosion in long-term perspective. Analysis showed the stability of foundation rock of the Håckren dam in term of mechanical displacements and flow in evaluated period of time.

1 Introduction

In virtually in all rock mechanics analysis one has to make some assumptions to simplify the problem and allow calculations. A common assumption is that the rock material is linearly elastic. However, in reality, the rock mass contains fissures, fractures, bedding planes, contacts and zones of altered rock, so it is not perfectly elastic. The extent of plastic deformation due to load cycles may be as important as design [1]. This process is very important for dam engineering because seasonal variation of the water in the storage basin induce cyclic loading on the foundation rock mass. As the water level in the storage basin in front of the dam rises, the rock under the dam deforms [e.g. 2]. When the water level subsequently is reduced, the rock mass rebounds elastically, however, not completely because there are still some plastic, permanent displacements remaining. Repeated cycles of loading and unloading in response of cyclic variation of the water in the storage basin produce a series of loops, hysteresis (Figure 1). In the long-term perspective, the plastic displacements generated by subsequent loading and unloading cycles accumulate in the foundation rock mass under the dam. The stiffness in the intact rock is greater than that of the discontinuities [e.g. 3], and because the in situ stress magnitudes are small near the surface, it logical to assume that all displacements are occurring along the discontinuities in the rock mass.

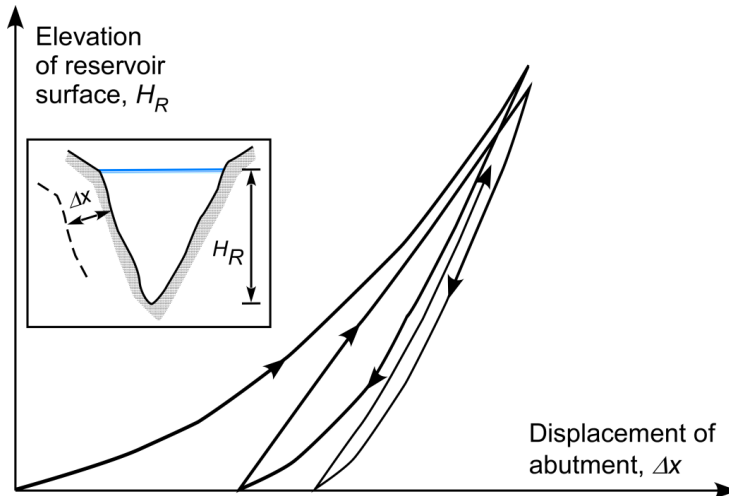


Figure 1. Schematic view of the accumulating plastic displacements occurring in a rock mass [modified after 1].

Knowledge and control of the water flow in the fractured rock mass is critical for maintaining stability and functionality of a dam. It is important to account for water flow in the design and construction of a hydropower dam, and in the subsequent production. Consequently, the

hydraulic properties of rock joints are studied by many authors using different approaches, e.g. evaluation of the bulk hydraulic conductivity, and statistic- and stochastic methods [e.g. 4; 5; 6]. The major part studies investigate the hydraulic conductivity of fractured rock mass, where the fracture network is not affected by processes occurring in the media in time, such as water flow, displacements, and changes in the state of stress [e.g. 7].

Loads imposed by dam construction, exploitation and seasonal variation of the water table in the storage basin causes relative displacements both in tangential- and normal direction to the plane of discontinuity, therefore altering the hydraulic properties of preexisting fractures [e.g. 8; 2]. These movements degrade the dilatancy angle and the asperity of joint surfaces, which may modify the flow characteristics [9; 10]. The characteristics of water flow are also influenced by weathering and alteration of the morphology of the joint surfaces, and the distribution of void spaces [11; 12; 13].

A change in the distribution of void spaces due to displacements may alter the water flow paths, and induce highly irregular preferential flow paths with widely varying velocities, up to about twenty times higher than through other channels [12; 14]. Such significant velocity contrasts, combined with long-term exposure to the flow water in a rock mass under hydropower dam (considering the lifetime of the dam) may result in an erosion process of the joint surfaces and the joint fill gouge material [15; 16], which may gradually deteriorate the grout curtain.

There are a few investigations that evaluate how shearing influence the hydraulic conductivity of a fracture [7; 14; 15]. These studies suggest that asperity degradation due to shearing and the resulting changes in the hydraulic aperture is more difficult to model, compared to asperity degradation due to normal joint displacements.

In this study, we are aiming at investigating the roles of shear- and normal displacement on fracture erosion. It consists of two parts, in which we successfully developed two 2D coupled hydro-mechanical discrete-element UDEC models over the Håckren dam complex in central Sweden (Figure 2) in Part I [17]. UDEC allows the study of deformation along existing discontinuities [18], which is thought to occur in the rock mass in response to annual cyclic variations of water table in the basin. The Håckren dam is a large class 1A embankment dam in central Sweden, i.e. it is a high consequence dam in case of dam failure [19], which is reaching 50 years of operation in 2015. In this paper (Part II), we are investigating the relationships between shear- and normal displacements, and hydraulic conductivity of the discontinuities to forward the understanding of, and to relate the observed displacements with the fracture erosion process within the discontinuities.

This paper (Part II) is divided into three parts: the first reviews the approach, rational and background for the analyses; the second describes the development of the numerical model and

how input data parameters were acquired; and the third validates and discusses the obtained model and our approach. The first part of this paper briefly reviews relationships between shear- and normal displacements, and hydraulic conductivity of discontinuities. We also discuss fracture erosion, and how it is influenced by variations in flow path and –velocity of water. The second part of this paper is concerned with the two UDEC models and the results of ten cycles of varying the water load in the storage basin. The final part of this paper discusses the coupling between the observed shear- and normal displacements and fracture erosion within the Håckren dam rock mass.

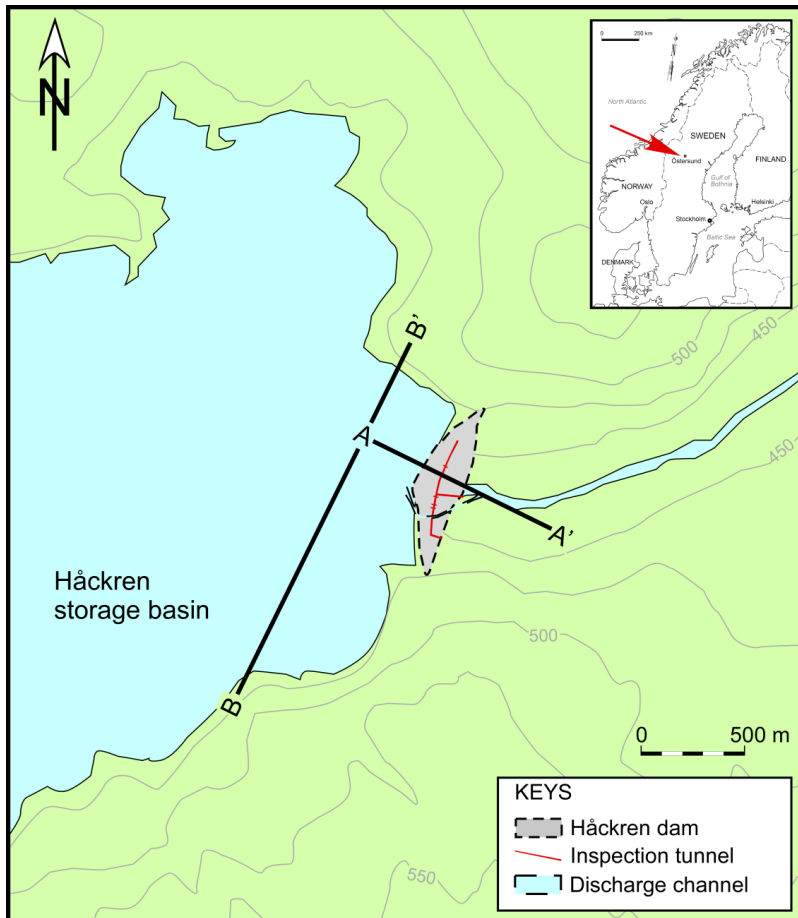


Figure 2. Map of the Håckren dam and the eastern most part of the Håckren storage basin. The red arrow in the inserted map shows the study area. Profiles A-A' and B-B' shows the location of UDEC Models A and B, respectively.

2 Effect of joint degradation on hydraulic properties of rock and fracture erosion

2.1 Phases of shear displacement of discontinuities and its implication on conductivity

Displacement of a discontinuity may take any of the following forms: normal closure, opening, shear and dilation [14], and they all alter the hydraulic properties of the rock mass. To make a model combining all these displacements, it necessary to know a precise characterization of joint roughness morphology and its development with shear displacement in the case of the shear loading conditions [14]. Several studies have focused on hydro-mechanical coupling problems under normal loading conditions [e.g. 10; 13]. The hydro-mechanical coupling is more sophisticated for shear loading conditions, and experimental work is more difficult to perform [20; 7; 15]. One difficulty is to understand the evolution of roughness morphology on discontinuity surfaces under normal stress loading and development of shear displacements [14]. The effect of normal loading is very important for the hydraulic conductivity at process of shearing [9; 14; 15]. Increase of the normal stress results larger damaged zones, reduction of cumulative dilatancy with fewer void spaces and decrease of aperture for the same shear displacement on the discontinuity plane. For lower normal stress and longer shear displacement the aperture in the void spaces will be larger because of the greater cumulative dilatancy. Perturbations of closure-opening (contractancy - dilatancy) for a matched joint under shearing loading will occurs within 2 mm of shear displacement, or even less [14]. The fluid flow will follow the tortuous paths, around the contact areas with widely varying velocities and preferential channels. [14]. This non-linear flow is a result of inertial losses arising from entrance and exhaust boundaries, constrictions and obstructions, and initiation of turbulence due to localized eddy formation [15] .

Movement of water along flow channels in the discontinuities results in water-rock interaction. This interaction includes physical and chemical reactions. Colback and Wild [21] showed that the influence of water-rock interaction on rock mass strength is significant.

Bates and Jackson [22] define wear under geological conditions as the reduction in size or the change in shape of clastic fragments by one or more of the mechanical process of abrasion, impact or grinding. Erosion in turn is the mechanical destruction and the removal of the material by running water, waves and currents, moving ice or wind. Erosion is subdivided into groups a) corrasion – rock is mechanically removed and worn away by the abrasive action of solid materials moved by wind, waves and running water b) corrosion (chemical erosion) – rock is removed or worn away by natural chemical process.

Construction of dam and following filling of the storage basin transmits large loads to the foundation and causes changes in aperture of the discontinuities, which in turn modifies the

natural flow path. Additionally the rock mass is subjected to large difference in hydraulic head between upstream and downstream side of the dam. The cyclic loading caused by variation of water in the storage basin contributes to continuous change in flow path [1; 23]. Vasconcelos Braga Farinha [23] reported that the weathering in the rock mass is responsible for the majority of recorded failures. Subsurface erosion and dissolution were the most significant. These processes resulted in loose of strength and lack of shear resistance along weak planes of unfavorable direction.

Process of erosion is very complicated. However our understanding of long-term behavior of rock mass during geological wear and erosion may be drawn from the results of accelerating testing methods [16]. High-speed fluid flow tests show that two most important parameters influencing the erosion performance, which are flow velocity and exposure time [16]. The functions for both parameters in turn may be subdivided into two sections: an incubation period and an erosion period. Incubation period is characterized by “invisible damage”, because no material is removed and the target material seems to be undamaged. The critical flow velocity, which is also called “erosive velocity” separates incubation and erosion period. It is the velocity of water in a channel above which erosion occur. In term of dam stability, water pressure are the most crucial aspect, however the discharge is also relevant factor. It is connected very close with seepage velocity, which should be limited in order to avoid erosion of material in open discontinuities [23].

3 Numerical simulations

The static load on the rock mass under the Håckren dam is generated by the self-weight of the overlying rock mass and the weight of the embankment dam. The water table in the storage basin is generating additional load that varies over the year. These loads alter the mechanic- and hydraulic properties of the rock mass. Bondarchuk et al. [2] observed that one year of variation in water load in the storage basin caused accumulation of displacement in the foundation rock. This changes the discontinuity roughness morphology and hydraulic conductivity, which is followed by changing the properties of the flow water and its paths [e.g. 14]. To better understand the response of the rock mass under the dam and in the storage basin in long-term perspective, the case study (Håckren dam) has been applied. In the first part of this study [17] the development of the numerical models and its validation is described in detail. Below follows a brief description of the two UDEC models A and B, and the calculation sequence that have been applied.

3.1 Numerical model

We have constructed two 2D UDEC models. In UDEC Model A (Figure 3A) the dam is located in the central part of the free surface and is composed from two layered block corresponding to the core and the support of the dam. In UDEC Model B (Figure 3B), the storage basin is located in the central part of the model and it reveals the topography of the upstream side of the dam.

Table 1 of Bondarchuk et al [17] shows the properties of the UDEC computational mesh, which describes the rock mechanic response of the dam body, the underlying rock mass, and the interface between the two. Three parameters describe the behavior of intact rock block, whereas six parameters describe the rock mechanic response of discontinuities in the dam body and the interface, and nine parameters describe their response in the rock mass.

The dam consists of a support and a core, with low bulk density (2.1 t/m^3) and low bulk- and shear modulus (1 and 0.1 GPa, respectively) to allow produce the correct load pattern (soft material) on the foundation rock. The support and core have been assigned with identical properties for five of the six rock mechanic parameters of the discontinuities: The normal and shear stiffnesses are both set low, to 1 GPa/m, whereas high values have been assigned to the friction angle (85°), and the cohesion and tensile strength ($1 \cdot 10^{14}$ MPa). It is only the aperture that differs, with an impermeable core with zero aperture, and 1.5 mm wide aperture for the support. The interface under the dam is subdivided the same way as the dam. With the exception of zero cohesion, tensile strength and friction angle, the two parts of the interface has the same properties as its corresponding parts of the dam.

The intact rock properties of the rock mass are slightly higher than those of the dam (the bulk density is 2.7 t/m^3 , the bulk modulus is 14 GPa, and the shear modulus is 8.4 GPa). The properties of the open discontinuities depend on depth, and whether the discontinuity has been grouted or not. Above 25 m depth, there are open and grouted discontinuities. Below this depth there are only open discontinuities, no grouting. The open discontinuities above 25 m have normal- and shear stiffness (14.27 and 0.6 GPa/m, respectively), friction and residual friction angles of 26° , the aperture and residual aperture of 0.152 and 0.05 mm respectively. Cohesion and tensile strength are zero for these discontinuities. The grouted discontinuities have almost the same properties with exception for cohesion (0.6 MPa), tensile strength (0.6MPa), residual friction angle of 21° and initial aperture of 0.05mm. Below 25m, the open discontinuities have normal- and shear stiffness (93.81 and 1.1 GPa/m, respectively) and the initial aperture of 0.05 mm. The rest of the parameters are the same as in discontinuities above 25 m.

To shorten computational time the models are divided into three areas, with zone sizes 2 m, 6 m, and 18 m. The intact blocks are discretized into triangular finite-different zones, but the discontinuity characteristics of the rock mass are only applied into the inner area with a zone size

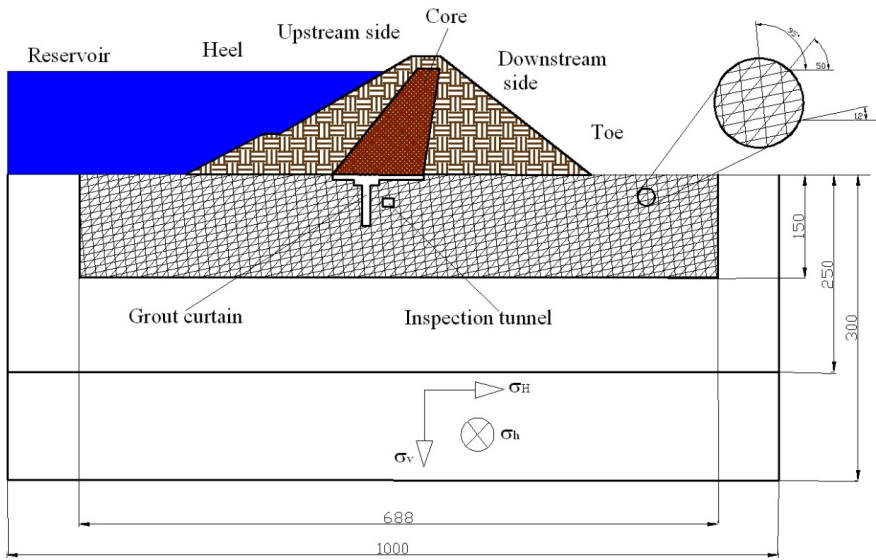
of 2 m. UDEC model A consists of three sets discontinuities, whereas only two discontinuity sets is included in UDEC model B. To account for an upper zone with very fractured rock, the rock mass is subdivided into an upper layer (0-25 m in UDEC model A, and 0-83 m in UDEC model B) and a lower layer down to 300 m depth, to the lower boundary of both models (Figure 3). The blocks are analyzed using an elastic model, and the discontinuities are modeled using an elastic-plastic with Coulomb slip failure and residual values constitutive model. This criterion implies that if the shear- or tensile strength is exceeded in a discontinuity, the residual values for friction, cohesion and tension will be used in all subsequent calculations [18].

The models have roller boundary conditions on all sides. The permeability of all boundaries is set to zero. The level of ground water table is established at the level of bottom of the dam for UDEC model A and at the level of upper part of the storage basin for UDEC model B. A fully coupled hydro-mechanical analysis is used, in which the fracture conductivity is dependent on mechanical displacement and joint water pressure affects the mechanical computations [18].

3.2 Calculation sequence

As analyses in this paper are completely based on the methodology and the results of Part I [17]. In this paper, the calculation sequence is forwarded to include cyclic loading on the rock mass in UDEC models A and B due to the variation of the water level in the storage basin. These variations are carried out by first reducing the water table to 25 m, and then increasing the water table to 50 m in both UDEC models. Each iteration is finalized by brining the models to equilibrium. During this process, data on shear- and normal displacements are recorded, together with inflow data into the inspection tunnel and flow velocities around inspection tunnel. Each iteration changes the water level in the storage basin by 25 m, which represents the critical levels for the Håckren dam. However according to the monitored data such variations occur only within the period of several years, which implies that full cycle (reduction by 25m and raising by 25m) may represent the period of the several years for the dam. Therefore the term “idealized year” has been used which describes the full cycle of the water table in the storage basin. The monitoring of the rock mass for both UDEC models A and B has been done for 10 idealized years.

A



B

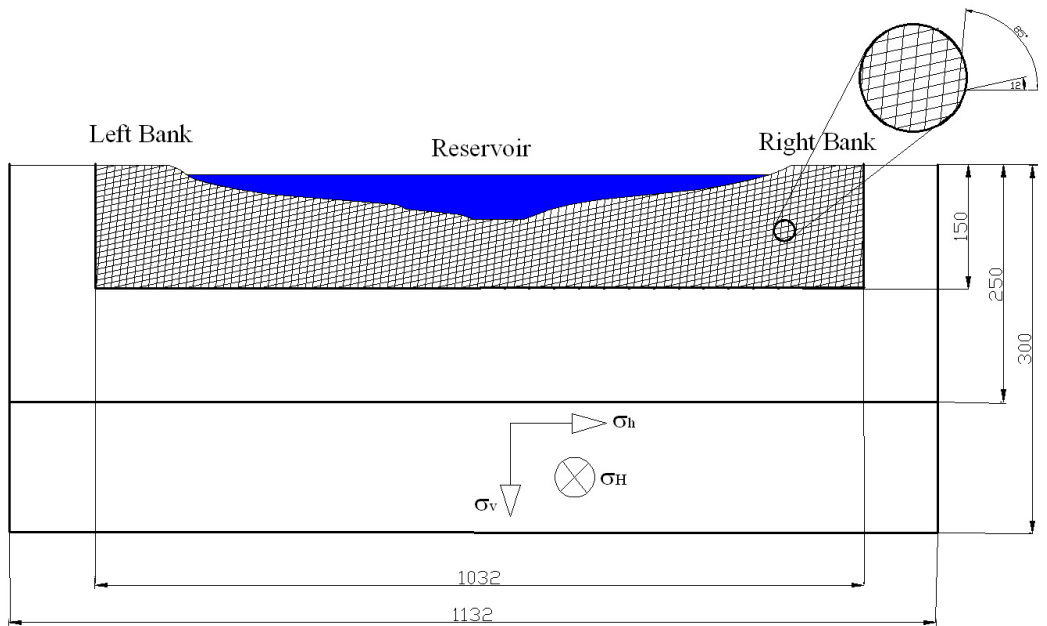


Figure 3. Layout of the UDEC models of the Håckren dam. A, UDEC Model A. The maximum horizontal stress is oriented in-plane (and strikes in the WNW – ESE direction) and the minimum horizontal stress is oriented out-of-plane; B, UDEC Model B. The maximum horizontal stress is oriented out-of-plane and the minimum horizontal stress is oriented in-plane. Figure 2 shows the location of profiles A-A' and B-B'.

4 Results

Table 1 shows the magnitudes of maximum shear- and normal displacements monitored in the rock mass and grout curtain in numerical simulation corresponding to a production time of 10 idealized years. The majority of the observed displacements in the rock mass are concentrated in two areas along UDEC model A (A-heel and A-toe) (Figure 3, 4A). Small, but yet significant displacements is also observed in the grout curtain (A-grout). In UDEC model B, there are three areas with concentrated displacements in the rock mass, the left and right banks (B-left and B-right respectively), and near floor of the storage basin (B-floor) (Figure 4B). In the following text the discontinuities with dip angle of 12° are referred as subhorizontal, with 50° as intermediate, and with 95° as subvertical.

Table 1. Maximum shear- and normal displacements of rock mass obtained from numerical models

Year	WT (m)	Rock mass displacement										Grout curtain displacement	
		Shear (mm)					Normal (mm)					Shear (mm)	Normal (mm)
		Model A-heel	Model A-toe	Model B-Left	Model B-Rht	Model B-floor	Model A-heel	Model A-toe	Model B-Left	Model B-Rht	Model B-floor		
0.5	25	0.62	0.45	0.15	0.16	0.49	0.10	0.13	0.04	0.05	0.39	0.050	0.006
1	50	0.61	0.84	0.25	0.35	0.56	0.08	0.05	0.18	0.07	2.04	0.164	0.008
1.5	25	1.14	0.82	0.24	1.66	14.30	0.25	0.13	0.06	15.00	13.30	0.060	0.012
2	50	1.30	0.85	0.32	0.57	8.50	0.12	0.12	0.21	0.31	22.00	0.172	0.011
2.5	25	1.84	0.82	0.34	3.20	9.16	0.50	0.13	0.04	13.70	8.36	0.062	0.012
3	50	1.46	0.86	0.32	0.65	6.60	0.16	0.12	0.22	0.52	5.70	0.177	0.012
3.5	25	2.00	0.83	0.33	1.81	8.10	0.35	0.13	0.04	16.40	7.50	0.077	0.012
4	50	1.65	0.86	0.32	0.69	6.34	0.19	0.12	0.21	0.32	5.43	0.175	0.012
4.5	25	2.22	0.82	0.33	1.45	7.90	0.17	0.13	0.03	1.16	7.40	0.081	0.013
5	50	1.83	0.86	0.33	0.53	6.14	0.15	0.12	0.22	0.34	5.30	0.178	0.013
5.5	25	2.34	0.82	0.33	3.05	8.00	0.17	0.13	0.06	26.50	8.00	0.083	0.013
6	50	2.00	0.85	0.32	1.98	5.90	0.14	0.12	0.21	0.72	5.10	0.146	0.010
6.5	25	2.20	0.83	0.33	1.53	8.22	0.17	0.13	0.06	1.24	9.00	0.084	0.013
7	50	1.82	0.86	0.35	1.52	5.88	0.13	0.12	0.22	0.99	7.80	0.178	0.013
7.5	25	2.30	0.82	0.33	0.90	8.60	0.22	0.13	0.06	0.41	11.00	0.088	0.013
8	50	2.00	0.86	0.35	0.89	6.43	0.17	0.12	0.21	0.33	23.00	0.174	0.013
8.5	25	2.48	0.82	0.31	2.21	16.60	0.21	0.13	0.06	12.80	18.10	0.089	0.013
9	50	2.10	0.86	0.35	0.52	5.30	0.17	0.12	0.21	0.14	15.80	0.176	0.013
9.5	25	2.40	0.82	0.32	2.32	25.50	0.21	0.13	0.05	0.05	25.70	0.091	0.014
10	50	2.15	0.86	0.35	1.49	6.55	0.18	0.12	0.21	1.57	6.94	0.176	0.013

Key, WT, water table

There is a practical reason for presenting the results separately for these subsets of UDEC models, rather than for the entire model. Thanks to the geometry of the discontinuities, they form

small loose blocks at the surface in front of the dam. These small blocks are those that are displaced the most in the entire model (Figure 5A). We are using the curtain command in UDEC to identify the area of highest displacement. This command plots the range from 100 to 20% of the maximum displacement. As an example, after ten idealized years of operation, the maximum shear displacement in the dam model shown in Figure 5A is 88.43 mm. Using the curtain command, the minimum shear displacement plotted is 17.69 mm, and only the small loose blocks at the surface of the model in front of the heel of the dam is subjected to this amount of displacement. Table 1 shows that the maximum shear displacement is 2.15 mm under the heel of the dam. This maximum value is used as cut-off value in Figure 4B, resulting in that shear displacements from 2.15 to 0.43 mm are plotted in red. The removal of large displacement of small near-surface blocks allows us to see that shear displacements under the heel of the dam is mainly occurring along some inclined discontinuities, down to over 50 m depth, whereas shear displacements under the toe of the dam is occurring along the subhorizontal discontinuities downstream of the toe of the dam, almost to 50 m depth. In addition, some shearing has also occurred to ~10-15 m depth upstream of the dam core.

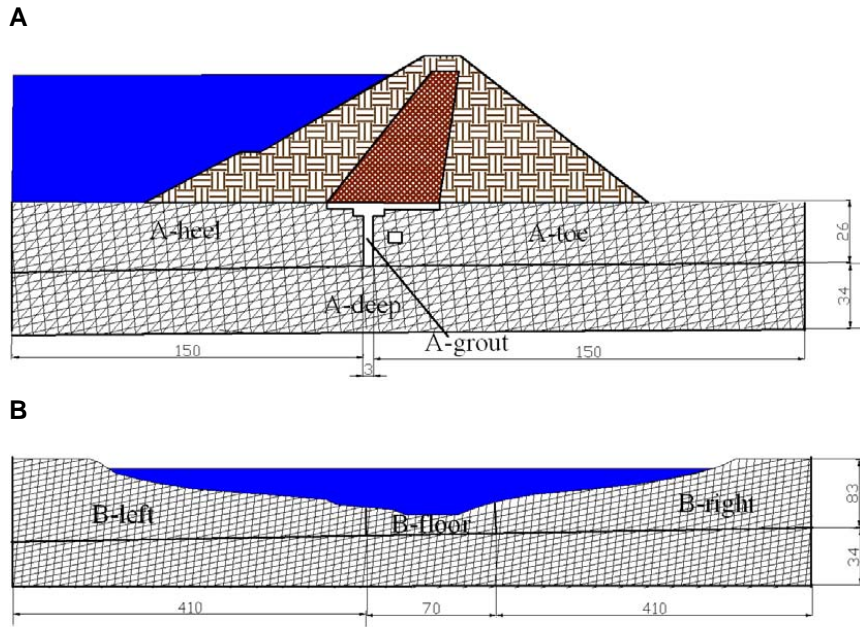


Figure 4. Areas of interest in foundation rock. **(A)** Areas of interest in Cross-section A are denoted as A-heel, A-grout, A-toe and A-deep. **(B)** Areas of interest in Cross-section B are denoted as B-left, B-right and B-floor.

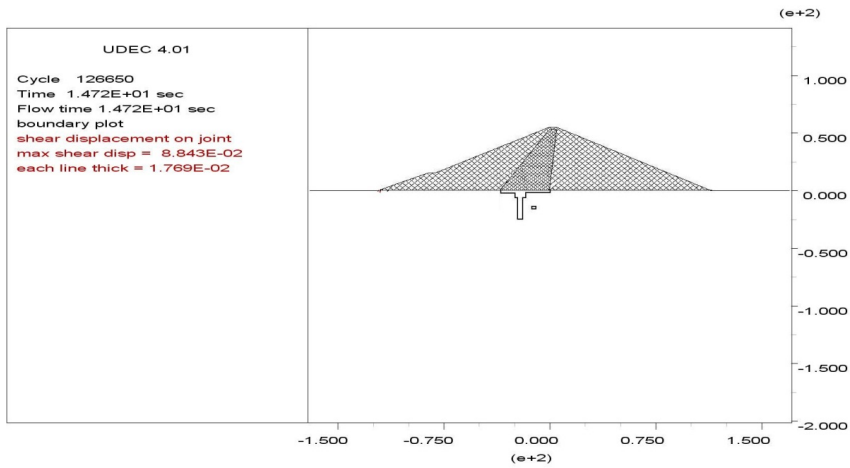
4.1 Shear- and normal displacements in the rock mass and grout curtain

The filling of the water storage basin for the first time resulted in the development of maximum shear displacements of 0.61 mm and 0.84 mm in the rock mass of UDEC model A under the dam heel and toe, respectively (Table 1). Under the dam toe, the order of maximum shear displacements remains rather constant and varies from 0.82 – 0.86 mm during the ten years of idealized operation. These displacements occur along subhorizontal discontinuities (Figure 5B). A different view is observed under the heel of the dam, at which there is a general gradual increase in maximum shear displacements from ~0.6 mm at year 1 to over 2 mm shear displacement after year 10 (Figure 6A). These displacements occur along inclined discontinuities that dip towards the storage basin (Figure 4B). We note that there is a tendency that larger shear displacements are occurring in the rock mass at 25 m water table than at 50 m water table (Figure 6A) after second year. We attribute this behavior to the fact that total deformation occurs in the direction of the dam. When we apply 25 m water table it reduced loads on the rock mass so it simplifies the deformation in the direction of the dam, however when we apply 50 m water table it increases load on the rock mass therefore reduces the total shear deformation. The amount of shear displacement is largest during the first years of operation, but appears to gradually decrease in size beyond that time (Figure 6A). The maximum shear displacements located close to the grout curtain gradually increases from 0.05 mm after the first filling of the storage basin to 0.18 mm after year 10. With exception for year 6, the gradual increase in accumulated shear displacements during subsequent loading and decrease while unloading mirrors that of Goodman [1] (cf. Figures 1 and 6B).

The first filling of the storage basin and variation of the water table has a very small effect on the normal displacements of the discontinuities on both sides of the dam (A-heel and A-toe). The magnitude of these displacements is less than 0.50 mm. There largest normal displacements are occurring along subvertical discontinuities under the dam heel, while the displacements are much localized and mostly concentrated on the intersection of the discontinuities in under the dam toe. The close monitoring the response of the grout curtain (A-grout) showed that construction and exploitation of the dam has very small effect on the grouted discontinuities. The magnitudes of shear- and normal displacements in this area do not exceed the value of 0.178 mm and 0.014 mm, respectively (Table 1).

A

Job Title :



B

Job Title :

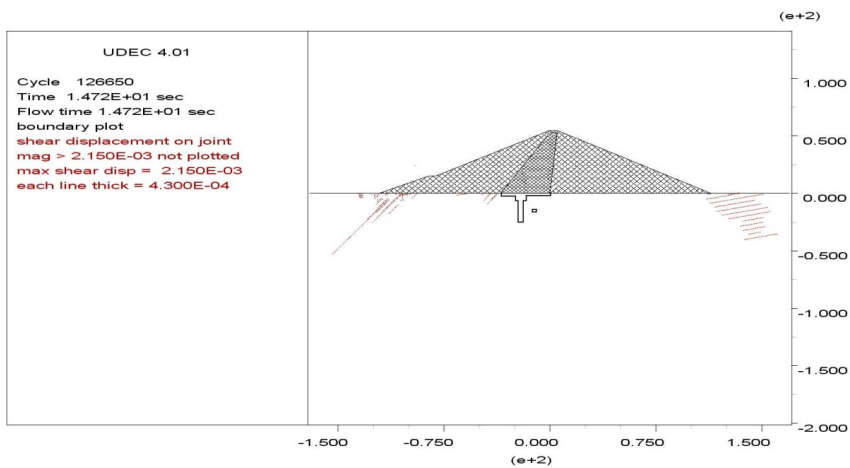


Figure 5. Examples of the application of the curtain command for UDEC model A after ten idealized years of operation. The curtain command only plots the values from 100 to 20% of the maximum shear displacement. A, The curtain command plots displacements from 100 to 20% of maximum shear displacement (i.e. 88.43 – 17.69 mm). B, Values over 2.15 mm are cut off in the curtain command. Shear displacements from 2.15 to 0.43 mm are included.

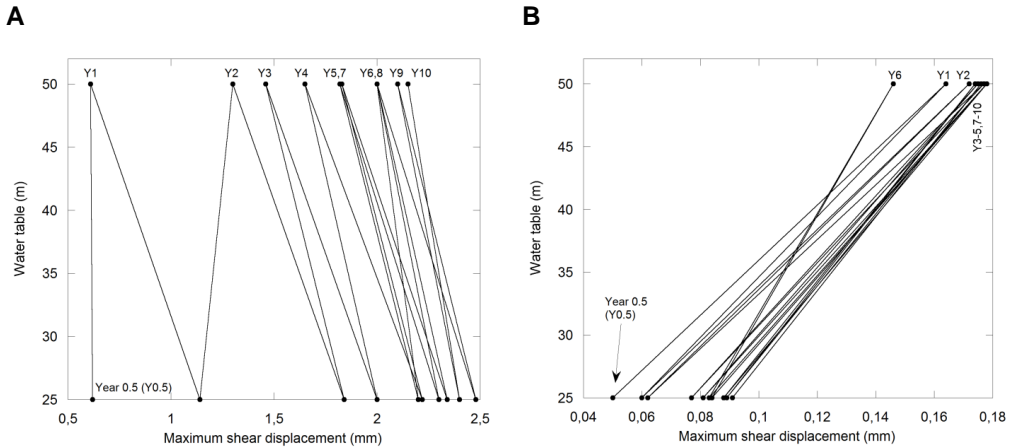


Figure 6. Accumulation of maximum shear displacements in the rock mass along model A versus the depth of the water table. A, The rock mass under the heel of the dam. B, The rock mass within the grout curtain. Y1-Y10 refers to idealized year 1 to 10 or numerical operation.

The overall variation in shear displacements in UDEC Model B varies from 0.05 – 25.50 mm over the entire simulation time (Table 1). The first filling of the storage basin with the following variation of water table results in the shear- and normal displacements in the banks and the bottom rock mass in UDEC model B. The majority of these displacements are localized within 5 m depth, and are occurring along subhorizontal discontinuities. The banks of the storage basin (B-left and B-right) identify almost the same magnitude of the shear displacements (Table 1), whereas the floor of the storage basin accommodates higher shear displacements, up to 25.50 mm. Unusually normal displacements are in the order of 10% of that of shear displacements. However, maximum normal displacements in the same order, or greater than the shear displacements are obtained in all sections of Model B (Table 1). Maximum normal displacements is about ~26 mm.

4.2 Total inflow in the tunnel and velocity of inflow

Table 2 shows the total inflow into the inspection tunnel, considering an active length of the tunnel of 150 m [17] and the velocity of water. In the first idealized year of numerical simulation, there is a rapid increase in water flow up to 32.6 l/min, with a velocity up to 1.65 cm/s (Table 2, Figure 7). After this rapid initial increase, there is a gradual and sublinear increase in inflow and velocity (Figure 7). Low water levels in the storage basin is associated with somewhat higher values of inflow and velocity.

Table 2. Total inflow into the inspection tunnel and water flow velocity around the tunnel

Year	Water table, m	Inflow, l/min	Velocity, cm/s
0.5	25	22.7	1.15
1	50	32.6	1.65
1.5	25	32	1.71
2	50	33.5	1.71
2.5	25	32.3	1.74
3	50	33.7	1.74
3.5	25	32.4	1.76
4	50	33.8	1.75
4.5	25	32.5	1.76
5	50	33.9	1.75

Year	Water table, m	Inflow, l/min	Velocity, cm/s
5.5	25	32.6	1.77
6	50	33.7	1.75
6.5	25	32.5	1.76
7	50	33.9	1.76
7.5	25	32.7	1.78
8	50	33.9	1.76
8.5	25	32.7	1.78
9	50	34	1.77
9.5	25	32.8	1.79
10	50	34	1.77

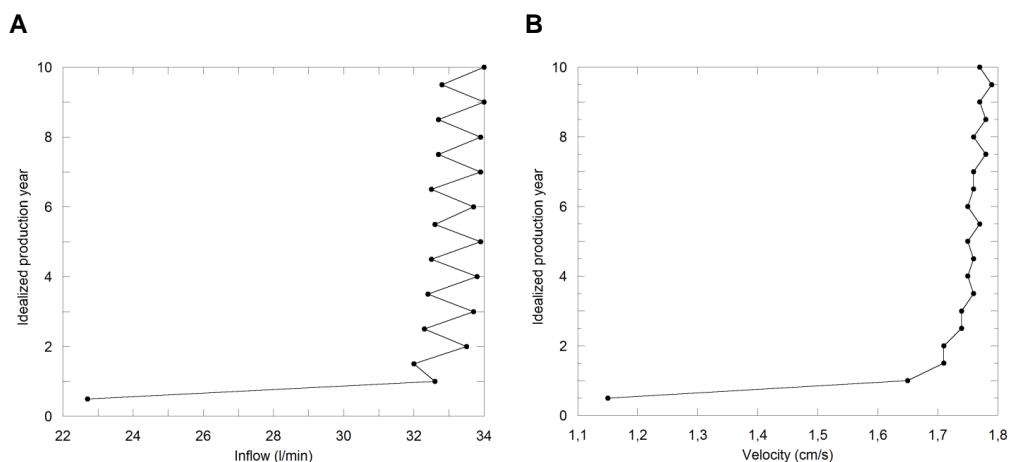


Figure 7. A, Water inflow versus idealized year of numerical simulation. B, Velocity of water versus idealized year of numerical simulation.

5 Discussion

The first filling of the storage basin is very significant in dam engineering practice and therefore it is usually performed along an extended period of time with close monitoring of the foundation rock and dam. Our results suggest the beginning of sliding of the dam along subhorizontal discontinuities in A-toe area in the first year. The peak shear strength of these discontinuities has been reached so they start to slide. The results from the simulation of the cycling loading along the next 9 idealized years shows that this sliding process has stopped after the first filling (Table 1). This implies that the rock mass on the downstream side of the Håckren dam initially was exposed to shear displacements, but that the subsequent loading is insufficient in size for driving this process any further. The observed low magnitudes of normal

displacements in this area are probably due to small roughness of the surface which could cause dilation of discontinuities and lower pore pressure than on upstream side of the dam. The measured mean value of JRC is between 4 and 5.

The different picture is observed on the upstream side of the dam, in A-heel area. The majority of shear displacements here are occurring along intermediate discontinuities in the area adjacent to the grout curtain and to the end of the dam. The combination of high pore pressure on the upstream side of the grout curtain and highest load caused by the weight of the dam probably result to this behavior. It should be noted that these displacements are within 15 m depth from the interface dam / foundation. These shear displacements are not observed in the area of grout curtain which means that strength of grouted discontinuities is high enough to withstand such loads. Higher shear displacements are observed in the intermediate discontinuities closer to the end of the dam in A-heel area. It may be a result of the most unfavorable orientation of the intermediate discontinuities in term of direction of displacement of the rock mass, compare to subhorizontal and subvertical ones which results to higher reduction of the effective stress, which in turn reduce the shear strength of the discontinuity. More importantly these shear displacements were developing along more extensive period of time compared to A-toe area (Figure 4), but closer to the end the rate of grow of shear displacements become very low. The registered magnitude of normal displacements is almost the same as in downstream side of the dam, A-toe, with except of three peaks (Figure 5). Such behavior is explained by low dilation angle of the discontinuities (low JRC). These analyses imply that most shear displacements of rock mass on upstream side of the Håckren dam are concentrated close to the surface, with very small normal displacement of the discontinuities.

Such behavior is supported by analysis of the rock mass in UDEC model B. Analysis show the extensive shear and normal displacements of the rock mass (Figure 6) at the bottom of the storage basin along the ten years. All registered displacements were obtained within the depth of 10 m from the surface. The high peaks of normal displacements on the right bank of the storage basin are a result of numerical approach. The introduced discontinuities in the model created a small block in the right side of the storage basin, which leads to such high displacements with the variation of the water table in the storage basin.

The monitoring of the displacements in the grout curtain showed that these displacements are very small and do not develop with variation of water table in the storage basin (Table 1). This implies that loads caused by the Håckren dam and water table in storage basin are not high enough to damage the grout curtain of the dam.

The monitored inflow into the tunnel raised during the first filling of the storage basin and stayed almost on the same level along the ten idealized years of exploitation of dam (Table 5) which allows assume the integrity of grout curtain. However the velocity of water flow around the tunnel shows a slight increase with time. This may be an interesting fact in turn of erosion considering that most important parameters influencing the erosion performance are flow velocity and exposure time [16].

Results of the analysis show that all the displacements are concentrated in the A-heel and A-toe areas close to the surface. The loads caused by the dam are not high enough to cause significant displacements within the grout curtain. This implies that there is a small chance for development of erosion path within the upper part of the foundation rock for Håckren dam. The monitored at Håckren dam site and registered in numerical analyses inflow of water into the inspection tunnel is a good indicator of it.

6 Conclusion

The analysis of the jointed rock mass response to the construction and exploitation of the Håckren dam along 10 idealized years was carried out by UDEC with application of hydro-mechanical model. The rock mass was modeled as a discontinuum media with the intent to analyze the progress of shear and normal displacements in the rock mass under the dam and in storage basin, the change in total inflow into the inspection gallery and variation of the velocity of water flow. Afterwards there have been done attempt to evaluate such conditions of the rock mass in terms of possible development of erosion along the discontinuities.

The numerical analysis shows that dam tends to slide along subhorizontal discontinuities on the downstream side after first filling of the storage basin. However the following cyclic loading caused by the water in storage basin does not contribute to the development of this sliding. On other hand first filling and exploitation of the Håckrem dam results in the shearing and opening of the discontinuities close to the surface on the upstream side. This effect is clearly observed in both UDEC model A and B. The total inflow into the inspection tunnel is stabilized after the first year and keeps staying on the same level, while the flow water velocity shows a slight rate increase which may raise a question about erosion in time. Analysis showed the stability of foundation rock of the Håckren dam in term of mechanical displacements and flow in evaluated period of time. However it should be kept in mind that water flow in rock mass may cause higher degradation of the strength properties of the rock mass in longer time perspective than the residual values used in this analysis. The usage of such simple analysis proved to be valid for the

first step evaluation of the conditions of the Håckrem dam rock mass. Hence this approach may be applied for preliminary evaluation of other embankment dams.

6 Acknowledgements

The research presented was carried out as a part of "Swedish Hydropower Centre - SVC". SVC has been established by the Swedish Energy Agency, Elforsk and Svenska Kraftnät together with Luleå University of Technology, The Royal Institute of Technology, Chalmers University of Technology and Uppsala University. www.svc.nu

7 References

- [1] Goodman RE. Introduction to rock mechanics. John Wiley and Sons; 1980.
- [2] Bondarchuk A., Ask M.V.S., Dahlström L-O., Nordlund E. Rock mass behavior under hydropower embankment dams: a two dimensional numerical study. *Rock Mechanics and Rock Engineering*, Springer, 2011. DOI 10.1007/s00603-011-0173-2
- [3] Rutqvist J. Modeling and field testing of coupled hydromechanical behavior of rock joints. Licentiate thesis, Lulea University of Technology; 1990.
- [4] Long JCS, Gilmour P and Witherspoon PA. A model for steady fluid flow in random three-dimensional networks of disc-shaped fractures. *Water Resources Res.*, 18 (3), 1985, pp. 1105-1115
- [5] Braester C. Discrete and continuum approaches to solution of flow problems in fractured rocks. *Proc. of the Fourth Canadian-American Conf. on Hydrogeology - Fluid flow, heat transfer and mass transport in fractured rocks*. Banff, Alberta, Canada, *Aim. Res. C.* and *N.W.W.A.*, 1988, pp. 223-229
- [6] Cacas MC, Ledoux E, de Marsily G, Tillie B, Barbreau A, Durand D, Feuga B and Peaudecerf P. Modeling fracture flow with a stochastic discrete fracture network: calibration and validation. 1: The flow model *Water Resources Res.* 26 (3), 1990, pp. 479-489
- [7] Boulon MJ, Selvadurai APS, Benjelloun H and Feuga B. Influence of rock joint degradation on hydraulic conductivity *Int. J. Rock Mech. Min. Sci. & Geomech. Abstr.*, 30, 7, 1993, pp. 1311-1317
- [8] Pine RJ and Batchelor AS. Downward migration of shearing in jointed rock during hydraulic injections, *Int. J. Rock Mech. Min. Sci. & Geomech. Abstr.* 21, 5, 1984, pp. 249-263
- [9] Bandis SC, Makurat A and Nik G. Predicted and measured hydraulic conductivity of rock joints. *Proc. of the Int. Symp. on Fundamentals of Rock Joints* Björkliden, Norway; 1985.

- [10] Barton N, Bandis S and Bakhtar K. Strength Displacement and Conductivity of rock joints. *Int. J. Rock Mech. Min. Sci. & Geomech. Abstr.* 22, 3, 1985, pp. 121-140
- [11] Elsworth D and Goodman RE. Hydro-mechanical characterization of rock fissures of idealized sawtooth or sinusoidal form *Proc. of the Int. Symp. on Fundamentals of Rock Joints* Björkliden, Norway; 1985.
- [12] Hakami E. Water flow in single rock joints Licentiate thesis, Lulea University of Technology; 1988.
- [13] Billaux D and Gentier S. Numerical and laboratory studies of flow in a fracture. *Proc. of the Int. Symp. on Rock Joints* Loen, Norway, Balkema ed. Rotterdam, The Netherlands, 1990, pp. 369-374
- [14] Archambault G, Gentier S, Riss J and Flamand R. The evolution of void spaces (permeability) in relation with rock joint shear behavior *Int. J. Rock Mech. & Min. Sci.* 34:3-4, paper No. 014; 1997.
- [15] Chen Z, Narayan SP, Yang Z and Rahman SS. An experimental investigation of hydraulic behavior of fractures and joints in granitic rock *Int. J. Rock Mech. & Min. Sci.* 37, 2000, pp. 1061-1071
- [16] Momber AW. Wear of rocks by water flow *Int. J. Rock Mech. Min. Sci.* 41, 2004, pp. 51-68
- [17] Bondarchuk A, Ask MVS, Dahlström L-O and Nordlund E. Rock mass stability of the Håckren hydropower embankment dam in central Sweden: Part I - Developing and validating 2D UDEC numerical models. Submitted for publication in the *Rock Mechanics and Mining Science*; 2012.
- [18] Itasca. *UDEC* version 4.0. Manual. Minneapolis, ICG; 2005.
- [19] Bartsch M, Mill O, Birkedahl J, Brandesten C-O, Hammar L, Norstedt U, et al. Peer Review of Swedish High Consequence Dams. Test of a model for “special examination” of dam safety – A compilation of facts and experiences from 5 reviews performed in 2006 – 2008. Svenska kraftnät 2009: PM 17 June 2009, 19 pp. Available at [www.svk.se/Om-oss/Var-verksamhet/Dammsakerhet/Rapporter on 25 February 2012](http://www.svk.se/Om-oss/Var-verksamhet/Dammsakerhet/Rapporter%20on%2025%20February%202012)
- [20] Makurat A, Barton N, Rad NS, Bandis S. Joint conductivity due to normal and shear displacement Rock Joints, Barton & Stephannson (eds.), Balkema, Rotterdam, 1990, pp. 535-540
- [21] Colback PSB and Wild BI. Influence of moisture content on the compress strength of rock Proceedings of third Canadian rock mechanics symposium, University of Toronto, 1965, pp. 385-391
- [22] Bates RL and Jackson JA. Glossary of geology end ed. Falls Churrch: Amer. Geolog. Inst.; 1980.

- [23] Maria Luisa Mendes de Vasconcelos Braga Farinha. Hydromechanical behaviour of concrete dam foundations. In-Situ tests and numerical modeling, Doctoral Thesis, Technical University of Lisbon; 2010.

